UNIVERSITÉ DE MONTRÉAL

COATABILITY OF CEMENT CLINKER ON BASIC REFRACTORIES

Zongqi GUO

DÉPARTEMENT DE GÉNIE PHYSIQUE ET DE GÉNIE DES MATÉRIAUX

ÉCOLE POLYTECHNIQUE DE MONTRÉAL

THÈSE PRÉSENTÉE EN VUE DE L'OBTENTION

DU DIPLÔME DE PHILOSOPHIAE DOCTOR (Ph.D.)

(GÉNIE MÉTALLURGIQUE)

MARS 2001

UNIVERSITÉ DE MONTRÉAL

ÉCOLE POLYTECHNIQUE DE MONTRÉAL

Cette thèse intitulée:

COATABILITY OF CEMENT CLINKER ON BASIC REFRACTORIES

Présentée par: GUO Zongqi

En vue de l'obtention du diplôme de: Philosophiae Doctor

A été dûment acceptée par le jury d'examen constitué de:

M. ALLAIRE Claude, Ph.D., président

M. RIGAUD Michel, D.Sc.A., membre et directeur de recherche

M. WILLIAMS Paul, Ph.D., membre

M. TANGUAY G. Marc, Ph.D., membre

ACKNOWLEDGMENTS

I would like to express my sincere gratitude to Professor Michel Rigaud for his constant encouragement, expert guidance, and constructive criticism throughout the entire duration of the thesis, and also for providing me with the opportunity to study here at Ecole Polytechnique.

I would also like to thank Prof. Jinxiang Wang, president of Luoyang Institute of Refractories Research, for kindly allowing me to study at CIREP.

Special thanks go to Dr. S. Palco, not only for his valuable help for the microstructural analysis, but also for his readiness to discuss any problem. Other thanks also go to Mrs. H. Q. He, Mr. V. Kovač and Dr. K. Cherif for their help at the beginning of this work. Acknowledgments are due to Dr E. Paransky for his aid with the electron probe microanalyzer and Mr. E. Planque for his help with DTA and TGA analysis.

I gratefully acknowledge the useful discussions and assistance of Dr. N. S. Zhou, Dr. C. L. Feng, Dr. X. Cheng, Dr. S. Afshar, N. Ntakaburiumvo, R. Pelletier, J. Sebbani, Dr. K. Dehghani, E. Divry, and C. Gaubert.

My particular thanks are due to J. P. Bouchard and H. Rioux at CIREP for their technical and secretarial helps.

I would like to thank my wife for her continuous sacrifice and encouragement and to my child who was often neglected during the years to achieve my educational goal.

RÉSUMÉ

Le croûtage dans la zone de cuisson joue un rôle prépondérant sur la durée de vie des réfractaires dans les fours rotatifs à ciment, sur l'opération des fours et la consommation énergétique par tonne de clinker produit. Il est apparu impératif de développer une méthode pour évaluer, a priori, ce phénomène en laboratoire. C'est là le but principal de cette thèse, au cours de laquelle seront déterminés les paramètres qui influencent l'adhérence du croûtage et les mécanismes des réactions sur les briques basiques couramment utilisées.

Au départ, les matières premières constituant le cru ont été caractérisées. Les analyses chimiques, minéralogiques et granulométriques ont été effectuées. L'évolution du cru en fonction de la température a été vérifiée par analyses thermiques différentielles (ATD) et thermogravimétriques (ATG). L'apparition de chaux libre a été confirmée à partir de 1000 °C, la formation de belite, C_2S, et l'apparition de phases liquides, à partir de 1350 °C, la présence de chaux libre étant encore présente à 1450 °C. Sous les conditions expérimentales qui seront celles de tous les essais, il faut atteindre 1550 °C pour que le phase alite, C_3S, devienne la phase prédominante, au détriment des phases C_2S et C (pour CaO libre), lorsque la montée en température est de l'ordre de 4 °C/minute.

Le protocole expérimental pour mesurer l'adhérence du cru après calcination sur des échantillons de briques dûment sélectionnés, a été développé, en constituant un

sandwich: deux tranches de briques avec le cru calciné entre. Durant la calcination, il s'est avéré nécessaire d'imposer une charge compressive sur le sandwich. La mesure de l'adhérence est le résultat d'un essai en flexion à trois points; les essais avec un mode de chargement en traction donnent des valeurs trop faibles, donc difficilement reproductibles.

Les essais ont été effectués au départ avec un cru préalablement calciné à 1000 °C durant 4 heures, puis mélangé à de l'eau pour former une pâte avec environ 46 % de matières solides. Il a été démontré ultérieurement qu'un mélange de cru calciné sec, pouvait tout aussi bien être utilisé, et ce fut la démarche adoptée finalement.

Les sandwichs ont été préparés avec des échantillons de briques de 50 x 50 x 60 mm, coupés à sec. Six cubes ont été utilisés chaque fois, pour former 3 sandwichs, pour tester une brique donnée. De douze à quinze grammes de cru pulvérisé sont utilisés par sandwich.

Les sandwichs sont introduits sur la sole d'un four moufle. Un poids mort de 1325 grammes est déposé sur le dessus de chaque sandwich, ce qui équivaut à une contrainte de compression de 5.3 kPa. Les sandwichs sont chauffés jusqu'à 1550 °C, maintenus à cette température 30 minutes, les taux de mise en chauffe et de refroidissement contrôlés à 4 °C/min.

Le module de rupture sur chaque sandwich est mesuré en flexion à 3 points, selon la norme ASTM C133-97, à un taux de mise en charge correspondant à la vitesse de déplacement de la traverse de 1.0 mm/min. C'est la moyenne des valeurs obtenues sur l'ensemble des 3 sandwichs qui est considérée comme représentative de l'adhésion d'un cru donné sur une brique donnée.

Quatre plans expérimentaux ont été suivis pour évaluer les paramètres de l'essai. Trois plans factoriels partiels et un plan factoriel complet ont été exécutés, pour révéler l'importance des facteurs principaux et la robustesse de l'essai. Les analyses statistiques classiques sur la variance des valeurs de module de rupture mesurées ont été effectuées pour confirmer la reproductibilité et la répétitivité des essais. Il a été établi que les mesures de l'ordre de 5 MPa sont reproductibles à ± 0.5 MPa, ce qui est considéré acceptable, compte tenu de l'hétérogénéité des matériaux considérés.

Au total, 12 briques basiques de natures différentes, et cinq crus industriels de compositions différentes, ont été étudiés et plus de 600 sandwichs ont dû être testés. Une trentaine d'échantillons ont été analysés à l'échelle microscopique. Les conclusions suivantes ont été déduites de l'ensemble des résultats:

(1) Les effets les plus significatifs sur la valeur de l'adhérence du clinker sur une brique donnée sont, par ordre d'importance: la valeur de la contrainte de compression sur le sandwich, la nature du cru, la température de clinkérisation atteinte, le temps de

résidence à cette température. À propos du cru, le ratio silice est hautement significatif; ce ratio a une influence négative sur les briques de magnésie-spinelle (MA) et positive sur les briques de dolomie (D), le ratio alumine n'a que peu d'influence sur les briques MA mais une influence positive sur les briques D. La finesse du cru utilisé est aussi très marquée pour les deux types de brique. Par ailleurs, l'effet de la montée en température est plus marqué pour les briques MA que pour les briques D.

(2) Les valeurs d'adhérence obtenues ne sont pas sensibles à des écarts expérimentaux concernant la durée de l'essai lorsque compris entre 30 minutes et 120 minutes, l'épaisseur du cru en pâte utilisé, entre 2 mm et 5 mm, et la façon de préparer la pâte, au niveau du mélange. Pour des briques de dolomie, la déviation standard est de 0.47 MPa pour une valeur moyenne de 5.5 MPa, obtenues sur 30 valeurs (10 briques) portées à 1550 °C, pendant 30 minutes, sous une charge de 5.3 kPa.

(3) Les mécanismes réactionnels conduisant à l'adhérence des clinkers sont bien différents lorsqu'il s'agit d'une brique de dolomie, plutôt qu'une brique MA. Dans le cas des dolomies, c'est la formation de l'alite, C_3S, qui est, à l'interface clinker-brique, prépondérante; c'est la présence de chaux dans la dolomie qui est critique et qui justifie les observations rapportées en (1). Lorsque le ratio silice est faible, la proportion accrue de phase liquide accélère la réaction dolomie-silice et favorise l'apparition d'un film quasi continu de magnésie qui vient réduire la force d'adhérence entre le clinker et la brique, car il n'y a plus de réaction possible entre le clinker et la magnésie. Cela est

confirmé lorsqu'on compare l'adhésion d'un clinker sur des briques de dolomie-magnésie (valeur plus faible) plutôt que sur des briques de dolomie (valeur plus élevée). La présence d'un plus grand pourcentage de magnésie est nuisible.

(4) Dans le cas des briques de magnésie-spinelle, les grains de spinelle réagissent facilement avec les phases contenant de la chaux du clinker et ceci conduit à la formation de belite, C_2S, plutôt que de l'alite, C_3S, à l'interface clinker-brique. Plus le clinker contient de phase liquide (ratio de silice bas), plus la réaction est avancée, plus la force d'adhésion est élevée. Lorsque les briques MA contiennent non du spinelle synthétique, mais de l'alumine, la pénétration de la phase clinker est moindre et l'adhérence clinker-brique diminue.

(5) Des résultats obtenus en fin de thèse indiquent qu'il est possible d'exploiter le même protocole expérimental avec du cru non-préalablement calciné, ce qui représente une simplification majeure. Ceci méritera d'être confirmé dans les travaux futurs. D'ores et déjà, le protocole est considéré comme fiable et il est recommandé de passer à une comparaison inter-laboratoires des résultats. Les travaux futurs devraient aussi être orientés de façon à pouvoir évaluer l'incidence de l'atmosphère sur le croûtage, et notamment de la présence d'alcalins en phase gazeuse.

ABSTRACT

Since coating plays a key role in prolonged operation and reduced energy consumption of rotary kilns, it is imperative to explore a reliable evaluation technique of coating. Developing coating and making precise measurement are big challenges in laboratory made experiments. The aim of this work is to develop an effective and practicable method to evaluate the coatability of cement clinker on basic refractory bricks, susceptible to be translated in numbers. Determinations of the dominant influential factors, and assessment of reliability, as well as of coating mechanisms on different basic bricks, are to be tackled.

Raw meal has been investigated in terms of chemical and phase compositions, particle size distribution, using DTA and TGA, as well as x-ray diffraction and microstructural analysis after heating at different temperatures. Raw meal calcinated at 1000°C for 4 hours contains plenty of free lime. Over 1350°C, most of liquid phases and belite C_2S have formed. At 1450°C, there are still some clusters of free lime in clinker. Alite C_3S becomes dominant phase in clinker fired at temperature of 1550°C, with reduction of belite C_2S and depletion of free lime.

Preliminary trials mainly focused on obtaining adherence and then determining the appropriate mechanical testing mode for measurement. Exerting a compressive load on sandwich during firing is critical for developing solid adherence. Furthermore, testing

the sandwich in three-point bending flexural mode, instead of traction, leads to higher values of adherence strength; with the smaller values obtained in traction mode, the influences of the main factors were masked.

Prior to making sandwiches, the as-received raw meal is calcinated at 1000°C for 4h in an electrically heated furnace. The calcinated raw meal is then crushed and pulverized. Calcinated raw meal was used during development of the sandwich method. Initially, tests were made using the wet paste of calcinated raw meal. It was shown later that dry mix can be used to obtain equal adherence strength and finally this was the preferred method because of its convenience.

Samples of 50×50×60 mm are directly cut dry from available bricks (without water-cooling) and the sandwich is prepared using the cut surfaces. At least six pieces are needed to have three sandwiches for all tested brands of basic refractories. Sample at the bottom portion of sandwich is wrapped with "Scotch tape" around one cut surface to make a container. Twelve to fifteen grams of pulverized raw meal is poured into it. A cut surface of the upper portion of the sandwich is then superimposed and pressed by hand. The raw meal is also compacted around "Scotch tape", to avoid its dropping-off when the tape burns out.

The sandwiches are then introduced in an electrically heated muffle furnace. A dead weight of 1325 grams is applied on top of the sandwich, which is equivalent to a

pressure of 5.3 kPa. The assemblages are heated at 1550°C for 0.5h, with heating and cooling rates of 4°C/min. According to ASTM C133-97, modulus of rupture is measured using a universal mechanical machine with 3-point bending flexural mode, 90 mm span, and strain rate of 1.0 mm/min. Mean value of the modulus of rupture obtained from three replicates is considered as representative of the adherence strength of the coating.

Statistical design of experiments was employed for evaluating this sandwich test method. Three fractional factorial plans and one full factorial plan were executed to efficiently generate data that reveal the significance of some specific factors and the ruggedness to the method. Statistical process analysis was also used to plan and carry out experiments carefully so as to confirm repeatability and reproducibility of the sandwich protocol. Variability of ± 0.5 MPa is considered to be acceptable on a 5 MPa measured value.

In total, over 12 brands of various basic bricks and five batches of raw meal from different cement plants were used to test their mutual adherence. More than 600 sandwich bars were tested to develop the sandwich protocol. About 30 samples were analyzed by reflecting microscopy, some using cathodoluminescence technique. The following conclusions can be derived from the results:

(1) The most significant effects on adherence strength are the compressive loads, the nature of the raw meal, the heating temperature and the holding time, ranked in the

order of importance. Silica ratio of raw meal has a highly significant influence on adherence strength with a negative effect on magnesia spinel brick and a positive effect on doloma brick. Effect of alumina ratio is not significant on magnesia spinel brick, but is a significant positive effect on doloma brick. Effect of heating rate on adherence strength is noticeable on magnesia spinel brick. Particle size has a significant effect on both magnesia spinel and doloma bricks.

(2) A ruggedness test indicates that the sandwich test is insensitive to minor changes, in holding time, paste thickness and mixing mode of the paste. The sandwich test is repeatable with small variability across trials, and is reproducible, having small variability across operators. The standard deviation of 0.47 MPa has been obtained, for adherence mean value 5.5 MPa on doloma bricks fired at 1550°C for 30 min and under a load of 5.3 kPa. With this sandwich test, it is possible to differentiate between the aptitude of various basic bricks for "coatability". The results reflect practical, accepted coating performance of basic bricks in rotary kilns. It is then a meaningful test.

(3) Adherence mechanism of cement clinker on doloma brick is due to participation of lime from doloma brick in clinkerization of raw meal and formation of alite phase rich zone at the brick/clinker interface. High adherence strength can be obtained in the case of raw meal with high silica ratio. A large amount of liquid existing in clinker with low silica ratio accelerates reactions between doloma grain and silica

from raw meal to form a continuous layer of agglomerated MgO, which then reduces adherence strength. There is no reaction found between MgO and clinker phases. Magnesia-doloma brick consists of doloma aggregates and magnesia matrix that restricts the contact of lime with clinker. The lower adherence strength of magnesia-doloma brick, as compared with doloma brick, is attributed to the limited reaction between lime of the brick and clinker.

(4) Fine, crystalline spinel easily reacts with lime containing phases from clinker to form low-melting phases and belite zone at the clinker/brick interface; this explains adherence on magnesia spinel brick. The more liquid in clinker, that is with low silica ratio, the faster is the reaction between spinel and clinker; with high silica ratio, reactions occur just at contact points of spinel and clinker, and thus adherence strength on such a magnesia spinel brick is low. On a brick consisting of magnesia and fused alumina grains, formation of a spinel ring around the alumina grain was observed. Microstructural analysis on its sandwich indicates that little penetration of clinker phases was found and limited reaction between spinel ring and clinker occurs at the brick/clinker interface. As a result, such a brick has poor adherence of clinker.

(5) Further work should confirm the possibility to simplify the protocol using raw meal without precalcination step. A full round robin testing needs to be launched between different laboratories in order to promote the standardization of this sandwich test. Influences of alkalis on the coatability of clinker need to be evaluated.

CONDENSÉ

Ce projet de recherche a été entamé dans le cadre d'un projet subventionné par un consortium d'entreprises industrielles manufacturant du ciment Portland d'une part (trois compagnies), et manufacturant des briques réfractaires d'autre part (trois compagnies), avec l'appui financier du Conseil National de Recherche en Sciences Naturelles et en Génie.

Le but du projet était d'élucider le rôle des différents réfractaires, dits basiques, utilisés dans les zones de transition et la zone de cuisson, des fours rotatifs à ciment, sur le phénomène bien connu du croûtage. Il s'agissait de pouvoir mesurer l'adhérence de ce croûtage lors de la clinkérisation du cru, et de déterminer si la nature du réfractaire et la texture des produits pouvaient avoir une influence détectable et quantifiable.

Le plan expérimental de cette thèse a été élaboré après une revue bibliographique exhaustive sur les différentes méthodes de caractérisation du croûtage et une série d'essais préliminaires conduits par différents chercheurs au sein du CIREP, la Chaire Industrielle sur les Réfractaires de l'École Polytechnique (Dr. Khaled Cherif, Mme Huiqing He, M. Vladimir Kovač).

Cette thèse a été scindée en sept chapitres, en commençant par la description de l'envergure du travail effectué, pour préciser l'importance technico-économique de ce

phénomène très familier aux cimentiers, du croûtage, et pour décrire les buts visés:

(1) Détecter l'importance des paramètres susceptibles d'influencer le croûtage, tels que: la température et le temps de clinkérisation, ainsi que la nature des crus chargés, et quantifier leur rôle sur la force d'adhésion du croûtage sur la paroi réfractaire.

(2) Évaluer de façon systématique la méthode dite du sandwich préalablement identifiée, mais en y ajoutant une contrainte de compression, lors de l'essai. Ceci conférait au départ un aspect original à ce travail.

(3) Déterminer les mécanismes réactionnels qui puissent permettre d'expliquer les résultats et justifier les observations déjà bien établies concernant les performances des briques de dolomie et de magnésie-spinelle, mais aussi de toute la gamme des produits existants, incluant les dolomies enrichies de magnésie, enrichies de zircone ou de magnésie et de zircone, les magnésies-spinelle avec spinelle synthétique et/ou formation de spinelle in-situ.

La revue bibliographique effectuée initialement par MM. Rigaud, Cherif et Kovač, référence 14, a été reprise et mise à jour au chapitre deux, en précisant la définition des différents ratios utilisés pour caractériser un cru (mélanges de matières premières) pour obtenir un ciment Portland de qualité. Dans ce chapitre, on passe aussi en revue l'évolution physico-chimique en fonction de la température des principales phases

présentes, aspect central pour l'interprétation des résultats. C'est aussi dans ce chapitre que sont décrites les principales caractéristiques du croûtage dans la zone de cuisson d'un four industriel. Il est rappelé qu'un croûtage-type est très poreux (35 % de porosité), constitué volumétriquement d'alite, C_3S, (35 %), de bélite, C_2S, (15 %), de ferrites de calcium, C_4AF, (10 %), d'aluminates, C_3A, (5 %). À la température de clinkérisation, cette croûte peut être formée massiquement de 50 % d'alite, 20 % de belite et jusqu'à 30 % de phase liquide (ferrites + aluminates). Il est important toutefois de noter que l'épaisseur de cette croûte peut dépasser les 500 mm et que le gradient de température sur cette épaisseur est considérable (1450 °C et plus à la face chaude, entre 1200 °C et 900 °C à la face froide, à l'interface clinker-brique). À partir de ce constat, les paramètres de l'étude sont fixés, des points de vue thermique, chimique et mécanique.

Le chapitre trois porte sur la définition précise du protocole expérimental en vue d'établir les conditions préalables. Les résultats des caractérisations des crus utilisés sont dûment rapportés et les bases du test sandwich avec compression sont définies.

Le cœur de la thèse se retrouve au chapitre quatre. Les résultats de trois plans expérimentaux, avec 4 facteurs chacun, à deux niveaux, plan factoriel partiel, du type 2^{4-1}, donc incluant 8 essais avec 3 répliques (3 sandwiches pour chaque choix des conditions expérimentales) sont présentés et analysés statistiquement, en effectuant chaque analyse de variance appropriée, selon le programme ANOVA.

Le premier plan expérimental a été effectué sur des briques de dolomie de même nature dénommées LD1. Les quatre facteurs considérés ont été: la valeur de la charge compressive (2.4 kPa et 5.3 kPa), la température (1450 °C et 1550 °C), le temps de maintien en température ultime (30 minutes et 300 minutes) et la nature du cru (dénoté par C et L, correspondant à 2 crus industriels distincts). Le protocole suivi a été celui du mélange pâteux sur cru pré-calciné. Les modules de ruptures mesurés ont fluctué entre 2.18 MPa et 6.02 MPa, différence très significative. Les 4 facteurs principaux: charge compressive, nature du cru, température et temps ont une influence toute significative, et sont cités ici par ordre d'importance, du plus au moins important. De plus, l'interaction charge et nature du cru est aussi hautement significative. Tous les effets sont positifs, sauf l'influence du temps qui elle est négative, ce qui signifie que, après 300 minutes, le module de rupture des sandwiches est moindre qu'après 30 minutes. Cette influence du temps sera éclaircie ultérieurement au chapitre six.

Le deuxième plan expérimental, aussi du type 2^{4-1}, a été effectué sur une brique de magnésie-spinelle particulière (HMA3). Les quatre facteurs considérés ont été cette fois, la taille des particules du cru calciné, broyé à D_{50} = 5µm ou à D_{50} = 40µm, l'indice de silice, de 2 ou 3 défini par le rapport $SiO_2/(Al_2O_3+Fe_2O_3)=\frac{C_3S+1.325C_2S}{1.434C_3A+2.046C_4AF}$, l'indice d'alumine de 1 ou 1.5, défini par le rapport Al_2O_3/Fe_2O_3 ou l'expression 0.64+1.15 C_3A/C_4AF, et enfin le taux de montée en température de 4 °C/min ou de 8 °C/min, de façon à monter jusqu'à 1550 °C, avec un temps de maintien de 30 minutes,

et cette fois en utilisant le protocole avec cru calciné à sec (sans eau de mélange), et une charge compressive de 5.3 kPa. Les modules de rupture mesurés ont fluctué entre 0.0 kPa et 4.09 kPa. Les facteurs statistiquement influents sont toujours par ordre d'importance: l'indice de silice (effet négatif), le taux de montée en température (effet négatif), la taille du cru (effet négatif), les interactions taille-indice d'alumine, taille-taux de montée en température et taille-indice de silice ayant les 3 des effets positifs.

Le même plan expérimental, c'est-à-dire avec les mêmes facteurs, a été repris dans les mêmes conditions, toujours avec 3 répliques, mais sur la brique de dolomie LD1. Cette fois, les valeurs de module de rupture mesurées qui reflètent la force d'adhésion du clinker sur le réfractaire, ont fluctué de 2.02 MPa à 8.93 MPa. Le facteur le plus important s'est révélé être encore l'indice de silice, mais cette fois avec un effet très nettement positif; plus l'indice de silice est élevé plus l'adhérence du clinker sur la dolomie est forte. Le deuxième effet principal est la taille du cru (effet négatif signifiant que plus la taille est élevée, plus d'adhérence est faible). Cette fois, l'indice d'alumine a un effet légèrement significatif et positif alors que le taux de montée n'est plus significatif, selon l'analyse de la variance. L'interaction indice de silice-taille de particule a par contre un effet négatif sur l'adhérence.

Il ressort donc au total que les variables principales qui déterminent la valeur de l'adhérence d'un clinker sur une brique donnée sont:

la charge compressive;

la nature du cru utilisé;

le taux de montée en température;

le temps de maintien.

Pour le cru, l'indice de silice est le principal facteur, l'effet étant très important mais inversé sur l'adhérence clinker-dolomie par rapport à clinker-magnésie-spinelle. L'indice d'alumine est un facteur important sur l'adhésion clinker-magnésie-spinelle ; le degré de finesse du cru est toujours important, donc à contrôler. Ces résultats font donc ressortir l'importance de la cinétique de la clinkérisation, l'importance du frittage solide-liquide qui s'opère alors, mais aussi l'importance du réfractaire lui-même.

Pour confirmer l'ensemble de ces premiers résultats, un test de robustesse au niveau statistique avec encore un plan d'expérience, cette fois factoriel complet à 3 facteurs, a été exécuté. Il a été clairement démontré que le protocole tel que défini était bel et bien robuste, en fonction de l'épaisseur du cru utilisé (2 mm ou 5 mm), du temps de maintien (entre 30 et 120 minutes) et du mode de préparation du cru. Des essais de reproductibilité et de répétitivité ont aussi été effectués sur des briques de dolomie, 9 lots distincts, dont 3 à 6 mois d'intervalle.

Les résultats avec le cru pré-calciné mélangé en pâte, ou à sec, ont aussi pu être réconciliés entre eux, et ce avec trois expérimentateurs distincts pour préparer les sandwiches.

Tous ces nouveaux résultats ont été consignés au chapitre cinq, en incluant des résultats sur 2 types de briques de dolomie, 2 de dolomie-zircone, 1 de dolomie-magnésie et 2 types de magnésie-spinelle. Suite à ce travail, il a été possible de confirmer que d'une part ce sont les briques de dolomie (sans addition) qui offrent la meilleure adhésion au croûtage, suivies dans l'ordre des briques de dolomie-zircone, dolomie-magnésie et magnésie-spinelle. D'autres essais ont permis de mettre en lumière l'influence de la texture des briques en considérant non plus 2 mais 4 briques distinctes de magnésie-spinelle.

Pour justifier et expliquer ces résultats, toutes les observations microscopiques effectuées sur une trentaine d'échantillons, au niveau des interfaces clinker-réfractaire, ont été regroupées au chapitre six.

Les mécanismes réactionnels régissant l'adhérence et l'évolution du clinker aux interfaces ont été révélés, faisant ressortir les différences fondamentales entre dolomie et magnésie-spinelle. Dans le cas des dolomies, la phase chaux présente dans la brique permet la formation de C_3S (alite) à l'interface. La continuité clinker-brique alors ainsi créée se traduit par une adhérence élevée qui s'établit très rapidement, mais qui cesse par après lorsque seule la phase magnésie devient restante et quasi continue. Ceci permet de comprendre que lorsque le croûtage s'effondre de temps en temps dans les fours industriels, il y a écaillage au sein de la dolomie. Les résultats concernant le rôle des

indices de silice et d'alumine sont aussi facilement interprétables, en tenant compte alors de l'importance du frittage solide-liquide, et donc de la présence de la phase liquide, qui accélère en fait la formation de la couche de magnésie et tend à diminuer l'adhésion du clinker.

Dans le cas des briques de magnésie-spinelle, la phase liquide dans le clinker s'attaque aux grains de spinelle et les dissout, ce qui favorise la formation de belite (C_2S) à l'interface clinker-réfractaire, une pénétration accrue au sein du réfractaire, mais qui retarde la formation de C_3S, qui se retrouve, au-delà de l'interface, et qui ne contribue que peu à l'adhésion du clinker sur la brique. Dès lors, l'adhésion est moindre sur les magnésie-spinelle que sur les dolomies. Il a été toutefois démontré que la texture des briques MA joue un grand rôle et que la nature du spinelle utilisé est déterminante. Il ne faut donc pas classer toutes les briques magnésie-spinelle dans le même panier.

Dans le dernier chapitre (sept), on retrouve la discussion générale, les conclusions et les recommandations concernant des travaux futurs.

Il est clairement démontré que les buts fixés initialement ont été atteints. Cette thèse a permis de mettre au point un test reproductible, fiable, simple et peu coûteux pour mesurer a priori l'adhérence d'un cru donné sur une brique donnée. Ce test a permis de révéler les mécanismes réactionnels mis en jeu, permettant d'expliquer les différentes valeurs obtenues selon la nature et la texture du réfractaire. Les paramètres principaux

ont été étudiés et leurs incidences sur les résultats ont été analysées statistiquement à l'aide de différents plans d'expériences, factoriels partiels et factoriel complet.

Des résultats obtenus en fin de thèse ont permis de réaliser qu'il sera possible d'utiliser des crus sans avoir à les calciner au préalable, et des essais préliminaires ont permis de mettre en lumière l'incidence des sels alcalins. Ceci vient préciser l'orientation des travaux futurs. La principale recommandation de ce travail est de passer maintenant à des essais comparatifs inter-laboratoires, en vue d'homologuer la méthode et de la populariser en tant qu'essai standard. D'autres travaux seraient à envisager pour préciser le rôle des conditions oxydo-réductrices dans la phase gazeuse.

TABLE OF CONTENTS

LIST OF APPENDIXES

LIST OF TABLES

LIST OF FIGURES

CHAPTER 1. INTRODUCTION

Portland cement clinker is manufactured in rotary kilns by heating a finely ground and carefully blended mixture of limestone or chalk and shale or clay to a very high temperature. The essential demands on refractory materials used in rotary kilns are the lining durability and insulation [1], to maximize kiln's reliability and minimize energy consumption. Following the innovations in cement manufacturing technology, a variety of chrome free basic bricks have been developed to cope with large stresses in large-sized rotary kilns. Using waste-derived fuels and reacting to environmental issues have contributed also greatly to magnesia-chrome refractory replacement [2-6]. The two groups of chrome free bricks produced today are doloma based bricks and magnesia based spinel containing bricks. The type of refractory selected for use in rotary kiln is very dependent on the kiln process type and on the different zones within the kiln. The conditions in the burning zone and upper and lower transition zones vary and thus often require different basic refractories.

Bricks used in the upper transition zone are typically exposed to (1) transient coating condition that leads to thermal shocks, (2) increase in exposure to alkali sulfates and alkali chlorides, and (3) mechanical stressing due to shell flexure. Low permeability magnesia spinel and magnesia zirconia bricks are normally used in this area of the kiln, preferably those made with natural magnesite because of their superior coatability. The low permeability is necessary to reduce alkali, sulphur, chloride and clinker melt

infiltration. The frequent coating detachments require refractories with good thermal shock properties, with a reduced modulus of elasticity and low thermal expansion coefficient.

The burning zone refractories are usually protected by coating, however, corrosion by infiltrating clinker liquids will contribute to refractory wear. Under severe conditions of high thermal loading, refractory corrosion by clinker can be accelerated. The most commonly used refractory in this zone is doloma brick and doloma zirconia brick. Because of high refractoriness, good chemical compatibility with normal clinker melt and hence its good adherence strength to maintain stable coating in place, doloma is the best material for the application.

Refractories used in the lower transition zone are subject to a variety of stresses. These include higher thermal loading, thermal shock, corrosion by clinker, corrosion by alkali salts, redox conditions, abrasion by clinker and mechanical stress due to shell flexure. In the lower transition zone, magnesia spinel, magnesia enriched doloma with zirconia and doloma zirconia bricks are most commonly used. Thermal cycling conditions are severe in the lower transition zone because of the unstability of the coating.

In total in the 3 zones, refractories have to withstand (1) high temperature, (2) clinker liquid infiltration, (3) flame impingement, (4) thermal cycling and shock and, (5) REDOX conditions and reactions [7, 8]. Fortunately, it is possible for the clinker to

develop a pseudo-stable coating on the lining in the burning zone. The course of the lining wear depends first of all on this formation of coating. The most stable coating is a protection for the refractory lining. Its formation depends primarily on the temperature as well as the amount and viscosity of the melt in the clinker, but also on the composition and texture of the brick, the temperature gradient in the brickwork, the condition of the kiln and the operating practice. There is less coating formation when the reactivity of the refractory material to the clinker is low. The ability to rapidly develop a stable coating benefits not only to lining life but also reduces heat losses through the shell. Three cases may be considered as [9, 10]:

(1) The coating is stable with a certain thickness, which is normal in the burning zone of cement kiln. In this case, the stress on the refractory lining is at its lowest thanks to the protection of coating.

(2) The coating is unstable, which leads to very high stresses on the lining. Wear of lining takes place discontinuously due to the falling-off of lumps of coating, which are then also likely to take along pieces of the refractories that has been weakened by the stresses in the kiln. This case is typical in the transition zones on the inlet and also on the discharged side.

(3) Little coating forms because of too low temperature. This is typical for the lower transition zone and there is usually continuous wear from abrasion.

In some other cases, it can also happen that no coating forms due to troubles in operation of kilns, and the characteristics of the raw meal and refractories. Wear then occurs through splitting off of small brick pieces and through abrasion of the weakened or, if strongly infiltrated, brick's microstructure deteriorates. Therefore, in order to obtain a maximum life from the burning zone refractories, it is important to operate a cement kiln so that clinker coating forms on the bricks. A shift from a stable to intermittent coating can increase a brick susceptibility to thermal shock, infiltration by alkali sulfates and chlorides and abrasion by clinker.

Coating is a mass of clinker or dust particle that adheres on the hot face of the bricks laid in the kiln, having changed from a liquid or semi-liquid to a solidified state. The chemical composition and phase assemblage of coating closely resemble those of the clinker. Solidified clinker particles first adhere to the refractory surface and continue to build as long as the surface temperature of the coating is below the solidifying temperature of the particles. Coating formation will cease when the surface reaches this solidifying temperature.

In general, doloma based bricks have better coating attraction than magnesia based bricks do. Coating formation on doloma refractories occurs by a different mechanism than magnesia-spinel bricks. Doloma brick offers a large quantity of CaO-contacts with cement clinker that contains about 20-40% of dicalcium silicate. The primary reaction

mechanism appears to be that belite (C_2S) reacts with lime to form alite (C_3S). The reaction of lime from doloma with clinker increases the viscosity of the melts thereby stabilizing the coating on the brick surface. The penetration depth of clinker melts in doloma brick thus is limited. The main reaction is accelerated by the formation of liquids created by the Fe_2O_3 and Al_2O_3 fluxing agents. These liquids may not participate in the reaction but may simply increase the mobility of the dicalcium silicate. In such a case, the belite's mobility allows it to penetrate and react with the CaO in doloma brick to form C_3S rich zone at the brick-clinker interface and leads to a reliable and strong bonding between clinker and doloma brick. This protective clinker coating on doloma consisting mainly of alite and belite decreases the thermal and chemical load on the doloma refractory lining and thermal losses through the shell [10].

Clinker coating can also develop on magnesia bricks but the characteristics of the contact area are different, compared to doloma brick [11]. Magnesia is the only phase that can withstand the thermo-chemical attack of liquid clinker phases. The CaO-rich clinker also leads to a destabilization of brick phases and the formation of low melting components like brownmillerite (C_4AF), mayenite ($C_{12}A_7$) and dicalciumferrite (C_2F) [9]. The liquid phases of cement clinker can attack the secondary phases in magnesia based brick. Due to the low CaO-content of magnesia based bricks, only a thin layer of C_2S-contact phases is formed, depending on the brick type. The development of a C_2S layer between the brick and cement clinker in the presence of coating can be assumed to be well known. The conversion into γ-C_2S seems to be favored by the magnesia spinel

bricks so that shutdown with cooling to below 600°C seems not to allow the permanent adhesion of the coating, although in many cases a certain content of Al_2O_3 is found to promote coating [12]. A pronounced γ-C_2S formed when reactions take place between cement components and spinel grains, against which only β-C_2S develops with mixtures of cement and sintered magnesia [13]. Normally, coating adhesion on magnesia spinel refractories is much less than that on doloma brick. However, it is possible to improve coatability of this type of refractory, for instance, by carefully designing its texture.

It is commonly known that the performance of bricks in the burning zone and transition zones of the rotary cement kiln is significantly affected by the coating formation and its ability to adhere on the bricks' lining. Coating adherence is a key parameter to increase the kiln's output. Coating stability is needed to minimize the thermal load (direct exposure to an 1800°C-flame temperature), the corrosion and the thermal shock on the brick's lining. Coating has to be adhering well to resist kiln's fluctuating conditions, which would cause the coating to drop and subsequently to expose and shock the free surface of the bricks to extremely high temperatures and to aggressive corrosive environment.

Most of the knowledge about coating was obtained by inspection of lining after kiln's shutdown. Observation of coating in kilns may not reflect its actual situation during operating the kilns. The common aspiration of cement manufacturers and refractory workers is to evaluate coatability of different basic bricks, particularly for a newly

developed product. Approaches to test coatability of various basic bricks are still been looked in laboratory [14]. However, the inability to correlate laboratory data obtained with field behavior has frustrated many researchers. More efforts are needed to develop and standardize a coating-evaluating test.

The general objective of this work has then been to develop a protocol to test adherence of cement clinker on basic refractory bricks for evaluating their coatability. The results should reflect the observation of coating in real service conditions of cement rotary kilns. The following goals should be reached in this work:

(1) To determine the major factors affecting adherence strength in order to clarify the importance of the testing conditions, such as compressive load, heating temperature, and raw meal characteristics.

(2) To assess the reliability of the sandwich protocol in terms of ruggedness, repeatability and reproducibility, and adherence evaluation of various basic bricks in line with the accepted bricks' coating performance in rotary kilns, in the field.

(3) To tackle adherence mechanisms of various basic bricks exposed to different raw meal and to correlate the brick textures with their adherence ability, using the appropriate microstructural analysis.

Statistical design of experiments was employed for the evaluation of the tests; this has been a valuable tool for exploring the phenomena with detailed comprehension. Three fractional factorial plans and one full factorial plan were executed to efficiently generate good data and test the ruggedness of the method. Statistical process analysis was also used to confirm repeatability and reproducibility of the sandwich protocol, and to assess the precision of the measurement system used.

In total, over 12 brands of various basic bricks and five batches of raw meal from different cement plants were used to test their mutual adherence. More than 600 sandwich bars were tested to develop the sandwich protocol. About 30 samples were analyzed by reflecting microscopy, some with help of cathodoluminescence technique and scanning electronic microscopy.

This thesis is divided into seven chapters.

In Chapter 2, the literature review covers clinker burning in rotary cement kilns, coating in high temperature zones, influential factors on coatability and existing methods to evaluate coatability. The evolution of cement clinker phases from raw meal is based on complex reactions in rotary cement kilns. The liquid phases generate during chemical transformation of raw meal at high temperature and dominate the formation of clinker coating. The role and characteristics of coating are introduced with influential factors on coating formation and maintenance. In order to understand coating behavior on the

rotary kiln lining, many adherence testing methods have been developed to attempt judgement of coatability. The disadvantages and limitations of those existing methods lead to approaches for a new protocol, which is to be introduced and finally evaluated in the following chapters.

In Chapter 3, the descriptive evolution of the sandwich test leads to the use of a compressive load and using three-point bending flexural testing mode. The detailed protocol is provided; sandwiches were prepared either from paste or a dry mix of calcinated raw meal, heated at 1550°C for 30 min and under a load of 5.3 kPa. Once the cooled samples were tested in three-point bending flexural mode to obtain modulus of rupture representing the adherence strength of clinker on basic bricks. Raw meal investigations in terms of chemical and phase compositions, particle size distribution, and changes of minerals and microstructural characteristics after heating are reported. The chemical and physical properties of various basic bricks tested are defined.

The sensitivity to influential factors is dealt with in Chapter 4. In order to determine which factors influence values of adherence strength, three statistical designs of experiment according to 2^{4-1} two-level fractional factorial plan has been conducted. The influence of load, firing temperature, raw meal and holding time, as well as their interaction effect is determined by the variance of analysis in the first experiment. The second and third experiments evaluated the influences of particle size, silica ratio and

alumina ratio of raw meal, as well as heating rate, on magnesia spinel brick and on doloma brick, respectively.

The reliability of the sandwich protocol is evaluated in Chapter 5, including results on a statistically done ruggedness test, and repeatability and reproducibility study. A full 2^3 factorial design was selected for a ruggedness test to quantify the influence of the thickness of the paste, the mixing method to prepare the paste and the holding time at maximum heating temperature. A repeatability and reproducibility study was designed to address the issue of precision of adherence strength measurement. An analysis of variance (ANOVA) was made on experimental results with different operators and repeated measurements (trials). Repeatability can be assessed by taking into account differences among trials, and reproducibility, by taking into account differences among operators.

Chapter 6 documents the microstructural analyses on 4 brands of doloma based and two kinds of magnesia spinel bricks, which were exposed to different clinkers. Some correlations of brick textures with adherence strength have been established. Different adherence mechanisms are illustrated for magnesia spinel brick and doloma brick, by their microstructures.

Finally, the interpretation of the experimental results, summary and conclusions are presented in Chapter 7. In order to promote this sandwich protocol to become a standard

method to measure adherence strength, some considerations and suggestions are offered. All the initial goals and objectives have been met. It is believed that the information made available in this thesis will be directly useful to cement manufacturers to select refractories for the lining of their rotary kilns and to refractory producers to assist in the design their products.

CHAPTER 2. REVIEW ON COATABILITY AND EVALUATION METHODS

2.1 Clinker Burning in Rotary Cement Kilns

The formation of clinker coating is dominated by liquid phase generated during chemical transformation of raw meal at high temperature; important characteristics are the liquid amount, viscosity and surface tension with wettability onto solids. The interactions between the bricks and clinker are to be taken into account, as well as evolution of the mineral transformations occurring in the raw meal, as it progresses in the kiln. In order to better understand coating characteristics, the manufacture of Portland clinker will now be reviewed.

The raw mix for making Portland cement clinker is generally obtained by blending a calcareous material, normally limestone, with a smaller amount of an argillaceous one, typically clay or shale. It may be necessary to include minor proportions of one or more corrective constituents, such as iron ore, bauxite or sand, to the bulk composition. On the other hand, some argillaceous limestone and marls have compositions near to that required, making it possible to use a blend of closely similar strata from the same quarry.

Portland cement clinker mainly consists of CaO, SiO_2, Al_2O_3 and Fe_2O_3, all accounting for more than 95 per cent. The minor components, in total less than 3 per cent, are MgO, TiO_2, P_2O_5 and alkalis. In clinker, they are not present in individual oxide, but exist as

compounds formed by two or more oxides. The mineral phases are very fine, usually 30-60 μm and consist mainly of alite, belite, calcium aluminate and aluminoferrite. Alite (C_3S) is the most important constituent, 50-70% in normal Portland cement clinkers. It is tricalcium silicate (Ca_3SiO_5) modified in composition and crystal structure by ionic substitutions. Belite (C_2S) constitutes 15-30% of normal Portland cement clinkers. It is dicalcium silicate (Ca_2SiO_4) modified by ionic substitutions and normally presents wholly and largely as the β-polymorph. Calcium aluminate constitutes 5-10% of most normal Portland cement clinkers. It is tricalcium aluminate ($Ca_3Al_2O_6$), substantially modified in composition and sometimes also in structure by ionic substitutions. Calcium ferrite makes up 5-15% of normal Portland cement clinkers. It is a tetracalcium aluminoferrite (Ca_2AlFeO_5), substantially modified in composition by variation in Al/Fe ratio and ionic substitution [15].

To form those mineral constituents enough lime has to be available in the raw meal, but when the limit of the maximum lime content is exceeded, free lime must unavoidably remains in clinker. Lime Saturation Factor (*LSF*) is an important parameter, having usually a value in between 0.85-0.95, to avoid free lime formation [16].

$$LSF = \frac{CaO}{2.8SiO_2 + 1.18Al_2O_3 + 0.65Fe_2O_3}$$

where CaO, SiO_2, Al_2O_3 and Fe_2O_3 are the respective weight percentages in raw meal.

There are two other ratios to evaluate the composition of clinker [17]. The silica ratio is the ratio of the percentage by weight of silica to that of the sum of the alumina and ferric oxide, usually of the order of ~2.5. A high value of silica ratio means that more solid phases (C_2S and C_3S) and less liquid (C_3A and C_4AF) will be formed in clinker during heating. In this case, the raw meal is said to be more difficult to clinkerize. On the other hand, with low silica ratio, more liquid will form at the sacrifice of the strength-giving phases. As distinct from the silica ratio, the values of the alumina ratio, i.e., the values of the ratio of alumina to ferric oxide, cover, in practice, a much wider range, between 0.8 and 1.7. It influences the viscosity of the liquid formed in the clinker.

Modern cement plants always utilize rotary kilns, into which the raw meal is fed whether in dry powder or slurry form. Figure 2.1 is a schematic flow diagram of rotary cement kiln [18]. The kiln itself is a steel cylinder, sloping at 3-4% from the horizontal and turning from about one to three revolutions per minute. The material enters at the upper end and then slides and rolls down in a counter flow to the hot gases produced by a flame at the lower end. In a system employing a precalciner, the kiln is typically 50-100 meters long and its ratio of length to diameter is 10-15. It is the heart of the cement-making process. The maximum material temperature, of 1450-1500°C, is reached near the lower end of the kiln in the burning zone, in which the material spends 10-15 minutes. The kiln is lined with refractory bricks, of different types along its length, in accordance with the material temperatures. In the burning zone, bricks become coated

with a layer of clinker, which plays an essential part in the insulation of the kiln and in the bricks' life.

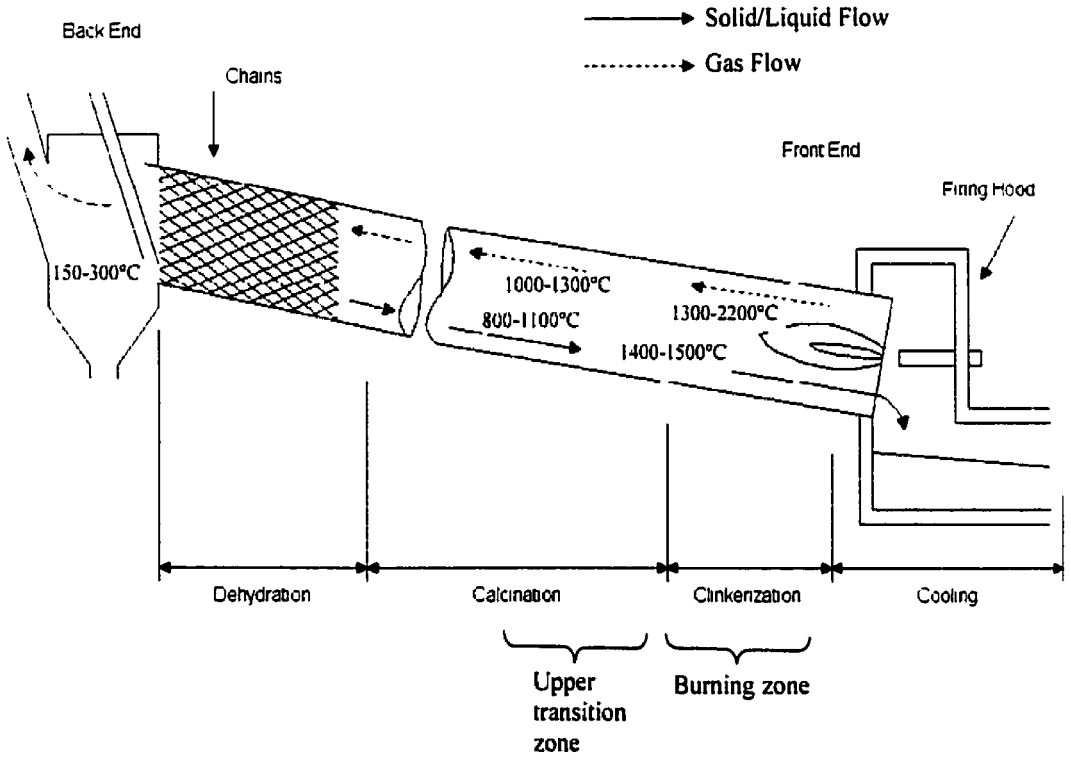

Figure 2.1 Schematic flow diagram of rotary cement kiln [18]

Reactions taking place in rotary kiln system are illustrated in Figure 2.2 [19]. On the left-hand is the feedstock comprising, in this case, calcite ($CaCO_3$), quartz (SiO_2), clay minerals (SiO_2-Al_2O_3-H_2O) and iron oxide (Fe_2O_3). Up to a temperature of about 700°C, activation through the removal of water and crystal structure changes take place. Within the temperature range 700-900°C, decarbonation of the calcium carbonate occurs, together with the initial combination of the alumina, ferric oxide and of activated silica

with lime. From 900 to 1200°C, belite forms. Above 1250°C and more particularly above 1300°C, the liquid phase appears and this promotes the reaction between belite and free lime to form alite. During the cooling stage on the right-hand side of the diagram, the molten phase goes to a glass or, if cooling is slow, the C_3A crystallizes out and in extreme cases the alite dissolves back into the liquid phase and reappears as secondary belite. Alkali sulfates condense out as a separate phase during the cooling process but these are not shown in Figure 2.2.

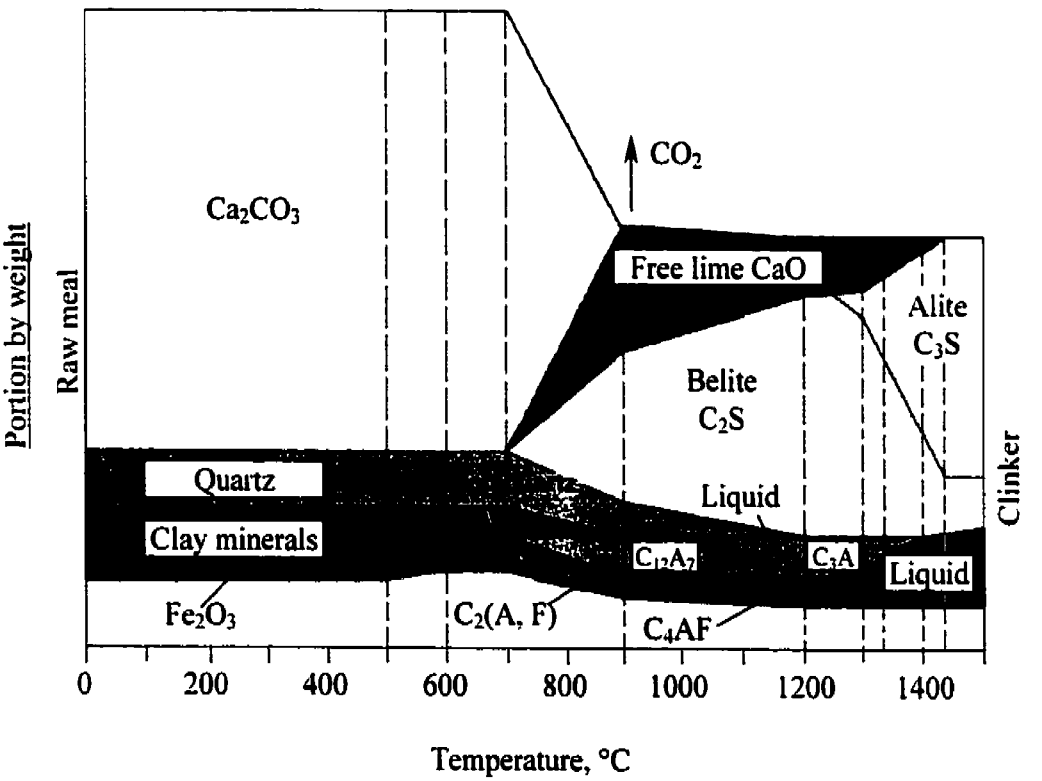

Figure 2.2 Reactions taking place during raw meal burning to clinker [19]

In modern systems of cement manufacture, the retention time of the material in the kiln is 30 to 40 minutes, of which the major part is in the burning zone. The temperature of the material increases rapidly from 850°C to 1250°C to 1300°C, at which temperature clinker melt is formed. In the burning zone, the chemical and physical changes of the material take place simultaneously; it is important with respect to the kinetics of clinkerizing reactions and agglomeration processes. The exact temperature of melt formation depends on the chemical composition of the feed.

Under certain conditions, melt may be formed at temperatures lower than ~1250°C. For instance, quartz grains in the kiln feed will give rise to melt at 1200°C or lower. The surrounding CaO will partly agglomerate and form crystals of belite, which can be identified in the clinker as belite nests. Also, the alkalis, sulfates, and chlorides present in the kiln system will form liquid phases at lower temperatures than the proper clinker liquid. However, the largest amount of clinker melt is formed within a narrow temperature interval and over a short distance in the rotary kiln. The coating formed on the brick lining reflects this. In the upper transition zone or the entrance to the burning zone, the soft, relatively thin coating changes to a dark, clinkerlike, hard, thick coating within half a meter [20].

The amount of the melt can be calculated according to the formula derived by Lea and Parker [16], or using Dahls [21] formulas. From these formulas, the amount of clinker melt can be calculated from the chemical composition of the mixture in the burning zone

and its temperature. Figure 2.3 shows the amount of melt as a function of temperature for different clinker systems [22]. As can be seen, the amount of melt is a discontinuous function of the temperature. There is a eutectic temperature, T_E, for each system below which no liquid is formed. At T_E, almost all of the melt of a given temperature is formed, and above T_E the increase in the amount of melt with the temperature rise is very small. In the four-component system, $CaO\text{-}SiO_2\text{-}Al_2O_3\text{-}Fe_2O_3$, the eutectic temperature is 1338°C. In the system $CaO\text{-}SiO_2\text{-}Al_2O_3$, it is 1460°C.

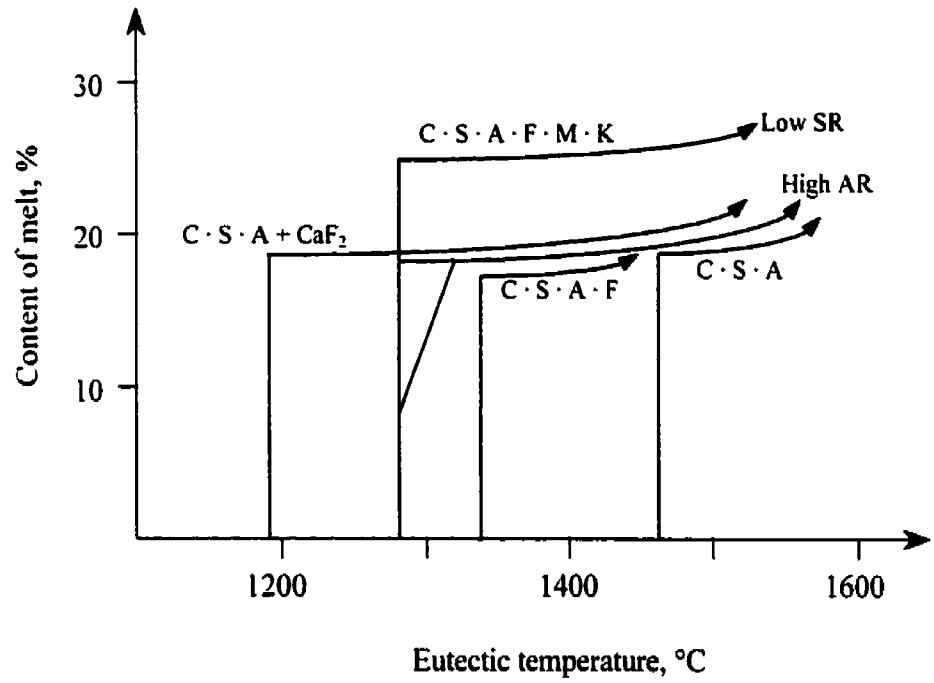

Figure 2.3 Diagram showing variation of melt content,
vs. temperature for selected clinker systems [22]

The level of the near-horizontal part of the curves depends on the chemical composition represented by lime saturated factor and silica ratio. The T_E depends on the alumina ratio; and the highest amount of melt at T_E occurs for the alumina ratio of 1.4. Values of the alumina ratio larger and smaller than that give less melt at T_E. The approximately horizontal parts of the curves extend to about 1550°C. Up to this temperature, the amount of melt increases 3% per 100°C increase in temperature. Above this temperature, the slopes of curves are steeper and at, approximately 1800°C, the typical Portland cement clinker will be completely melted.

The formulas for calculating the amount of melt at given temperatures are derived assuming equilibrium and that solid solutions in the C_3S and C_2S phases present are negligible. The Lea and Parker formula for calculating the amount of melt at 1400°C in the system $CaO\text{-}SiO_2\text{-}Al_2O_3\text{-}Fe_2O_3$ is:

$$\text{Percent liquid} = 2.95(\text{percent } Al_2O_3) + 2.2\ (\text{percent } Fe_2O_3)$$

By not taking solid solution into consideration, all the alumina and iron oxide would have to be available for the melt and this is not so [23]. Correcting for this, and assuming that alite and belite may contain 1% Al_2O_3 and 1% Fe_2O_3 in solid solution, the formula overestimates the amount of melt by about 5% absolute. This is in accordance with observations made when the amount of melt is estimated using the amount of interstitial phase determined microscopically on quenched, synthesized clinker [24].

The effect of adding minor components to the system $CaO\text{-}SiO_2\text{-}Al_2O_3\text{-}Fe_2O_3$ is, in general, to lower the T_E and increase the amount of liquid. One of the important minor components is MgO, which decreases the eutectic temperature of the system $CaO\text{-}SiO_2\text{-}Al_2O_3\text{-}Fe_2O_3$ to near 1300°C. In the system $CaO\text{-}SiO_2\text{-}Al_2O_3$, which is the model system for white cement clinker, the T_E correspondingly decreases from 1460° to 1400°C. Raw mixes for white cement are difficult to burn. The presence of 1 to 2% MgO in such raw mixes, compared to raw mixes without MgO, improves the burnability substantially.

Other important minor components are the alkalis, K_2O and Na_2O. Their presence in the melt further decreases the T_E by approximately 20°C. The simultaneous presence of sulfates and alkalis may complicate the situation [25-26]. The sulfates form immiscible melts with the clinker melt. The sulfates and chlorides also contribute to the internal circulation of volatiles between the kiln part and the preheater part of the kiln system. The alkali sulfates and alkali chlorides form melts at temperatures well below T_E, corresponding to the colder parts of the kiln system, where agglomeration will have a negative influence on the kiln operation. For these reasons, the content and amount of circulating volatiles are to be strictly controlled.

Shortly after arriving at the burning zone, the materials consist of solid particles and a liquid phase. During rotation of the kiln, the tumbling material starts to agglomerate and to form nodules. The physics involved is identical to that which takes place when water is added to a powdery material and it is nodulized in a drum or pan pelletizer. Good

strong nodules are formed when 90 to 95% of the voids between the densely packed particles are filled with liquid. The particle size also has an effect. Too small amount of liquid results in a few nodules in dust, too much in a pastelike mass. For the material nodulizing in the kiln. the amount of necessary liquid is between 15 and 25% by weight.

2.2 Coating in the Burning Zone

Those mixtures of solid and liquid adhere to the lining in the burning zone, reacting with components of the bricks and forming coating crust. Figure 2.4 represents the possible intermediate layers between cement clinker and the bricks, which changes from a semi-liquid to a solid depending upon its thickness and the cycling of the temperature profile in such a crust and the adjacent bricks [14].

The bricks, in the burning zone, should help to build a coating rapidly upon start-up, reacting with the burden but in a manner not extremely corrosive to itself. It should maintain the coating throughout changing conditions within the kiln as well as during subsequent start-ups and shutdowns. Furthermore, if the coating is lost for any given reason, the brick should be able to withstand the operating conditions in the kiln and quickly build new coating.

Schematically, the different steps in the formation and the drop-off of the coating are: 1) Chemisorption on the refractory surface of calcined meal, containing a certain

percentage of liquid phase, the amount dictated by the thermal and chemical conditions prevailing in that zone; 2) Infiltration of liquid clinker components and then dust and gaseous species; 3) Penetration and reaction within the bricks; 4) Solidification of infiltrates as a function of the prevailing thermal gradient; 5) Mechanical anchoring and growth of coating; 6) Building-up of internal stresses, in part due to the increased weight of coating; and 7) Eventually dropping or stripping of coating owing to erosion. impact. stresses, C_3S disintegration, and role of alkalis [9].

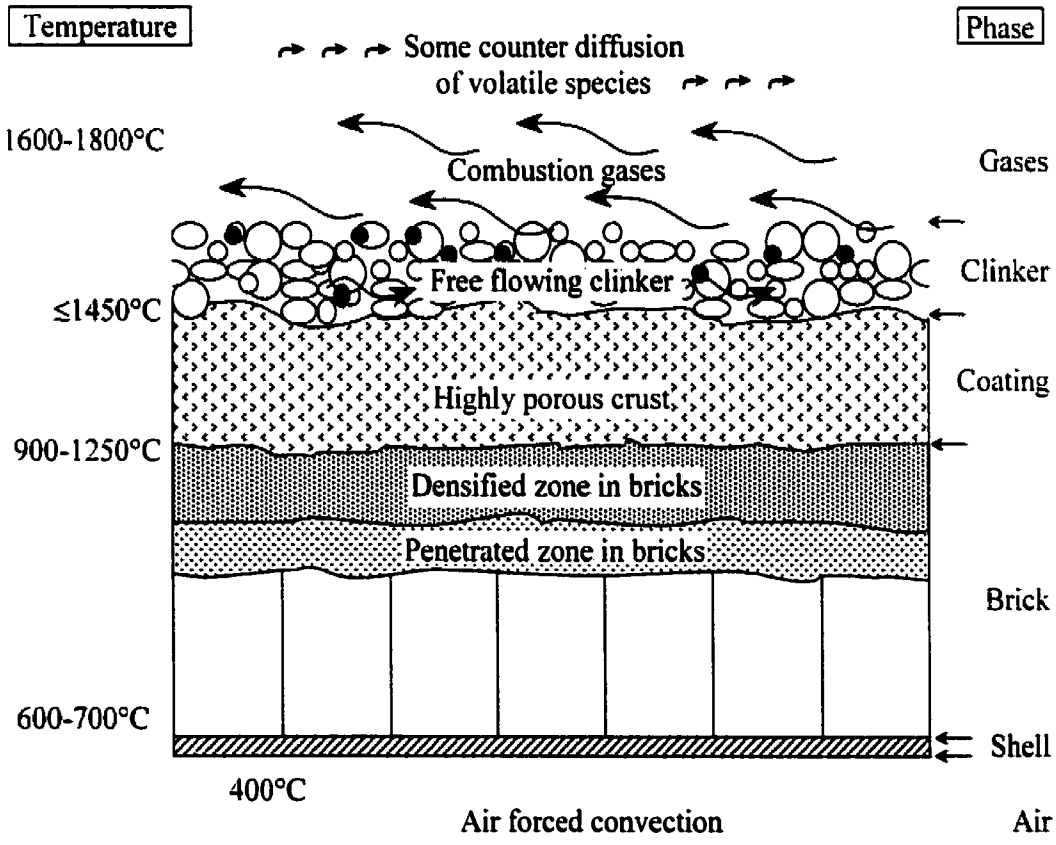

Figure 2.4 Schematic representation of coating and its surrounding in rotary cement kiln [14]

The cement coating in the burning zone shows a very uneven surface with a typical maximum thickness of 500 mm, after the rotary kiln is shut down [27]. It is observed that the coating is strongly bonded to the bricks and difficult to remove in some area but in other areas the coating is not bonded and thus is quite easy to remove. The reason for these phenomena is not clear, but the areas of little or no bonding could happen as follows [28]:

(1) The temperature of the interface between the coating and the bricks is lowered by formation and growth of the coating. The bonding between the bricks and coating is broken by their different thermal expansion rate.

(2) Considering the $CaO\text{-}SiO_2$ phase diagram, the main components of cement, $3CaO\cdot SiO_2$, is metastable at low temperature. When it is exposed to a temperature less than 1250°C, $3CaO\cdot SiO_2$ decomposes into CaO and $2CaO\cdot SiO_2$. This breaks down the structure of the coating and destroys the bonding between the coating and bricks.

(3) The original bond strength between the coating and bricks is rather weak. Therefore, it is easily broken.

Depending on the thickness and the porosity's characteristics of the formed crust, the temperature of the hot face of the bricks, when in the floor position, can be lowered from

1450°C to only 1235°C, just with ~25 cm thick coating [14].

A typical coating in the burning zone could be composed volumetrically of 35% alite (C_3S), 15% belite (C_2S), 10% ferrites (C_4AF), 5% aluminates (C_3A), 35% porosity, and on a mass percentage 50% alite, 20% belite and 30% liquid (ferrites + aluminates). Of course, presence of minor phases including sulfur, alkalis and free lime is important. The apparent density of the crust could be of the order of 2.0 g/cm^3 in order to decrease thermal conductivity and place less burden on the kiln drive system, yet it should have sufficient strength to withstand the mechanical stresses created during the rotation of the vessel.

Therefore, coating is a protective crust adhering to the brick lining of rotary kiln, which isolates the lining from thermal impact, chemical corrosion and abrasive wear. Coating plays an important role in maximizing refractory life of the burning zone and in reducing heat losses. It is painfully evident to those associated with cement plant operation that rarely an ideal coating is maintained in the burning zone for extended periods of time. When this does occur, life of brick lining is generally excellent and production of clinker is maximized. The questions are: why do some operations more readily build and maintain coating than others? And why do some bricks tend to work more effectively than others? It is long known that many parameters have a direct or an indirect effect on the coating texture, thickness and stability. To control perfectly the situation, one has to consider all possible reactions occurring at the 7 interfaces and the volumetric transfer in

the 6 major phases, shown in Figure 2.4. Two extra interfaces have to be considered within the brick, realizing that in any used brick, one may distinguish between a penetrated densified zone, a more deeply penetrated and discolored zone and an unaltered zone.

2.3 Influential Factors on Coatability

Based on a bibliographical search and a literature review covering the theme of coating and adherence of coating in rotary cement kiln, the following factors have been identified, as shown in Figure 2.5.

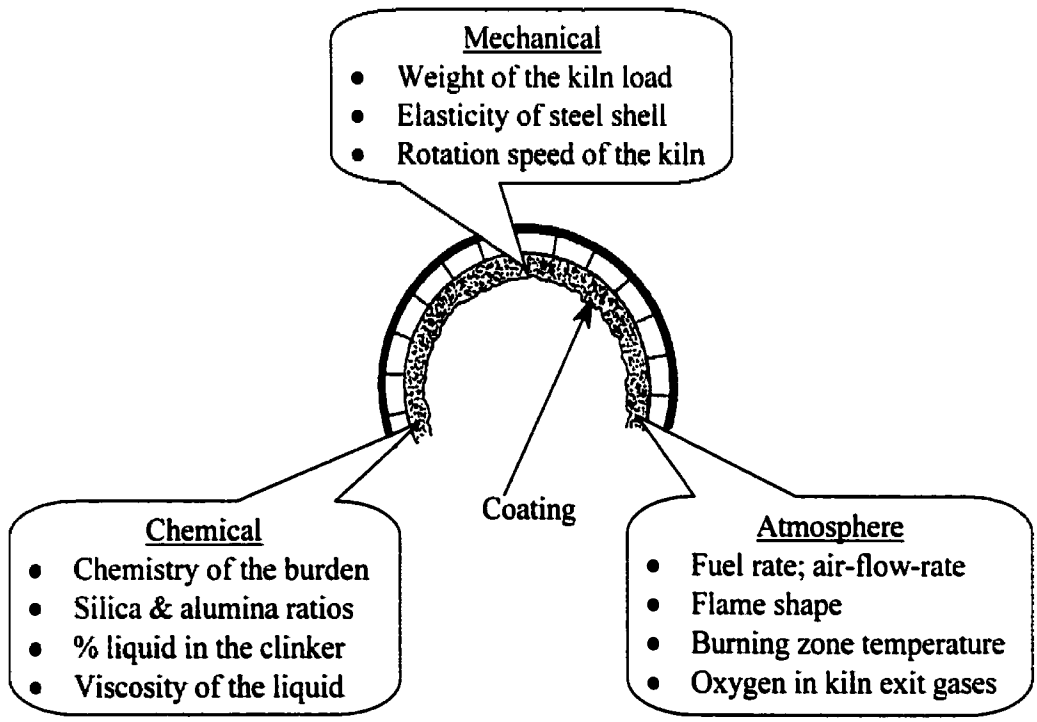

Figure 2.5 Main parameters to influence coating's formation

2.3.1 Microstructural Factor [11, 27, 29-38]

The role of refractory microstructure has been examined by many researchers, dealing with the role of porosity and permeability. It has been shown that differences in the porosity of refractory bricks manifest itself in different coating adhesion levels, but since the control of porosity in a brick is so much dependent upon the refractory manufacturing technology (grain size distribution, compaction and pressing, firing), no detailed analysis is yet available in the open literature. Of course, one may argue that it would be futile to produce, for a given class of refractories, the same quality brick with different porosity, since all commercially available bricks have been "optimized" already. The reality, it seems, is that this has not been tested, not only in terms of porosity but also more importantly in terms of pore-size distribution and permeability. Yet the role of liquid in the clinker phase, such as the percentage, its viscosity vs. temperature and its chemical nature, on the penetration mechanism into the brick should be influenced by the porosity and the connectivity of the pores. On the other hand, many researchers believe that the chemical nature of the dissolution mechanism is more important.

2.3.2 Refractory's Nature [39-51]

The role of the different aggregates or the refractory's nature is well documented. Doloma bricks in general appear to pick up coating very readily. Doloma bricks with up

to about 50% replacement of doloma by magnesia have almost as high an adhesion susceptibility (enough CaO). Within the category of magnesia-chrome bricks, there are some notable differences, which in several cases have been attributed precisely to the porosity of the various grades of bricks concerned. The lowest adhered area was found on bricks manufactured on the basis of synthetic sintered magnesia.

2.3.3 The Thermal Factors [52-59]

There are many thermal influences to take into consideration, like sudden changes in temperature, temperature variation of up to 200°C, due to the rotation of the kiln with a million times turns a year or so, which should cause thermal fatigue – a subject not treated as such in the literature. Of course, those thermal factors are related to the parameters controlling combustion: fuel types, fuel rate, thermal load (feed-rate), flame shape, incomplete combustion of fuels, but also brick characteristics, thermal shock resistance and thermal conductivity controlling more or less the thermal gradients, the later being influenced also by the cooling of the shell – wind factor, episodical rains, etc. Figure 2.4 provides a composite picture of the situation, from which the most important point is directly related with the solidus and interval of solidification of the melt present at the hot face, of either the coating's layer (with variable thickness) or the brick itself.

2.3.4 The Chemical Factors

The chemical influences are dictated by the presence of a liquid phase in the clinker, the kiln atmospheres, and the combustion and volatilization products. The first parameters to be considered are the raw meal composition indexes, such as silica ratio, alumina ratio, alkali/sulfur ratio, percentage of liquid in the clinker, burnability index. From the references [8-11, 27-29, 31-36, 47-48, 55, 58], the essential points are that:

- The ability to form coating depends on silica ratio of clinker. The lower the values of silica ratio, the higher the tendency to coating's formation is.

- Even when using coating friendly doloma products, coating will not form if the silica ratio is too high.

- After a certain period, even refractories made from high-grade synthetic magnesia become "contaminated" and eventually take on coating. This finding reinforces the point that the texture of the refractories should play a role on coating's stability.

- If one really wants coating to adhere rapidly after installation of new refractories, it is always possible to add iron oxide to the raw mix to lower the alumina ratio.

- Good coating adhesion can be achieved on most basic bricks with a liquid phase content in the clinker of the order of 30%.

- The strongest coating adhesion is attained if "normal" cement raw mixes are applied to doloma brick, but the testing of raw cement mixes with regard to their coating behavior belongs to the burning behavior or burnability index set of problems.

- In conclusion, keeping all the process parameters constant, it may well be possible to develop a suitable method to select refractory lining for a given optimized raw mix composition. As B. Scheubel [55] has shown, the raw material properties and the temperature profile are the two main factors influencing not only the refractory lining but also the clinker's quality.

2.3.5 The Mechanical Factors [36, 48, 52, 60-64]

These factors are related to the design of the kiln itself and the consequences are deformation of kiln shell, ovality, axial distortion; mechanical and thermomechanical stresses like abrasion by the bed of the clinker, and other stresses due to differences between shell and tire temperatures and due to inadequate clearance between shell spacer pads and bores of the tires, etc., all influencing the stresses on the refractory lining and then the coatability. It has to be noted here that coatings can form which do not always adhere to the kiln but are rather like a sleeve within it [65]. This latter observation, although not common, leads to interesting consequences on the role of refractories. To us, this "sleeve effect" means that any refractory could be used. This is

in intriguing thought, which does not fit with the accepted paradigm today, concerning the coatability on refractories. It is a thought that will be kept in mind, even if it contradicts some observations made on the chemical factors.

2.3.6 The Operating Parameters

The thermal, chemical and mechanical factors are affected in many ways, such as the rotation speed, the feed rate, the back-end temperature, zoning in kiln lining, inexpert lining construction, inopportune interruptions of the kiln due to a wide range of maintenance problems. All of those parameters then affect the coatability. In summary, the references [34, 35, 37, 43, 45, 47, 48, 50, 55, 62, 66] reveal why it will also be frustrating to compare laboratory tests to in-plant trials (how to simulate and how to keep the process parameters constant?).

2.3.7 The Kiln Atmosphere

Due to their inherent importance in coatability, the role of the volatized phases in the kiln has been differentiated from the chemical factors. All experts in the field agree with the importance of alkalis [40, 42, 67]. Some results and explanations are indeed valuable but do not provide a clear link between coatability and refractory behavior. Based upon post-mortem analysis of the bricks in the upper transition zone, the role of sulphate also has to be taken into account. A few thermodynamic studies have been done to establish

volatility and predominance diagrams of multicomponent systems [40, 42] and to illustrate the role of Po_2.

2.4 Existing Methods to Evaluate Coatability

At first the knowledge about coating just came from observations inside the kiln after shut down, but they are not real situations of coating during operation, for instance, in the case of coating drop-offs when the feed and heating stop, with the kiln still turning for clearance. Attempts to evaluate coatability in laboratories started with the advent of rotary cement kilns, being in need of new refractory products to withstand higher temperatures. Many testing methods have been developed, including static contact and clinker-renewed dynamic methods [14, 27-28, 68-69].

2.4.1 The Static Methods

Figure 2.6 is schematic representation of the static methods. They can be differentiated into 7 sub-classes. Their basic principle intends to make raw meal contact refractories and to develop clinker adherence by heating. All of those methods provide a crude qualitative evaluation of coating. Heating in most cases is done in electric furnaces, and it is then possible to monitor the influence of atmospheres, but the role of alkalis, sulfates and other volatile species cannot be tested without contamination and damages of the furnace refractories.

(1) DIN 51069 Method [8, 35]

The industrial standard, DIN 51069 (1959) was established in Germany, in which two procedures are included. One uses a cylindrical-shaped brick sample (Φ36 × 36 mm) that is buried in cement raw meal (60 g) and heated in an electric furnace for 30 minutes. The other uses crucibles made of refractory bricks. Holes are bored in the sample bricks with the dimensions Φ41 × 35 mm, Φ25 × 25 mm, Φ5 × 5 mm and filled with 70 g, 20 g, and 1 g of cement raw meal, respectively. The crucible samples are heated in an electric furnace with or without a cover for 3 hours, up to 45 hours.

(2) Tablets Method [35]

Cement raw meal is compacted into small tablets (5 g) and 6 tablets are put on the sample brick (45 × 45 × 45 mm). Samples with raw meal tablets are heated in an electric furnace for 3 hours or more. Hot brick is taken out from the furnace and cooled in their vertical position.

(3) Contact Method [30-33, 35, 51, 69]

Cylinder-shaped brick samples (Φ50 × 80 mm) are prepared and cement raw meal is compacted into a cylinder with the same diameter of sample. The cylinder of cement raw

meal is put on the brick sample and they are heated in an electric furnace for 3 hours or more with or without a cover.

(4) Sandwich Method [27, 35, 36]

Cement raw meal (6 g) is inserted between two pieces of brick (25 × 25 × 150 mm), and the assembly is heated in an electric furnace. Then, the adherence strength is measured by the three point bending test. In the case of measuring the adherence strength by a shear test, the sample is a plate shape (75 × 75 mm, thickness unspecified) and 40 g of cement raw meal is used. In the case of tensile strength, the sample is a cylinder (Φ20 × 150 mm) and 4 g of cement raw meal is used.

(5) Button Adherence Method [28, 32, 33]

Brick samples are buried in granular MgO to produce a temperature gradient. The chamber is quickly heated up to the test temperature by gas burner. Cylindrical cement raw meal buttons usually do not adhere to the brick sample on the first heating. After several times, coating started on the brick sample after putting on a new button and repeating the heating. In the static methods, only this one exerts thermal gradient while all other tests are isothermally run.

6) Weighing Balance Method [28]

This method is designed to measure the coating adherence using a weighing balance. Cement raw meal of 5 mm thick is put on a brick sample (55 × 55 × 15 mm) and heated in an electric furnace. After cooling, the adhering raw meal is divided into 10-30 pieces due to the shrinkage of the raw meal during heating. Then adherence strength of each piece is measured by a weighing balance and a hooked rod prying off the sticks.

In summary, the results of those adherence tests are commonly reported as the adherence ratio that is calculated by the area of adhering coating divided by the whole clinker contact area of the samples, or a few by the adherence strength.

The main advantage of these methods is their simplicity. They are designed to compare the behavior of different clinkers between themselves. Results are not conducive to good correlation with coatability in rotary cement kiln.

The sandwich methods have been designed to allow for a measurement of adherence. It has been a great surprise to find out that no effort of standardization had been made among the different researchers. At this point it is believed that the furnace atmosphere (Po_2), the temperature and the time all have an effect. No plan of experiments has yet been reported to ascertain the importance of such variables. Of course, the composition of the clinker, its burnability index, its C_4AF and C_3A content, are also very important to

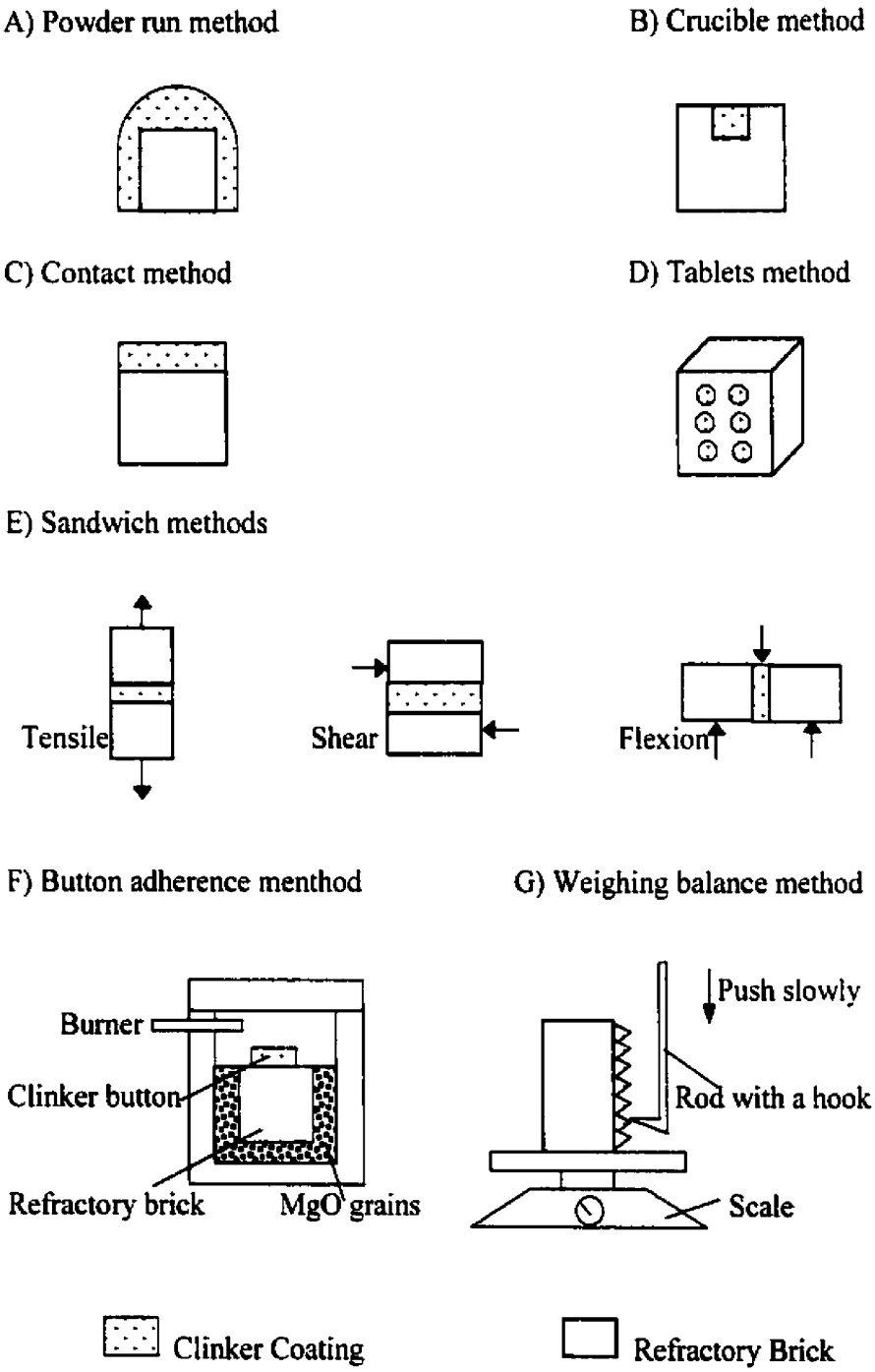

Figure 2.6 Schematic representations of the static methods

appreciate the results. If these tests are to reveal something about the nature of the refractories used, they are only expected to tell something of the very beginning of the coating process. There is no renewal of the clinker, no thermal gradient, and sample sizes are very limited.

2.4.2 The Dynamic Methods

Three different methods have been identified: the short rotary kiln, the pilot-plant kiln and the Holderbank test. Of the 3 methods, the short-rotary kiln is the most economical to run. These methods are designed to simulate a little bit better than the real conditions in a given kiln, but the limitations are still existing: temperature fluctuations, radial and longitudinal temperature gradients, feed-rate, load conditions, lack of control on coating growth, no easy evaluation of coating adherence. For the short rotary kiln, again the effect of the variables such as rotary speed, angle of inclination, feed rate of clinker and duration of test are not documented. Different values are used by each experimentator. It is then difficult to compare data from one to another.

(1) The Short Rotary Kiln Method [8, 30, 32, 70]

The short rotary kiln, as shown in Figure 2.7, is used to measure the coating adherence on the test bricks. Six brick samples in a hexagonal configuration are installed as the lining. The furnace, rotating at 1-5 rpm, is heated by gas burner to the temperature of

1400-1630°C, for a duration up to 24 hours. The temperature of the hot face is measured by an optical infrared radiation pyrometer. Calcinated raw meal is fed to the amount of 2-5 kg for each test.

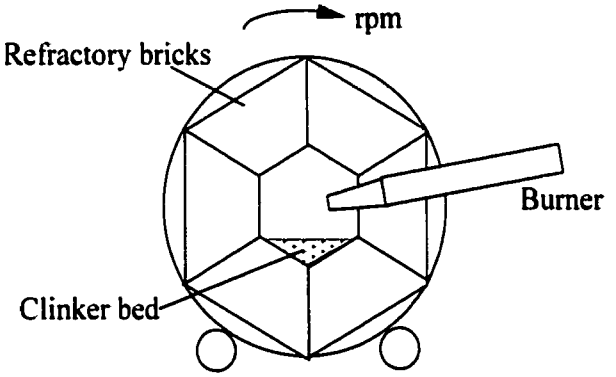

Figure 2.7 Schematic diagram of the short rotary kiln

(2) Pilot-Plant Rotary Kiln [35]

As shown in Figure 2.8, the kiln's lining is made of brick rings, with diameter of 1250 mm and 2500 mm in length. Raw meal of 900 kg is continually fed and testing duration can last up to 10 days. The kiln is heated by a gas burner.

(3) Holderbank Coating Test [11, 29, 35]

The method used by Holderbank involves setting brick samples (about 600 cm^2) on the floor of a gas-fired furnace, as represented in Figure 2.9. Raw meal of 3-5 kg is put on the brick samples, and at intervals added and pressed. Different temperatures can be reached and for a duration up to 40 hours. The backside of the samples is cooled by air to create a temperature gradient. The sample dimensions are not clear but a standard size would be assumed. Then, coating adherence is judged based on the ratio of the coated area.

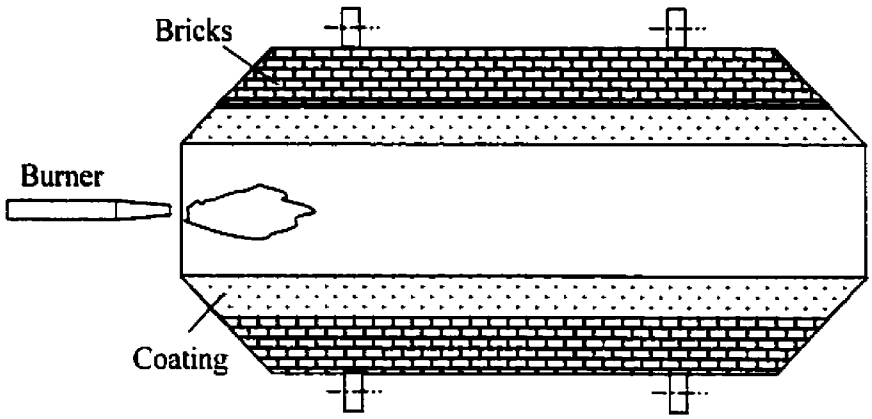

Figure 2.8 Schematic diagram of the pilot-plant rotary kiln

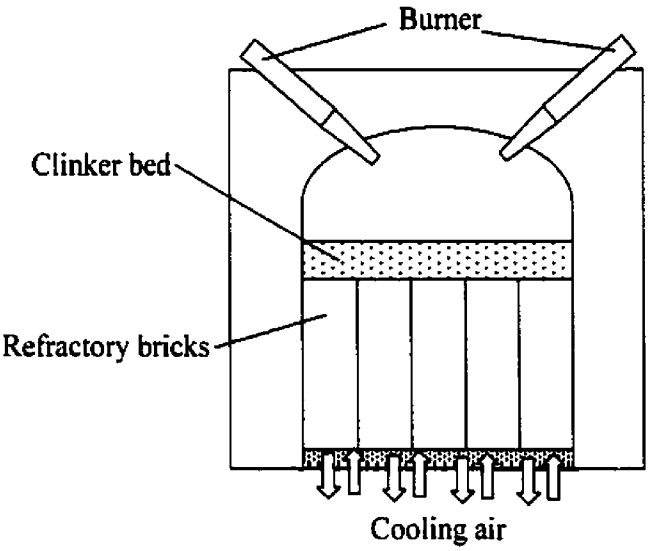

Figure 2.9 Schematic diagram of Holderbank method

CHAPTER 3. NEW PROTOCOL – THE SANDWICH TEST

Based on the review in Chapter 2, it can be concluded that a method does not yet exist to make reproducible and precise measurements of adherence, and no standardized laboratory test has yet been accepted to measure coatability. The Holderbank method, which seems to be the preferred one, is used only by Holderbank central laboratory, about 3 times a year, because of its high inherent cost. To overcome those limitations has been the raison d'être of the present thesis.

The list of parameters known to influence coating formation shown in Figure 2.5 is not exhaustive. It is clearly a great challenge to properly simulate all of the kiln conditions and to hope to correlate in-plant adherence values to laboratory measured values. Therefore, experimental strategy will be limited to the design of a new testing method to determine the influences of the refractory composition and texture, as well as raw meal composition, based on a sandwich test approach.

This chapter will deal with properties of raw meal and refractories used in all the experiments, determination of test configurations, magnitude of the compressive load, heating rate at temperature, and mechanical testing modes, in order to define a protocol worthwhile to go through a further standardization procedure.

3.1 Raw Meal

3.1.1 Chemical and Phase Compositions

All the cement raw meals were supplied by Lafarge Corporation. Five batches of raw meal were used from St. Constant, Brookfield and Exshaw plants. Results of chemical analysis by X-ray fluorescence (XRF) are shown in Table 3.1. It can be seen that the main oxides, CaO and SiO_2, are almost the same with a little fluctuation for the other components.

Table 3.1 Chemical compositions (wt-%) of the raw meals used

Chemical Composition	St. Constant Cement Plant	Brookfield Cement Plant	Exshaw Cement Plant
SiO_2	21.40	21.10	21.20
Al_2O_3	4.57	5.69	4.35
Fe_2O_3	2.79	2.03	2.93
MgO	2.70	1.56	4.34
CaO	64.40	64.20	64.30
Na_2O	0.66	0.18	0.26
K_2O	0.82	1.38	0.64
TiO_2	0.20	0.28	0.18
P_2O_5	0.25	0.05	0.05

The identification of various phases in the raw meal was obtained by X-ray diffraction and carried out using a Siemens powder diffractometer, model D5000 operating with Co $K\alpha$ (40 kV, 30mA) radiation and a graphite monochromator. The angular range was 3 to 100 degrees with 0.01-degree increments and 1.0 second counting time for each step. Figure 3.1 shows the XRD patterns for the raw meal powders. The semi-quantitative phase compositions of the raw meal are listed in Table 3.2.

Calcite and quartz are the major minerals, but raw meal from Exshaw contains much more dolomite than the other two raw meals. Brookfield's raw meal contains almost no dolomite but more mica. It is known that the reactivity of the carbonates decreases in the order: calcite → dolomite → ankerite.

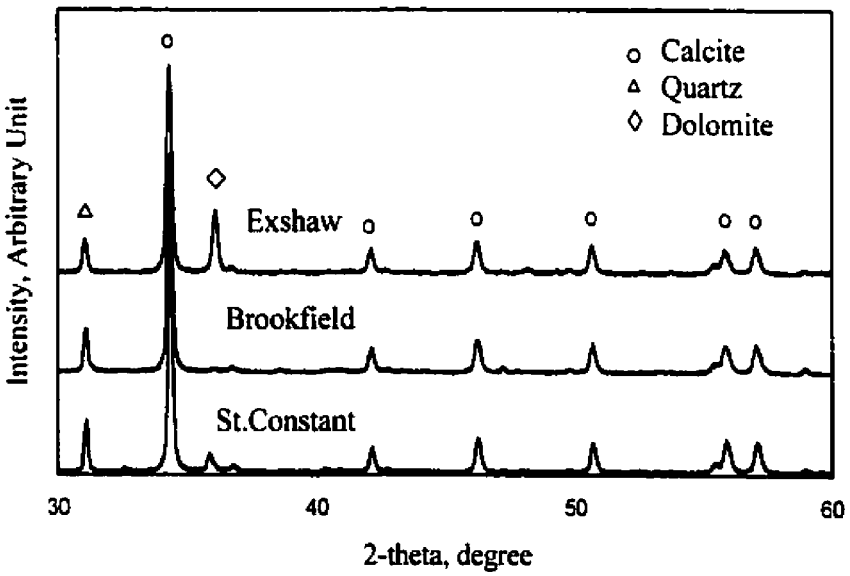

Figure 3.1 XRD patterns of the as-received raw meal

Table 3.2 The semi-quantitative mineral compositions of the raw meal (XRD)

Mineral	Brookfield	Exshaw	St-Constant
Calcite $CaCO_3$	72	53	68
Quartz SiO_2	19	15	19
Dolomite $CaMg(CO_3)_2$	1.2	30	9
Feldspar $NaAlSi_3O_8$	0.4	0.4	1.1
Mica $(K, Na)(Al, Mg, Fe)_2(Si_{3.1}Al_{10..9})O_{10}(OH)_2$	6.5	1.4	1
Chlorite $(Mg, Fe)_6(Si, Al)_4O_{10}(OH)_8$	1.3	0.4	1.2

3.1.2 Particle Size Distribution

The particle sizes of the raw meal were determined using an LS 200 Particle Size Analyzer from COULTER Corporation. The particle size distribution is shown in Figure 3.2 and numerical results are listed in Table 3.3. Obviously, raw meal from St. Constant is coarser than the other two. Specific surface area for St. Constant raw meal is 13.984 cm^2/ml, Brookfield's 20.545 cm^2/ml and Exshaw's 18.053 cm^2/ml. Brookfield raw meal has larger portions of fine powder, although the mean size value lies in the middle of the three tested raw meals.

Raw meal fineness doubtlessly has an influence on clinkerization. A more finely ground raw meal will yield a mixture that reacts quicker while showing a reduced tendency to form cluster-like concentrations of clinker minerals [71]. In general, coarse silica particles have a more detrimental influence on the ease of clinker combination and on the strength potential of the cement than does a similar quantity of coarse limestone particles [72].

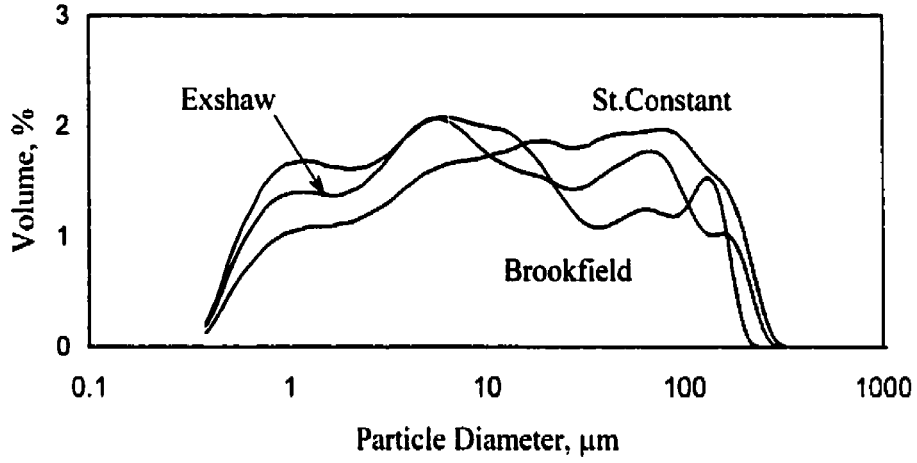

Figure 3.2 Particle size distribution of the as-received raw meal

Table 3.3 The percentages of the particle size distribution in raw meal

Cement Plant	10% ≤, μm	25% ≤, μm	50% ≤, μm	75% ≤, μm	90% ≤, μm	Mean μm
St. Constant	1.39	4.29	17.08	59.67	124.0	41.9
Exshaw	0.96	2.23	7.74	28.51	94.1	27.2
Brookfield	1.06	2.84	9.62	42.8	97.9	32.4

3.1.3 Differential Thermal Analysis and Thermogravimetric Analysis

Simultaneous differential thermal analysis/thermogravimetric analysis (DTA/TGA) studies were conducted using the thermobalance, Model Setsys DSC141, from Setraram, on ~55 mg of the as-obtained raw meal powders, under normal atmospheric conditions and over the temperature range from room temperature to 1400°C. Alumina crucibles and a magnesia reference were used, and the system was calibrated against the melting point of gold (1063°C). The heating rate was 5°C/min and the cooling rate 30°C/min. The temperatures of the DTA events were determined using the usual method, based on the intersection of the DTA baseline with the extension of the linear region of the peak rising slope. The temperature uncertainty was estimated to be less than 5°C.

The curves for differential thermal analyses on the three raw meal powders are shown in Figure 3.3. The exothermic peaks between 400°C and 600°C correspond with dehydroxylation of clay minerals before 500°C and transformation of β-quartz → α-quartz at ~573°C [72]. The endothermic peaks around 800°C reflect decomposition of carbonates during the early stages of cement clinkerization, the endothermic reaction $CaCO_3 \rightarrow CaO + CO_2$ accounting for much of the energy consumption in cement kilns. After decomposition, raw meal becomes stable in weight, as shown in Figure 3.4. The peaks at 1330°C in Figure 3.3 are indicative of liquid phase formation with appearance of alite crystals.

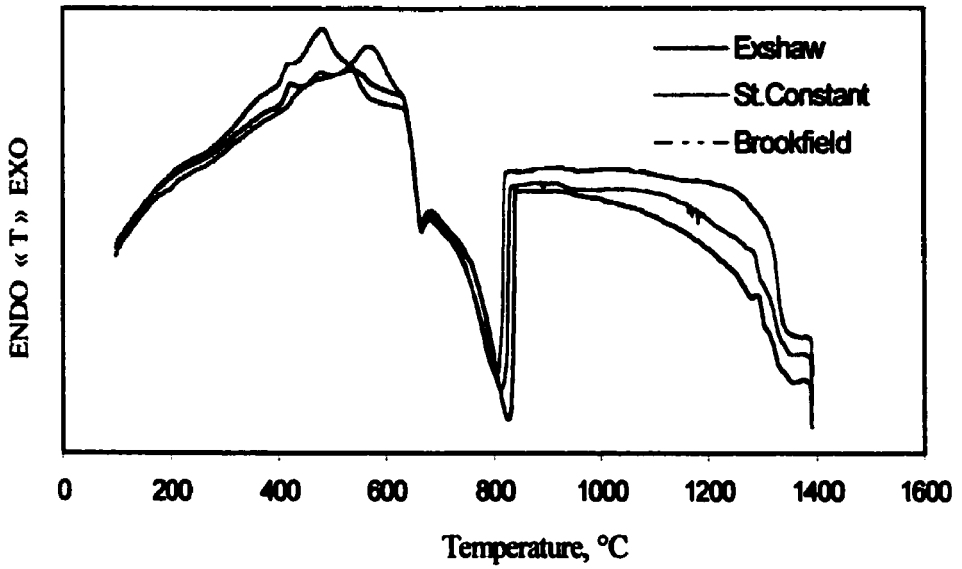

Figure 3.3 DTA curves of the as-received raw meals, at heating rate of 5°C/min

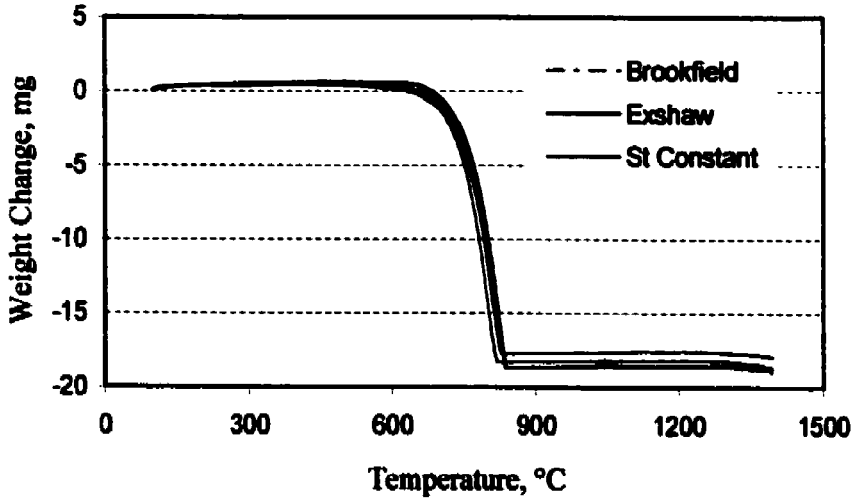

Figure 3.4 Thermo-gravimetric change of the raw meals, at heating rate of 5°C/min

3.1.4 Physical Changes after Heating

Raw meal samples were pressed into 20 × 40 × 60 mm compacts under pressure of 18 MPa. The compacts were fired at 1350°C, 1450°C and 1550°C for 30 min in an electrically heated furnace. The porosity of the fired compacts was measured using kerosene to avoid hydration, results being shown in Table 3.4. After firing at 1350°C and 1450°C, the compacts for Exshaw are the most porous, of the 3 raw meals, while at 1550°C, St. Constant clinker remains the most porous, of the 3. The compacts for Brookfield are easiest to densify at any temperature.

Table 3.4 Porosity and bulk density for fired compacts of raw meal

Raw Meal	Firing Temperature, °C	Apparent Porosity, %	Liquid Absorption, %	Bulk Density g/cm^3
St. Constant	1350	53	28	1.47
	1450	49	23	1.65
	1550	46	21	1.73
Exshaw	1350	58	39	1.13
	1450	53	27	1.54
	1550	44	19	1.81
Brookfield	1350	39	20	1.51
	1450	36	14	1.98
	1550	18	6	2.50

3.1.5 Mineralogical Evaluation after Heating

X-ray diffraction analyses were made on the samples treated at various temperatures. Semi-quantitatively, St. Constant raw meal, calcinated at 1000°C, for 4 hours, consists mainly of 58% lime (CaO) and 24% belite (C_2S = Ca_2SiO_4), quartz (SiO_2), hematite (Fe_2O_3), merwinite [$Ca_3Mg(SiO_4)_2$], and spurrite [$Ca_5(SiO_4)_2CO_3$] are in amount of 2-5%, respectively. Free lime is the dominant phase, and thus the reactivity of raw meal can be significantly increased by calcination. Figures 3.5-3.7 show XRD patterns of the fired samples. Semi-quantitative analyses of phase composition are listed for the samples fired at high temperatures in Table 3.5.

Table 3.5 Phase compositions of raw meals after firing at 1350, 1450 and 1550°C

Raw Meal	Firing Temperature, °C	C_3S	C_2S	C_3A	C_4AF	CaO
St. Constant	1350	35.4	26.3	11.5	7.5	11.9
	1450	46.0	22.0	11.2	8.9	6.2
	1550	59.4	14.9	11.3	8.8	1.3
Exshaw	1350	43.2	27.6	10.7	8.9	6.2
	1450	45.4	22.6	11.3	8.8	5.3
	1550	58.6	15.9	11.7	7.3	1.2
Brookfield	1350	39.3	27.5	23.1	5.2	1.5
	1450	41.0	28.4	20.2	5.2	1.0
	1550	55.1	10.8	23.5	5.4	1.1

It is known that at sufficiently high temperature belite (C_2S) does react with CaO to form alite (C_3S) if enough liquid phase is present [19]. The amount of alite (C_3S) increases with reducing belite (C_2S), until free lime is depleted. The liquid phases C_3A and C_4AF form at temperature of 1350°C, and their amounts do not change appreciably with increase of temperatures. Table 3.5 clearly shows that Brookfield clinker contains about 30% liquid phases, whereas St. Constant's and Exshaw's only have some 20% liquid with more C_3S and C_2S minerals. This is why the compacts for Brookfield clinker shrank much more than the other two, resulting densities being shown in Table 3.4. Free lime still exists at 1350°C in greater proportion for St. Constant's and Exshaw's than for Brookfield clinker.

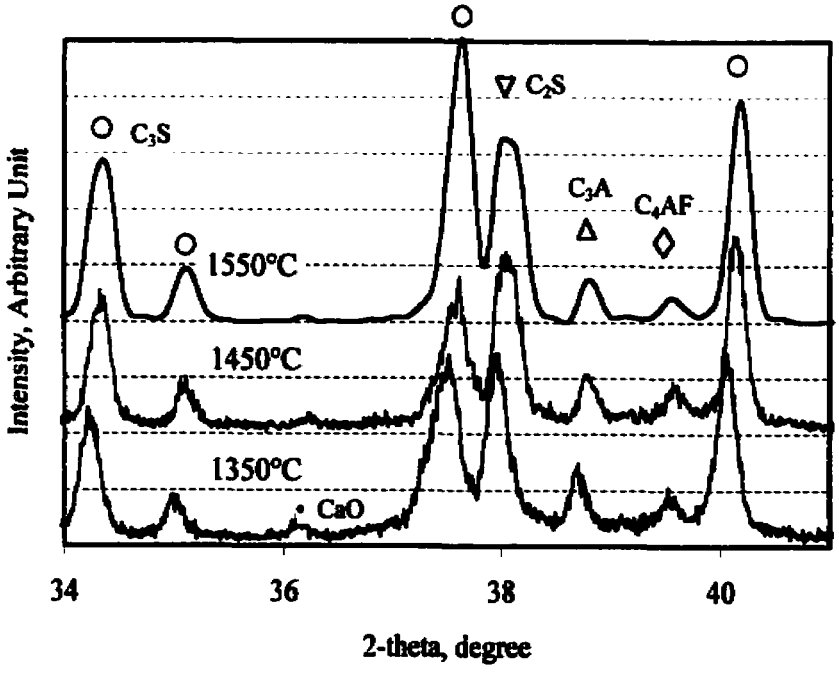

Figure 3.5 XRD patterns of St. Constant clinker

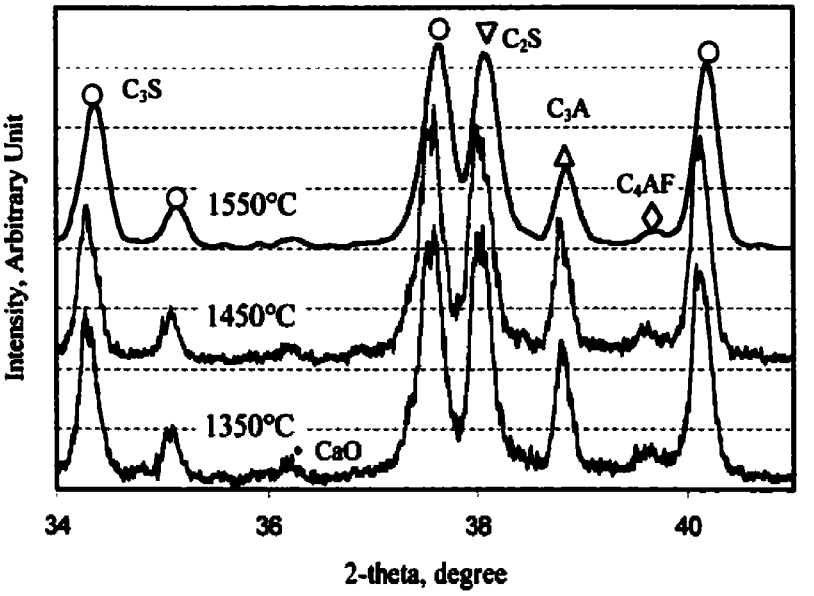

Figure 3.6 XRD patterns of Brookfield clinker

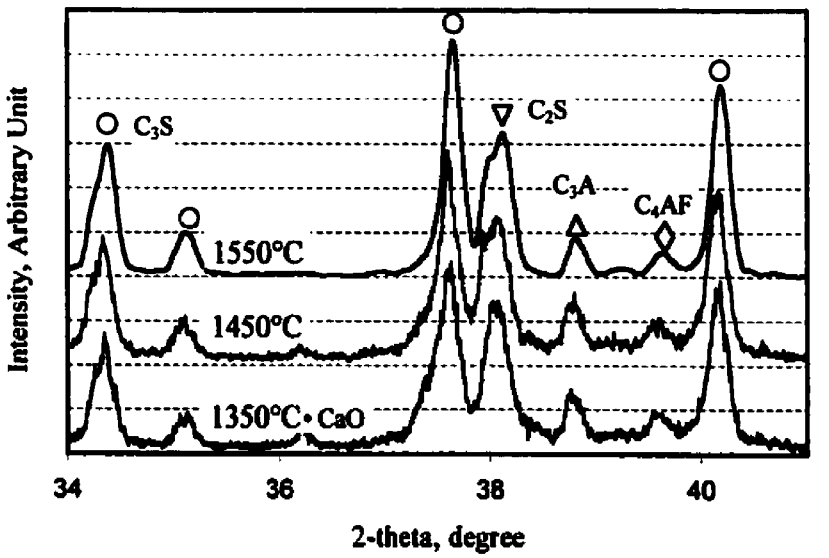

Figure 3.7 XRD patterns of Exshaw clinker

Further analysis was made by an optical microscope. A careful polishing process and the proper etching and staining techniques were adopted because of easy hydration and hard identification of cement phases. Samples were mounted in a polishing ring with epoxy resin. A vacuum was then drawn for thirty minutes to allow the epoxy to penetrate the open porosity. After hardening, the samples were fixed in an automatic polisher and taken down through succeedingly finer laps of 60, 120, 240, 320, 400 and 600 grit. Final polishing on the 6 micron, 3 micron and 1 micron diamond paste was accomplished, using Buehler lap oil as a lubricant, rather than water, to prevent hydration of the samples. Between each polishing, the samples were thoroughly cleaned by an ultrasonic cleaner in alcohol. The as-polished sample was examined just for porosity, as shown in Figure 3.8. The appropriate etchants (see Appendix 1) had to be used, in order to reveal the phases in contrast shown in other figures hereafter.

Figures 3.9-3.11 show the microstructures of the raw meal at 1350°C. The first impression is that the solid and liquid phases are distributed in Brookfield clinker more evenly than it is in the others. The interstitial phases - ferrite and aluminate are formed, resulting in formation of alite. The alite starts to crystallize into various sizes. The belite crystal growth is also observed. The reactivity of raw meal is affected by the dissociation of carbonates; calcite has a higher reactivity than dolomite or ankerite [72]. Cluster structures of free lime were found to be very big in Exshaw clinker, small in St. Constant clinker and few in Brookfield clinker. This is because of the larger amounts of dolomite or ankerite in raw meal of St. Constant and Exshaw, listed in Table 3.2.

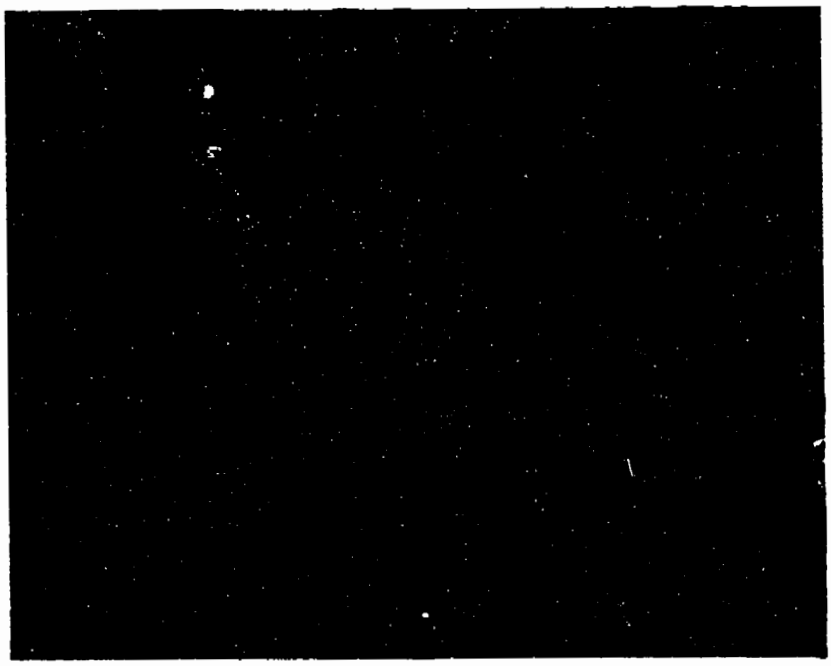

Figure 3.8 Brookfield clinker fired at 1350°C, prior to etching ×200

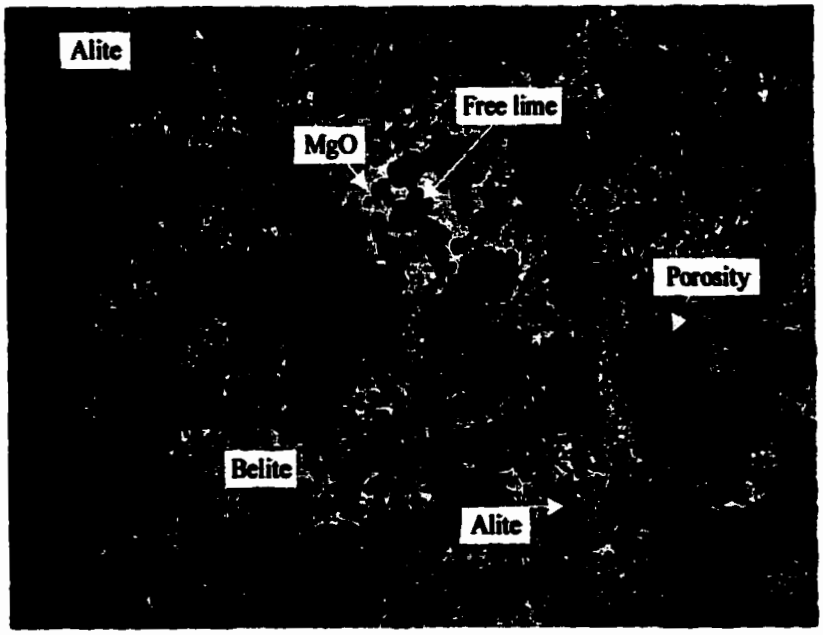

Figure 3.9 Brookfield clinker fired at 1350°C, once etched ×100

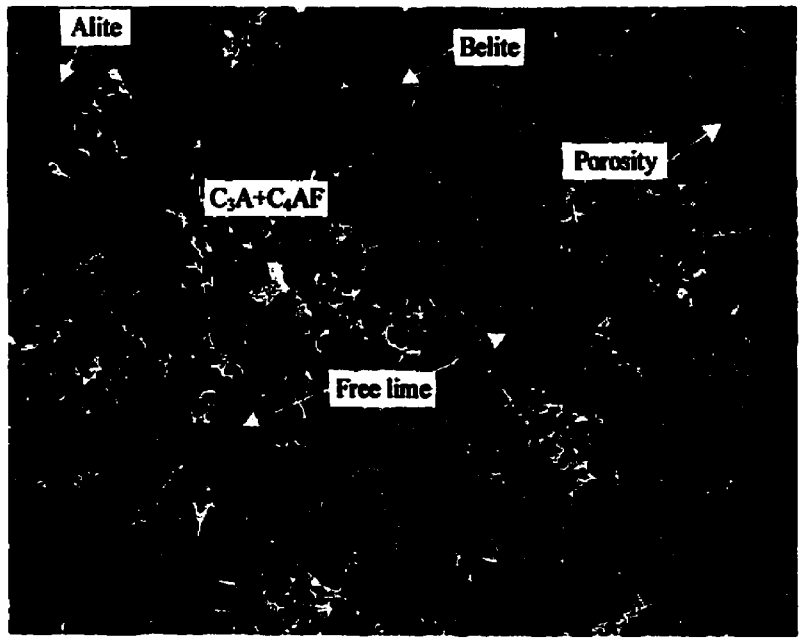

Figure 3.10 St. Constant clinker fired at 1350°C, once etched ×100

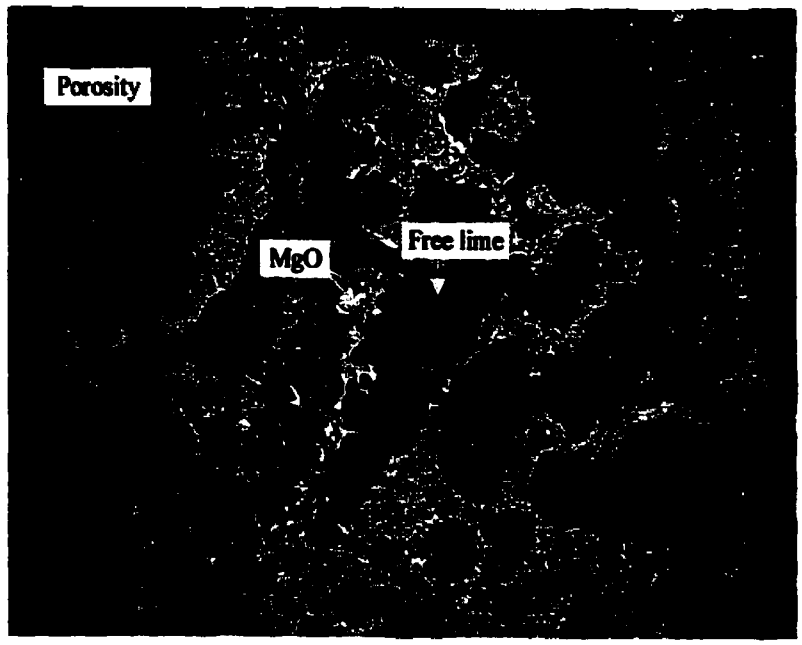

Figure 3.11 Exshaw clinker fired at 1350°C, once etched ×100

As shown in Figures 3.12-3.14 for the clinkers fired at 1450°C after etching, bigger alite and belite crystals are appreciably observed in all clinker microstructures, where the alite appears straw to brown colored and the belite is blue colored. The transformation from belite to alite is obvious, particularly for Brookfield clinker which shows more alite without finding free lime at all. Free lime still exists in St. Constant and Exshaw clinkers, showing a cluster with some hydration of black area in Figures 3.13 and 3.14. Magnesia is found to be adjoined with free lime, as a result of the residual dolomite's dissociation. The aluminate C_3A appears between alite (and/or belite) crystals. Porosity in St. Constant and Exshaw clinkers is much bigger than that evenly distributed in Brookfield clinker.

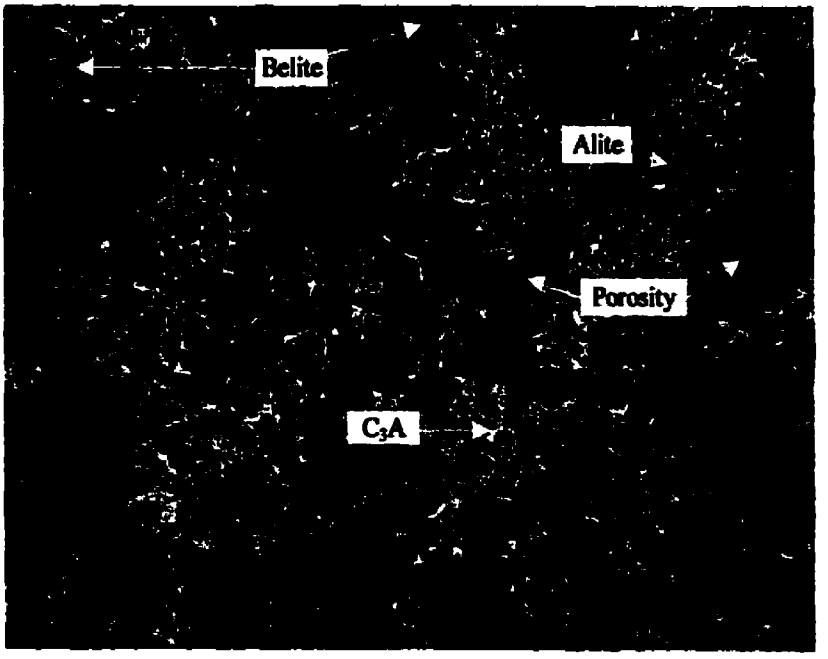

Figure 3.12 Brookfield clinker fired at 1450°C, once etched ×100

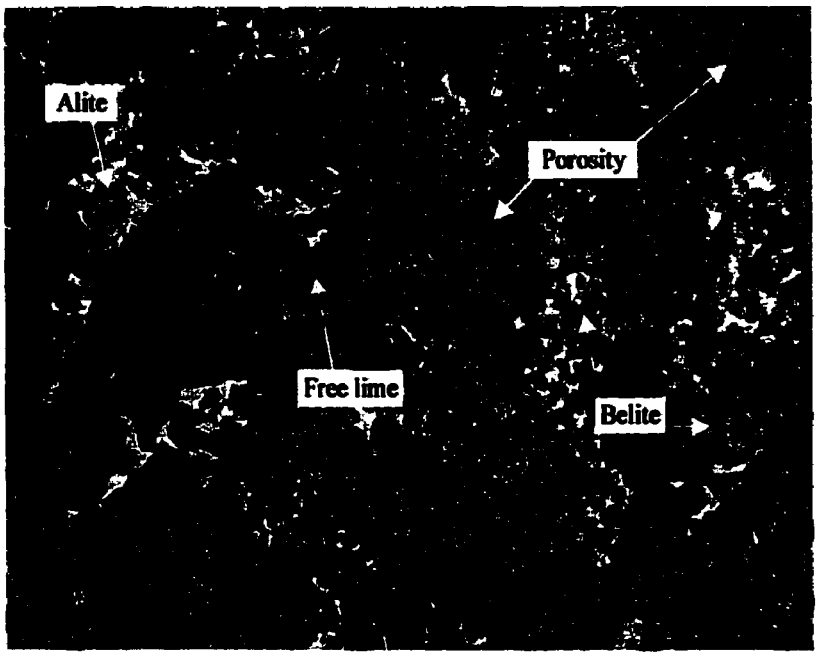

Figure 3.13 St. Constant clinker fired at 1450°C, once etched ×100

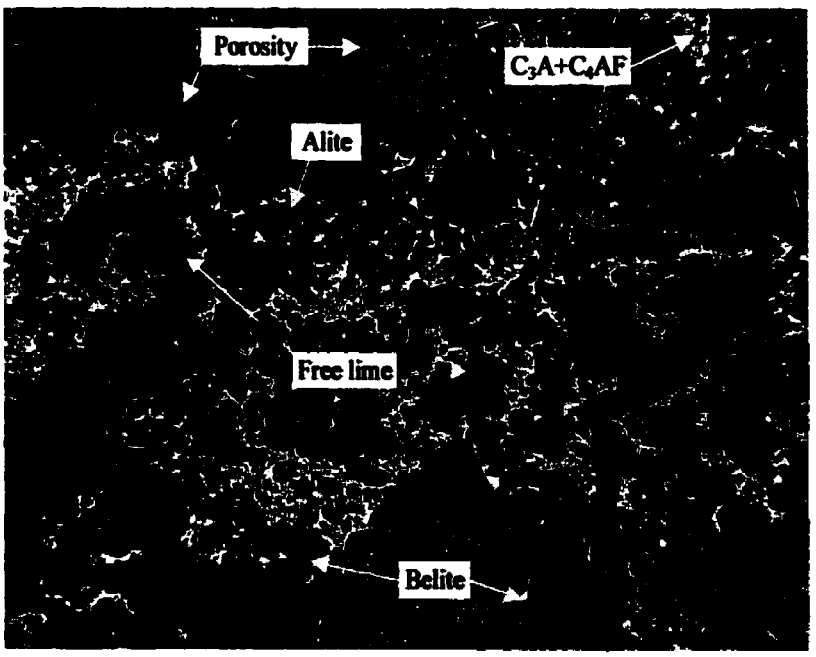

Figure 3.14 Exshaw clinker fired 1450°C, once etched ×100

The microstructures of the clinkers fired at 1550°C are shown in Figures 3.15-3.17. It is noted that no big differences are observed in the three clinkers at 1550°C, with the exception of less and smaller porosity in Brookfield clinker. The alite in all samples examined is the dominant crystalline phase. It is generally formed into continuous networks of large well-defined crystals. Occasionally, alite crystals with belite cores or fringe are found, which may be the result of incomplete conversion. The belite crystals tend to be smaller, rounded crystals organized in clusters, unevenly distributed throughout the samples. It is obvious that the aluminate appears as a gray interstitial phase and the ferrites as a light gray to white one. The latter is primarily a ferrite solid solution in which C_4AF is a member. Little free lime was found in all clinkers, which proves that it is better to conduct the sandwich test at 1550°C than at 1450°C in laboratory, although 1450°C is the prevailing temperature in most of rotary kilns.

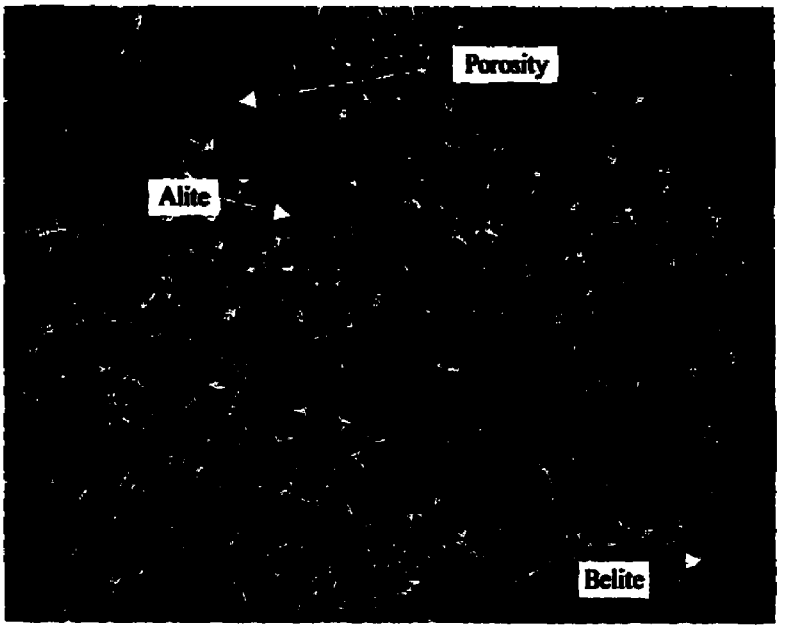

Figure 3.15 Brookfield clinker fired at 1550°C, once etched ×100

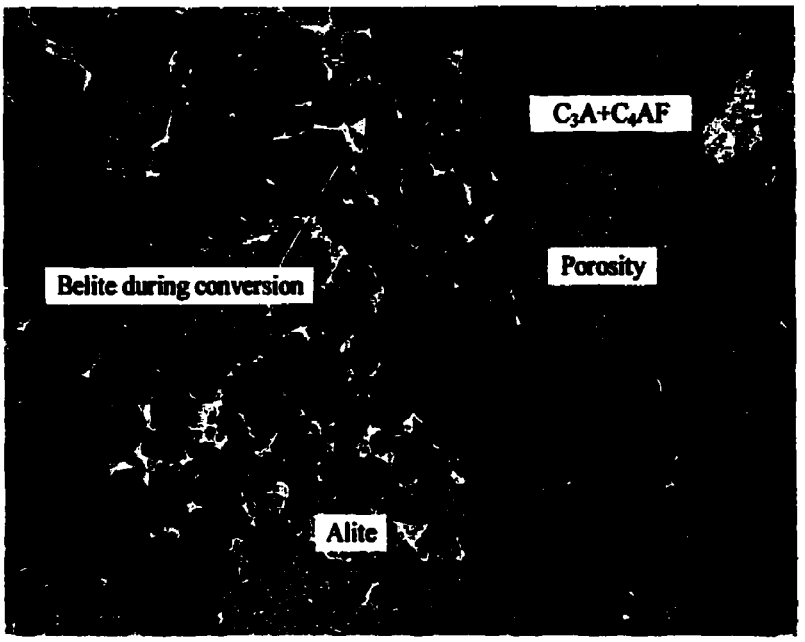

Figure 3.16 St. Constant clinker fired at 1550°C, once etched ×100

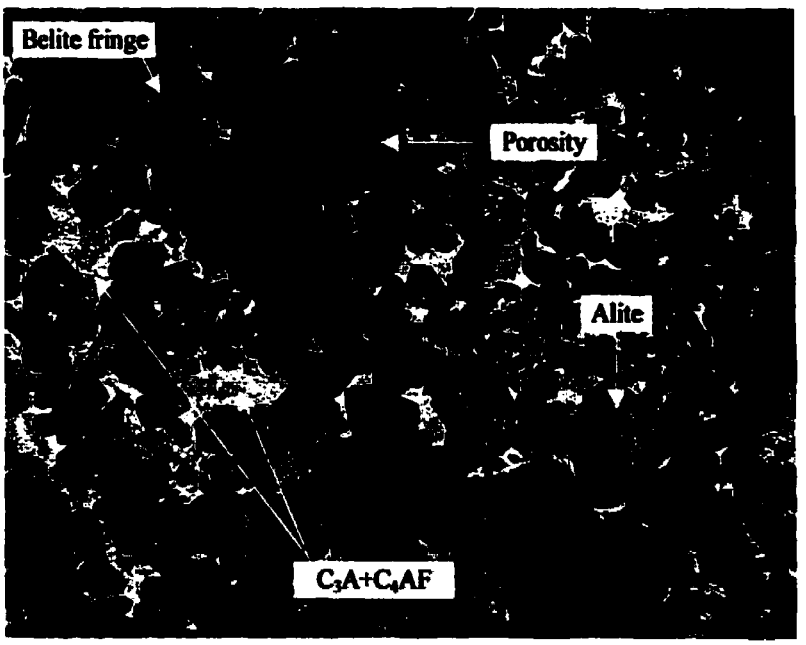

Figure 3.17 Exshaw clinker fired at 1550°C, once etched ×100

3.2 Basic Refractory Bricks

Historically, the fireclay and high-alumina bricks were the first-generation refractories of the cement industry, which, in fact, are still used in lower temperature zones of kilns. Basic bricks made of sintered magnesia and chrome ore became the dominant kiln lining when Al_2O_3–SiO_2 bricks no longer satisfied the increased chemical and thermal demands of the rotary kiln. Magnesia chrome bricks had a stable coating in burning zone, their performances mainly depending on the addition of refractory chrome ore. In relation to the environmental risk caused by disposal of the residual bricks that contain hexavalent chromium, the production of chrome-bearing bricks for cement industry has greatly declined, at least in North America.

Fired, direct-bonded doloma bricks have been used in burning zone for many years. Zirconia-containing doloma brick and zirconia-containing doloma-magnesia brick are also being in use. The novelty, during last decade, has been the use of direct-bonded periclase spinel brick. Some typical products, commercially prevailing in American and European markets of cement industry, were selected to test in this work.

In this thesis all of these types of bricks will be tested. To develop initially the test, work has been concentrated on using a given doloma brick. In Table 3.6, are listed the chemical and physical properties of the doloma-based bricks used. They are composed mainly of CaO and MgO, with or without the addition of zirconia [73, 74].

Table 3.6 The properties of the tested doloma-based bricks

Label		LD1	BD2	LDZ1	BDZ2	LDM1	BDM2
Chem. Comp., wt-%	MgO	40.0	40.0	38.8	39.0	57.0	60.0
	CaO	58.0	57.0	56.2	57.0	38.0	37.0
	SiO_2	0.8	0.9	0.8	1.2	0.8	1.1
	Al_2O_3	0.4	0.8	0.4	0.8	0.4	0.4
	Fe_2O_3	0.8	1.1	0.8	1.2	0.8	0.6
	ZrO_2	--	--	3.0	2.0-3.0	3.0	0.5-2.0
Bulk Density, g/cm^3		2.80	2.78-2.82	2.81	2.92	2.94	2.98
Apparent Porosity, %		17	12-15	17	16	15	12-14
Crush. Strength, MPa		60	27.6-41.4	40	--	50	--
Mod. of Rupture, MPa		--	9.0-12.4	--	6.2-9.7	--	6.5-10

Sintered dolomite is used to manufacture doloma bricks. Grains and powders, obtained by crushing and sizing, are mixed with a temporary binder, pressed into bricks and fired in a tunnel kiln at temperatures of up to 1700°C. Because CaO reacts very fast with air humidity to form $Ca(OH)_2$, doloma bricks are extremely sensitive to water and humidity, and so are impregnated with a special material. Although the binary system CaO-MgO shows a high melting temperature of 2370°C [75], the refractoriness of doloma bricks is rather limited due to a high plasticity by thermomechanical loads. Additionally, doloma

bricks are very sensitive against attack by SO_2/SO_3 and CO_2, forming CaS and $CaSO_4$ or $CaCO_3$. These reactions are always accompanied by a high volume effect destroying doloma bricks.

The properties of magnesia spinel bricks used in this work are shown in Table 3.7 [73, 74, 76, 77]. The stoichiometric composition of $MgAl_2O_4$-spinel is 28.2 wt-% MgO and 71.8 wt-% Al_2O_3. In the system MgO-Al_2O_3 [78], there is the only one compound of the cubic crystallizing spinel with a congruent melting point at 2135°C, and the two eutectics with temperatures of 2050°C and 1925°C. For cement kiln refractories, MgO-oversaturated spinel is preferred, as the eutectic of 2050°C is much higher than the typical burning temperature (~1450°C) of cement clinker. Spinel itself is produced either by fusion in an electric arc furnace or by sintering at temperatures of 1700-1900°C in a rotary kiln. Magnesia raw materials are either pure natural or synthetic materials with low iron content.

For production of classical magnesia spinel bricks, a mixture of pre-synthesized spinel and magnesia is pressed and fired, usually in tunnel kilns. Different thermal expansion coefficients between spinel and the surrounding magnesia matrix lead to generation of microcracks in the bricks, resulting in a significant increase of the brick modulus of elasticity without a negative influence on the brick strength. A further production method of magnesia spinel bricks is the direct addition of alumina to magnesia, the spinel forms during brick firing by an in-situ reaction. Magnesia spinel bricks are burnt

at temperatures up to 1700°C and above; their alumina content is typically between 3 and 18 wt-%. Magnesia spinel bricks are highly thermal shock resistant, not too sensitive against reducing/oxidizing conditions.

Table 3.7 The properties of the magnesia spinel bricks

Label		BM1	BMA1	HMA2	HMA3	HMA4	NMA5
Chem. Comp., wt-%	MgO	94.0	91.7	80.7	87.1	82.9	87.0
	CaO	2.8	1.5	1.4	1.7	1.6	2.1
	SiO_2	1.1	1.3	0.5	0.3	0.4	0.6
	Al_2O_3	0.4	4.7	15.8	10.4	14.4	10.7
	Fe_2O_3	0.5	0.6	0.9	0.3	0.3	0.5
	ZrO_2	1.0-2.0	--	--	--	--	--
Bulk Density, g/cm^3		2.91	2.85	2.93	2.88	2.88	2.91
Apparent Porosity, %		17	18	17	18	18	17
Crush. Strength, MPa		--	--	24	29	27	38
Mod. of Rupture, MPa		6.5	7.0	4.0	5.0	5.0	5.4

3.3 Preliminary Experiments

Many trial and error experiments had to be performed to define an acceptable protocol. At an early stage, it was shown that the coating study in a short rotary kiln, adopting the ASTM C 874 method for slag test of refractories [79], was inappropriate to obtain

quantitative results providing numerical values. Three variations of the sandwich test, shown by the configurations 'pastille', 'closed-cup' and 'sandwich without compression', in Figure 3.18, were then tried, and rejected, due to a lack of reproducibility of the results.

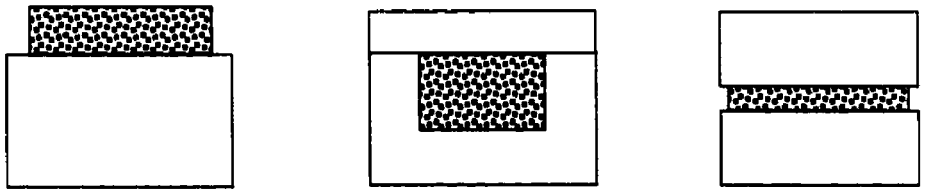

Figure 3.18 The early configuration of the sandwich test used in this work

3.3.1 Compressive Load

A key achievement was reached when a compressive load during heating was used. Without loading on sandwich, clinker does not stick well and adhesive coating can not be reproduced. Using a load was conducive to adherence of clinker in the sandwich.

Influence of load on tensile strength is shown in Figure 3.19, and on modulus of rupture shown in Figure 3.20. It is obvious that the bigger the load, the stronger is the adherence, no matter what mechanical testing mode is chosen and no matter what the heating temperature is between 1350°C and 1550°C and no matter what the holding time at temperature is.

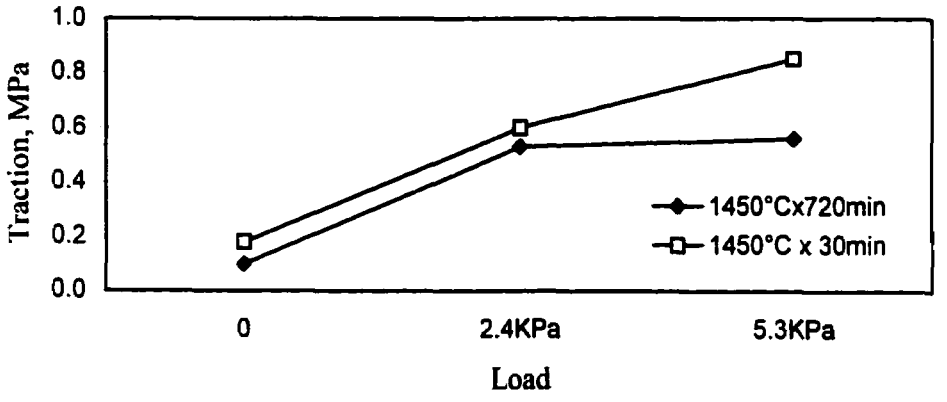

Figure 3.19 Influence of load and holding time on tensile strength (LD1)

As revealed in Figure 3.19, the holding time has a negative influence on adherence strength. Comparison between Figures 3.19 and 3.20 shows values of adherence strength being much smaller in traction mode than in flexion mode, and this is considered as an obvious result.

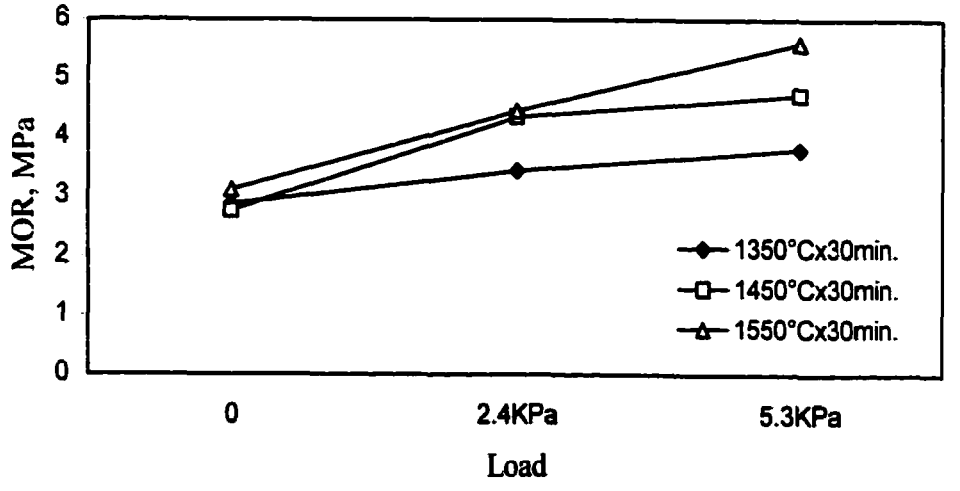

Figure 3.20 Influence of load and temperature on MOR (LD1)

Figure 3.20 also shows the importance of the firing temperatures on adherence strength. There is little influence of temperature on modulus of rupture in the case of no loading. It is farfetched to say that adherence strength increases with rising temperature under lower loading (2.4 kPa). The big differences of adherence strength under higher loading (5.3 kPa) illustrate that loading plays a critical role in adherence of the sandwich, with respect to firing temperatures. Therefore, 5.3 kPa is recommended for the load used in the sandwich protocol.

3.3.2 Raw Meal Treatment

The use of calcinated raw meal is another feature of the revised sandwich test. Paste made from calcinated raw meal was adopted for making the sandwich during the early development period. Raw meal and clinker obtained directly from St. Constant cement plant were first used to make the sandwich with paste. Lack of adherence strength with paste of raw meal or clinker led to the use calcinated raw meal, which was found to improve the adherence strength. Plenty of free lime existed in calcinated raw meal, as shown in Sections 3.1.3 and 3.1.5, which reacted with water in the paste to form a temporary hydraulic bond.

Raw meal was first calcinated at 1000°C for 4 hours either with bars pressed under a pressure of 20 MPa or bulk packed in an alumina crucible, prior to mixing with water for preparing paste. Mixing of the paste can be achieved using either a Hobart mixer or

simply a bowl and a spatula. The consistency of the paste and the variability due to paste preparation were also studied. The consistency of the calcinated raw meal from St. Constant with various water additions was measured on a vibrating table using ASTM C 860-91 method, which is a known technique to test flowability of castable [80]. This study showed that 46% water would be mostly appropriate without any interference with compressive load. Figure 3.21 illustrates influence of water addition on paste and adherence strength of doloma brick LD1, fired at 1450°C for 30 min under a load of 2.4 kPa. It is to be noted that many of the initial values were obtained using 42% water addition.

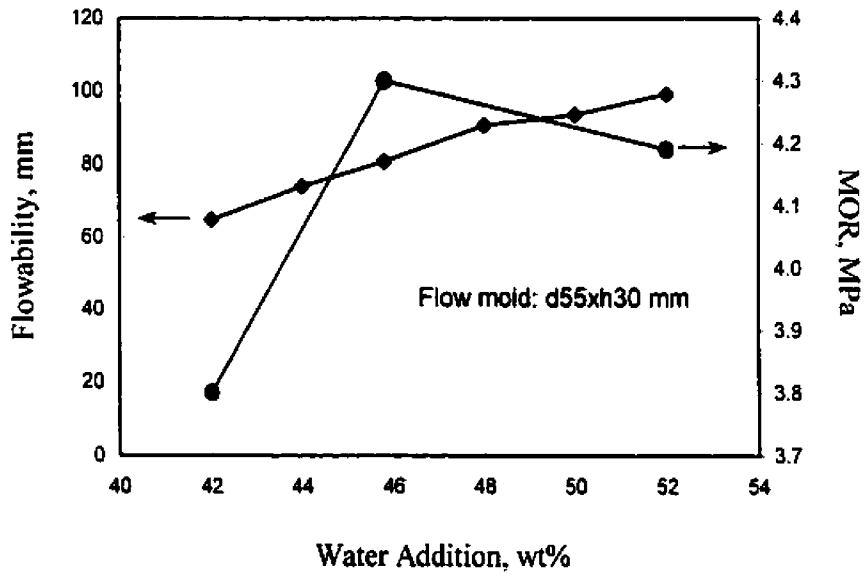

Figure 3.21 Influence of water addition on paste and adherence strength (LD1)

Practically, brushing sample surface with slurry of calcinated raw meal and water, before putting paste on sample, has been proven to be adequate. If so, measuring values

are essentially unchanged. In addition, cut surface leads to more reproducible values of adherence strength. For avoiding influence of sample surface, dry mix of calcinated raw meal is finally preferred with equal adherence and great convenience.

3.3.3 Mechanical Testing Mode

Our attempts obtaining numerical values of coatability are always to stride forward towards adherence strength. In measurement of the mechanical testing configuration, the early trials were done using a traction mode, which proved to be the wrong choice. The measured values were greatly influenced by the variability due to the fixing device itself. The results were difficult to interpret and then masked the influence of the main factors, which were recognized as important to start with. Their reliability was also challenged due to very small values of measurement, less than 1 MPa, which could masked the influence of factors. Such small values were also obtained in reference [81]

Figure 3.22 shows adherence strength of doloma (LD1), doloma-zirconia (LDZ1) and doloma-magnesia (LDM1) bricks, measured by traction and flexion modes after a clinkerization at 1450°C for 30 min, under a compressive load of 2.4 kPa. The ranking order is the same using the two sets of measurement, but it is more appropriately measured in flexion than in traction. This illustrates that the three-point bending flexural mode is an appropriate measurement of adherence.

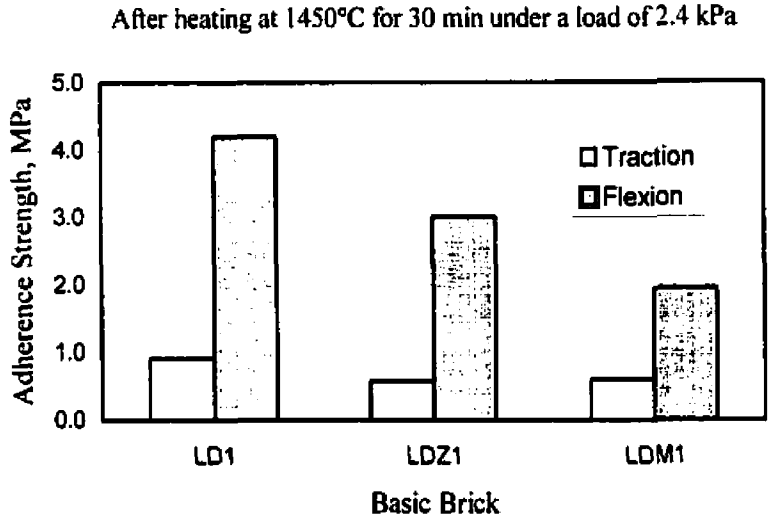

Figure 3.22 Comparison of tensile and flexion strength of adherence

3.4 The Sandwich Testing Protocol

The protocol, which has been used in this thesis, will now be described. The essential steps of the method are shown in Figure 3.23.

1. Calcination of raw meal

The as-received raw meal is calcinated, either by pressing the raw meal into bars under a pressure of 20 MPa or simply placing the raw meal into an alumina crucible. The material is then heated to 1000°C for 4 hours in an electrically wired furnace. The calcinated raw meal is then crushed and pulverized.

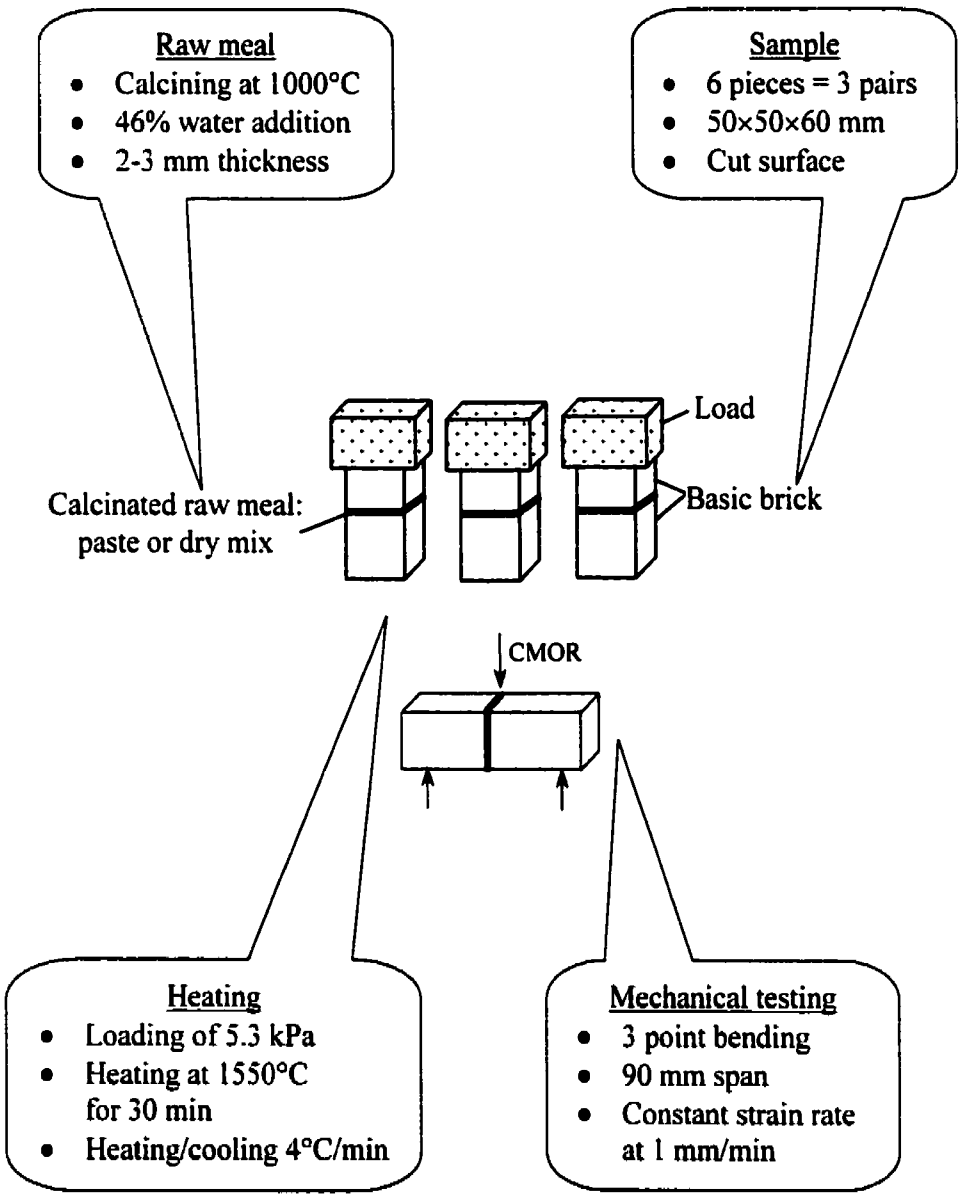

Figure 3.23 The essential points of the sandwich protocol for measuring adherence strength of coating

2(A). Making sandwich by paste

For three sandwiches, 50-gram calcinated raw meal is needed. About 42-gram water is slowly added into the calcinated raw meal and mixed using either a Hobart mixer or simply a bowl, mixing with a spatula. An exothermic reaction occurs. After 3-5 minutes, the paste is ready for making sandwich.

The paste consists of 54 wt-% calcinated raw meal and 46 wt-% water, which could be adjusted depending upon consistency.

The sandwich is to be prepared using a cut surface. Samples of 50×50×60 mm are directly cut dry from available bricks, without water-cooling. At least six pieces are needed to have three sandwiches for all tested brands.

Prior to applying the paste, slurry needs to be prepared, which consists of 33 wt-% calcinated raw meal and 67 wt-% water. One cut surface 50×50 mm has to be brushed with slurry, the 4-5 mm thickness of paste spreads on the brushed surface which constitutes the bottom part of the sandwich. The surface (50×50 mm) of the piece serving as the upper part of sandwich is also brushed with slurry, then superimposed and pressed by hands to reach a thickness of 2-3 mm for paste. Excessive paste is carefully removed on the 4 sides to obtain a 'clean' sandwich.

2(B). Making sandwich by dry mix

Sandwich is to be prepared using cut surface. Samples of 50×50×60 mm are directly cut dry from available bricks, without water-cooling. At least six pieces are needed to have three sandwiches for all tested brands of basic refractories.

Sample as the bottom portion of sandwich is wrapped with "Scotch Tape" around one cut surface to make a container. Twelve to fifteen grams of pulverized raw meal is poured into it and pressed lightly. A cut surface of the upper portion of the sandwich is then superimposed and pressed by hand. Using one finger the raw meal is compacted around scotch tape, to avoid its dropping-off when the tape burns out.

3. Heating

The sandwiches are then introduced in an electrically heated muffle furnace. A dead weight of 1325 grams is applied on top of the sandwich. The assemblages are heated at 1550°C for 0.5 hour, with heating and cooling rates of 4°C/min.

4. Measuring modulus of rupture

According to ASTM C 133-97 [82], the modulus of rupture is measured using a universal mechanical machine with 3-point bending flexural mode of 90 mm span and

the strain rate of 1.0 mm/min. A mean value of the modulus of rupture obtained from three replicates is considered as representative of the adherence strength of the coating.

CHAPTER 4. SENSITIVITY TO INFLUENTIAL PARAMETERS

The factorial design is the most popular class of experimental designs because of its wide applicability and ease of use and analysis. This chapter introduces the design, analysis, and interpretation of three studies in two systems of doloma-based brick and one magnesia-based spinel brick. Each study represents a blend of issues with different features which make each study unique. These experiments, which are all designed according to two-level factorial plans, give information that proved to be highly useful and illustrate a technique for simultaneously evaluating four variables. Three fractional factorial tests made will be introduced in this chapter. The first experiment involved the influences of the intensity of the compressive loading, the heating temperature, and the holding time, as well as the nature of raw meal. It was executed on doloma brick LD1. The second experiment involved the influences of the silica ratio, the alumina ratio, and the particle size based on a given raw meal, with two different heating rates, conducting on magnesia spinel brick HMA3. The third experiment was a repetition of the previous one but was made on doloma brick LD1.

Compared with one-factor-at-a-time experimentation and a series of trial and error tests, a statistically designed plan of experiments is a most effective method for identifying the key factors, to gain an understanding of the relationship between the factors and adherence strength, and to minimize costs by reducing the number of trials [83].

4.1 Two-Level Fractional-Factorial Design [84-87]

In complete factorial designs of p-factors, two-level factorial designs require making 2^p runs. As the number of factors gets large, it is easy to see that 2^p gets large. Fortunately, most of the information can be obtained from a fraction of the runs in a two-level factorial design. Fractional-factorial designs can be used to obtain information on main effects only or main effects and lower order interactions of variables. In addition, using fractional factorial design leads directly to improved efficiency and effectiveness of experimental design with great savings in resources. It is helpful, however, to understand what is given up when fractional-factorial designs are used. Two-level fractional-factorial designs are usually constructed assuming that it is of interest to estimate linear effects free and clear of two-factor interactions and that three-factor and higher-order interactions are not important. Three- and four-factor interactions rarely exist in nature, hence, little effort should be spent to estimate them, particularly at the beginning of an experimental program. Two-factor interactions, on the other hand, occur frequently and a good design is one which estimates them directly or separates them from the linear effects.

The two half-fractions of the 2^4 design are given by defining contrasts **I = 1234** and **I = -1234**. The points in these designs are shown in Table 4.1 and Figure 4.1. The balance and uniform distribution of points throughout the factor space is an important property of the design. Low (-1) and high (+1) levels of all variables are run in both half-

fractions. These two designs have equal statistical properties, the choice of which one to use is based on personal preference.

Table 4.1 Half-fractions of the 2^4 design

Defining Contrast	Run	X_1	X_2	X_3	X_4
I = 1234	1	-	-	-	-
	2	-	-	+	+
	3	-	+	-	+
	4	-	+	+	-
	5	+	-	-	+
	6	+	-	+	-
	7	+	+	-	-
	8	+	+	+	+
I = -1234	9	-	-	-	+
	10	-	-	+	-
	11	-	+	-	-
	12	-	+	+	+
	13	+	-	-	-
	14	+	-	+	+
	15	+	+	-	+
	16	+	+	+	-

The 2^{4-1} design has eight runs that allow the estimation of the effect summarized in Table 4.2. A study of the defining contrast **I = ±1234** shows that the linear effects are confounded with three-factor interactions and the two-factor interactions are confounded with each other in pairs. The calculated effect for variables 1 (E_1) estimates the sum of the linear effect of X_1 and $X_2X_3X_4$ interaction for the 2^{4-1} design with **I = 1234** and the difference between the X_1 and $X_2X_3X_4$ effects for the 2^{4-1} design with **I = -1234**. Similarly, in the case of 2^{4-1}**(I =1234)**, E_{23} estimates the sum of the X_2X_3 and X_1X_4 interaction effects. If the effects that measure the combinations of two-factor interaction were small, then it would be safe to conclude that the interactions were not important and that no further testing is needed. If the interactions were large, one might choose to complete the other half of the experiment to study the interactions.

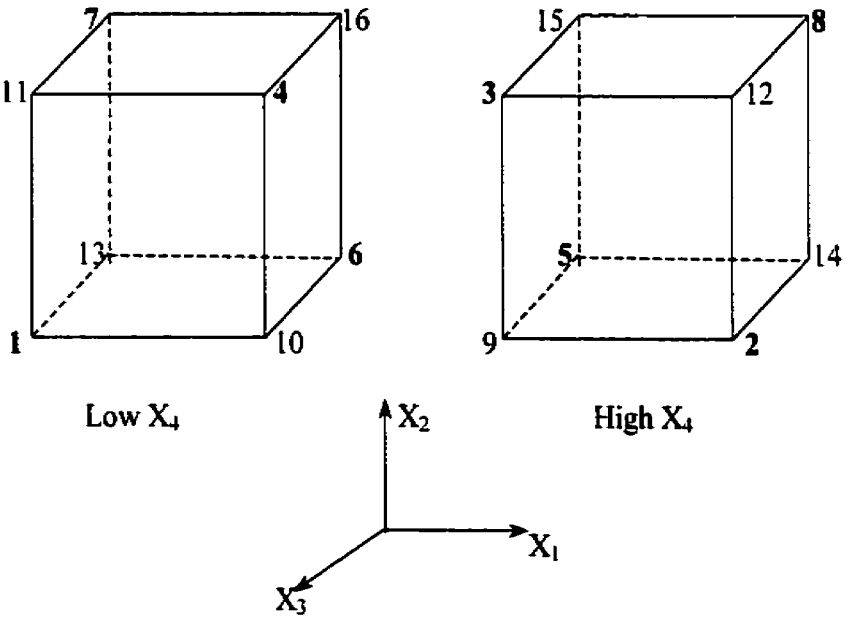

Figure 4.1 Two half-fractions of a 2^4 design

Table 4.2 Effects estimated by 2^{4-1} design

Calculated Effect	I = 1234	I = - 1234
E_1	$X_1 + X_2X_3X_4$	$X_1 - X_2X_3X_4$
E_2	$X_2 + X_1X_3X_4$	$X_2 - X_1X_3X_4$
E_{12}	$X_1X_2 + X_3X_4$	$X_1X_2 - X_3X_4$
E_3	$X_3 + X_1X_2X_4$	$X_3 - X_1X_2X_4$
E_{13}	$X_1X_3 + X_2X_4$	$X_1X_3 - X_2X_4$
E_{23}	$X_2X_3 + X_1X_4$	$X_2X_3 - X_1X_4$
E_{123}	$X_1X_2X_3 + X_4$	$X_1X_2X_3 - X_4$

4.2 Study of the Test Conditions

4.2.1 Executing a Fractional Factorial Experiment

Fractional factorial experiment will be accomplished in the following steps.

1. Identify a problem;
2. Perform a cause-and-effect analysis;
3. Select factors and their levels;
4. Select a fractional factorial experiment format;
5. Conduct the experiment and acquired data;
6. Graph the results;

7. Determine the effects;
8. Perform ANOVA – Analysis of variance.

Although some parameters of the sandwich test have been settled in Chapter 3, there is a need to know how much the adherence strength depends on them and how big influence they have when several variables are exerted simultaneously. A designed experiment was conducted to provide a better understanding of the interrelationships of adherence strength and process variables in the sandwich test. This would provide the inside needed for effective test control, to optimize the test conditions for the sandwich protocol. A satisfactory method was defined to be one of producing sufficient adherence strength for a specified brand of basic brick.

In setting up the sandwich test, four variables were noted as the principle contributors affecting adherence strength. These included compressive loading intensity, heating temperature, holding time and raw meals which were either from St. Constant or St. Laurent cement plants (The chemical composition of St. Laurent raw meal is 21.9% SiO_2, 3.95% Al_2O_3, 2.58% Fe_2O_3, 2.22% MgO, 66.20% CaO, 0.31% Na_2O and 1.60% K_2O). They were thought to have an approximately equal chance of influencing adherence strength. The four variables, considered at two levels, were studied using a 2^{4-1} factorial design with defined contrast **I = 1234** indicated in Table 4.1. Doloma brick LD1 was used as a reference refractory. Three sandwiches were prepared using the paste method and tested for each of the combinations of factors and levels, according to the description in Section 3.4 of Chapter 3. The eight-run plan and the measured MOR of

Table 4.3 The first 2^{4-1} factorial design and MOR responses

Run	Replicate	Raw meal	Temperature °C	Holding time min	Load kPa	MOR MPa
1	1	C	1450	30	2.4	2.33
2	1	C	1450	300	5.3	4.46
3	1	C	1550	30	5.3	5.63
4	1	C	1550	300	2.4	3.23
5	1	L	1450	30	5.3	2.64
6	1	L	1450	300	2.4	2.18
7	1	L	1550	30	2.4	3.88
8	1	L	1550	300	5.3	3.42
1	2	C	1450	30	2.4	2.60
2	2	C	1450	300	5.3	4.05
3	2	C	1550	30	5.3	6.02
4	2	C	1550	300	2.4	3.37
5	2	L	1450	30	5.3	3.69
6	2	L	1450	300	2.4	2.96
7	2	L	1550	30	2.4	3.35
8	2	L	1550	300	5.3	3.47
1	3	C	1450	30	2.4	3.64
2	3	C	1450	300	5.3	4.22
3	3	C	1550	30	5.3	5.26
4	3	C	1550	300	2.4	3.06
5	3	L	1450	30	5.3	3.78
6	3	L	1450	300	2.4	2.69
7	3	L	1550	30	2.4	4.08
8	3	L	1550	300	5.3	3.06

three replicates are listed in Table 4.3. It should be noted that two levels for each factor were assumed sufficient to describe adequately what was thought to be a linear relationship between the response variable and the factors of interest within the ranges selected.

4.2.2 Statistical Analysis and Interpretation

A statistical software package was used to analyze the results of the above plan of experiments [88]. The technical tool of process analysis was integrated with the advanced statistical technique ANOVA that partitions variations. At first, a look was made at the quality control chart to appreciate the deviations and to detect the excessive variability. Then the data were evaluated for level effects and graphed for visual analysis, being subjected to ANOVA to determine whether the effects are significant.

The Quality Control module can provide a procedure to monitor the sandwich test process. Figure 4.2 shows an X-bar chart and an S chart of the eight-run results, which are the most standard displays. In both line charts, the horizontal axis represents the different runs; the vertical axis for the X-bar chart represents the means for modulus of rupture, and the standard deviation is plotted in S chart.

Before interpreting the X-bar chart, the variability has to be sure under control by inspecting the S chart. As it is seen, the S chart contains no outliers, i.e., no points

outside of the upper control limits, so the variability is declared to be under control. Based on it, the X-bar chart is now reviewed to show three out of control runs, two points lying below the lower control limit and one point lying above control limit. In other words, the factors selected in the fractional factorial experiments, i.e., raw meal, heating temperature, holding time and compressive load, have an impact on adherence strength, with the sandwich test.

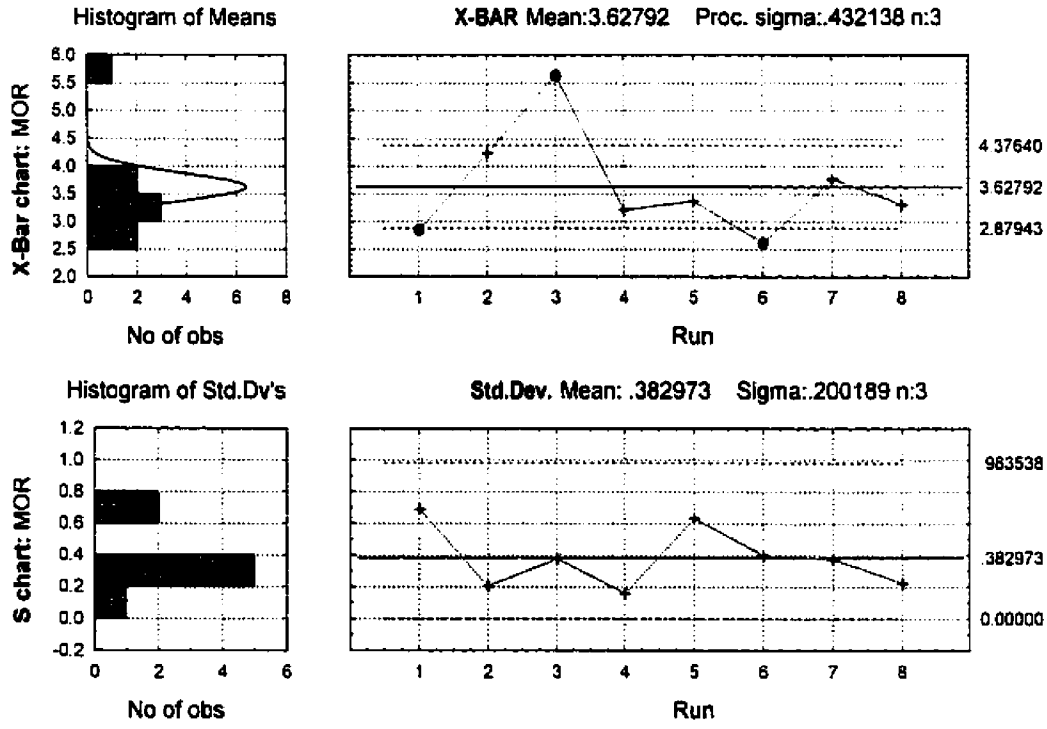

Figure 4.2 The X-bar chart and S chart of the test condition runs

Analysis of variance (ANOVA) was used to assess the significance of the main effects and interactions. The complete analysis of variance is summarized in Table 4.4, for the

data of MOR in Table 4.3. Typically, results that yield $p \leq .05$ are considered as the borderline for statistical significance but this level of significance still involves a pretty high probability of error (5%). Results that are significant at the $p \leq .01$ level are commonly considered statistically significant, and $p \leq .005$ level is often believed highly significant. Based on the p-values in table 4.4, or at the 99% confidence level, it is concluded that all the main factors are statistically significant and that there is significant interaction only between compressive load and raw meal.

Table 4.4 Analysis of variance for the experiment in Table 4.3

Factor	Sum of Square	Degree of Freedom	Mean Square(MS)	*F* ratio	*P*-Value
(1)Raw meal	3.13204	1	3.132037	17.39618	.000721
(2)Temp	3.07450	1	3.074504	17.07663	.000782
(3)Ho-time	1.88720	1	1.887204	10.48204	.005154
(4)Load	6.33454	1	6.334538	35.18373	.000021
1 by 2	0.15884	1	0.158438	0.88000	.362146
1 by 3	0.01260	1	0.012604	0.07001	.794705
1 by 4	4.58500	1	4.585004	25.46635	.000119
Error	2.88067	16	0.180042		
Total SS	22.06500	23			

The effect estimates of fractional factorial designed experiment were determined, as shown in Table 4.5. They are the deviations of the mean of the negative setting from the mean of the positive setting for the respective factor. If graphing these effects in *X-Y*

axis diagram, the slope of the line for main effect indicates the significance of the effect. The steeper the slope, the more significant the effect is.

Table 4.5 ANOVA effect estimates for the first factorial experiment

Factor	Effect	Std. err.	t(16)	*P*-Value	-95% confidence limit	+95% confidence limit
Mean/ intercept	3.6279	0.0866	41.886	.000000	3.4443	3.8115
(4)Load	1.0275	0.1732	5.9316	.000021	0.6602	1.3947
1 by 4	0.8742	0.1732	5.0464	.000119	0.5069	1.2414
(1)Rmeal	0.7225	0.1732	4.1709	.000721	0.3553	1.0897
(2)Temp	0.7158	0.1732	4.1324	.000782	0.3486	1.0831
(3)Htime	-0.5608	0.1732	-3.2376	.005154	-0.9281	-0.1936
1 by 2	0.1625	0.1732	0.9381	.362146	-0.2047	0.5297
1 by 3	0.0458	0.1732	0.2646	.794705	-0.3213	0.4131

In the Pareto chart of effects, the ANOVA effect estimates are sorted from the largest absolute value to the smallest absolute value, as shown in Figure 4.3. The magnitude of each effect is represented by a column and a line going across the columns indicates how large an effect has to be statistically significant by the p= .05 threshold. This chart clearly identifies the main effects for load, raw meal, temperature, and holding time as the most important determinants of resultant strength. The four main factors are ranked

in the order of importance as: load, followed by load-raw meal interaction, raw meal, holding time and temperature, all having significant influence on adherence strength. Therefore, they have to be specified for the sandwich test. Again, the first rank of the load effect on adherence strength proves its correctness and its critical importance. The interaction between load and raw meal, also very significant, can be understood by distinct role of load on firing evolution of different minerals in raw meal.

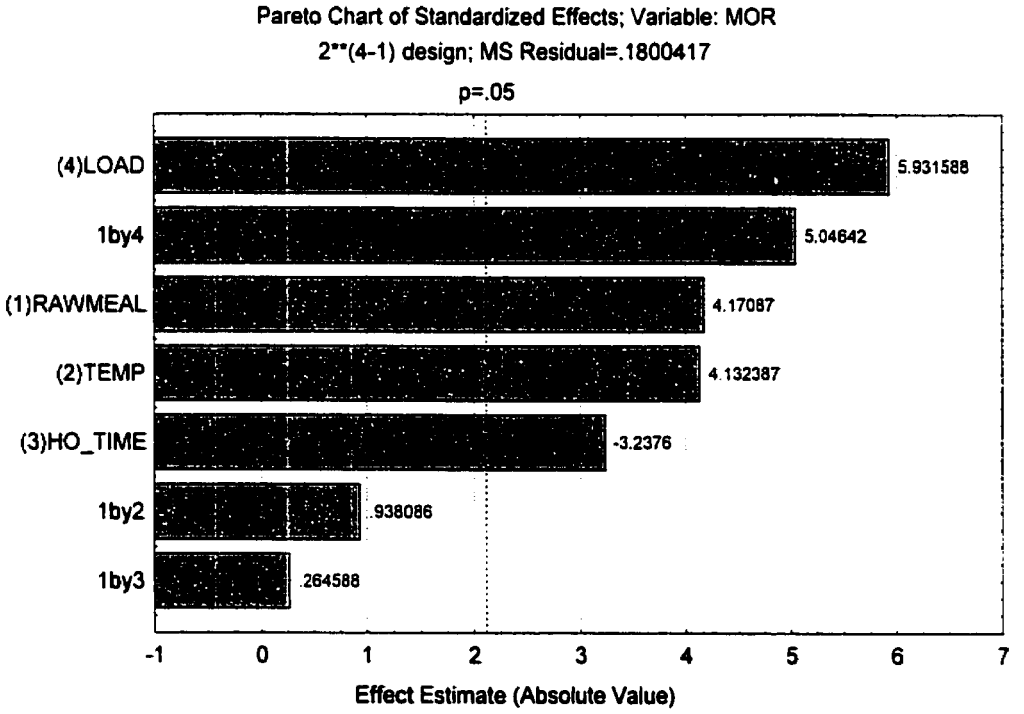

Figure 4.3 Pareto chart of the effects for the test conditions

It should be noted that the effect value for holding time is negative. Thus, the longer holding time at high temperature, the lower adherence strength. This was mentioned in

Section 3.3 of Chapter 3, which showed the lower adherence strength of 12-hour heating than that of 30 min heating. It is confirmed that under the fixed other conditions the modulus of rupture reduces with substantially prolonging heating time and changes a little in a narrow range of time with the sandwich test, as shown in Figure 4.4. It is then adequate to execute holding time of 30 min in the sandwich protocol.

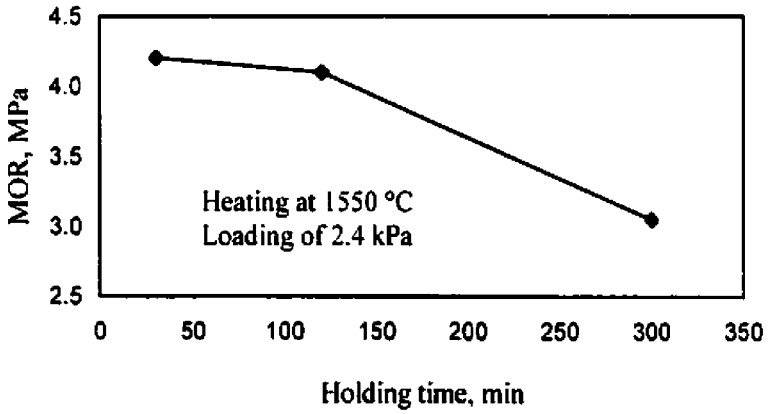

Figure 4.4 Influence of holding time on adherence strength

The analysis so far for dependent variable – adherence strength has revealed significant main effects for compressive load value, nature of the raw meal, heating temperature, and holding time, as well as interaction between load and raw meal. But how well this model fits the data? The fitted model has to be checked and illustrated in Figures 4.5 and 4.6. The predicted values cluster fairly close and homogeneously around the diagonal line in Figure 4.5, indicating a good fit of the model. The distribution of the residual values is computed as the difference between the predicted values and the observed values. It is assessed how closely a set of residuals follows a theoretical distribution in

Figure 4.6. It appears that residuals follow the normal distribution very closely. The four-main-effects model provides a good fit for the dependent variable strength.

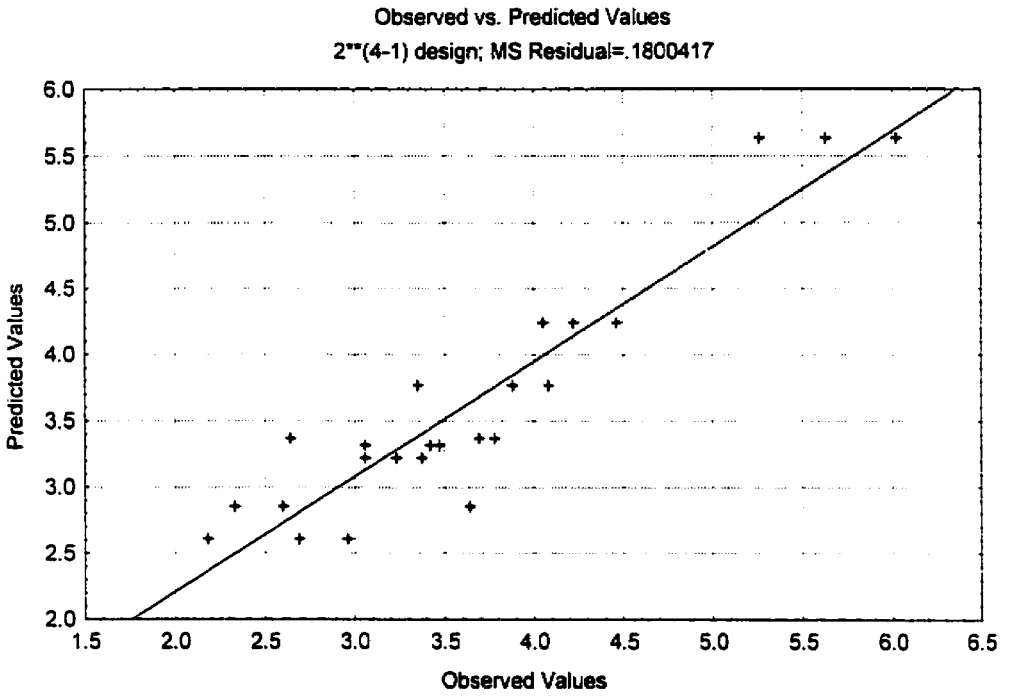

Figure 4.5 Predicted value vs. observed value in study of test conditions

4.3 Study of Raw Meal with Magnesia-Spinel Brick

Raw meal significantly influences adherence strength. This is illustrated by another set of results shown in Figure 4.7, for raw meal from three different cement plants, tested on magnesia-spinel brick HMA3. There are big differences in adherence strength with different raw meals. In order to figure out such a result, the statistical design of experiment was considered again to identify some other variables responsible for such changes in adherence strength.

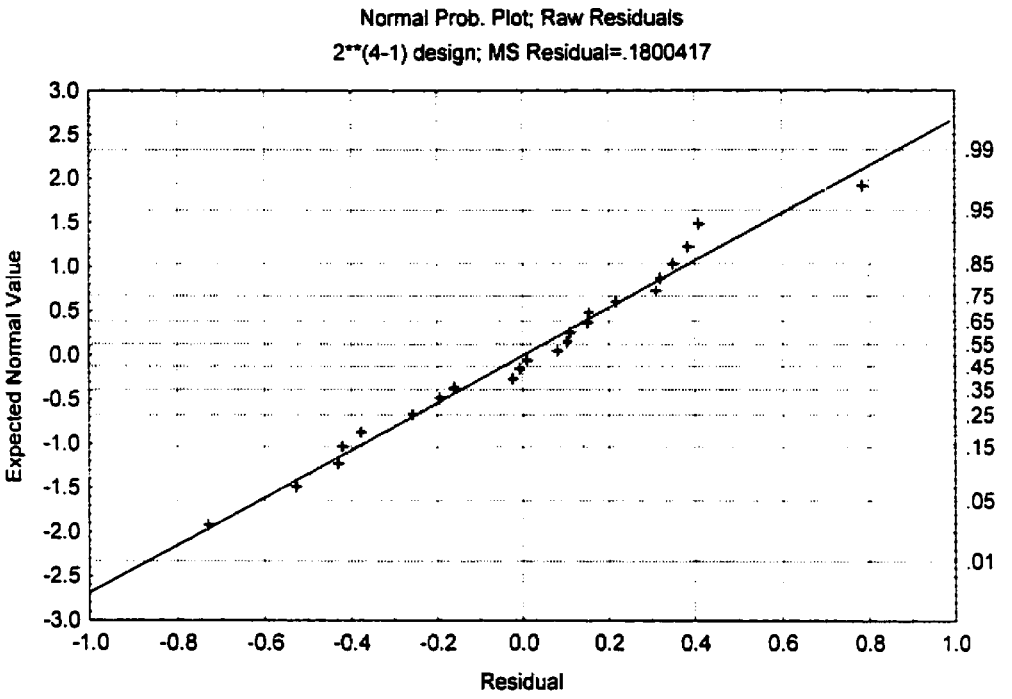

Figure 4.6 Normal probability plot of residuals in study of test conditions

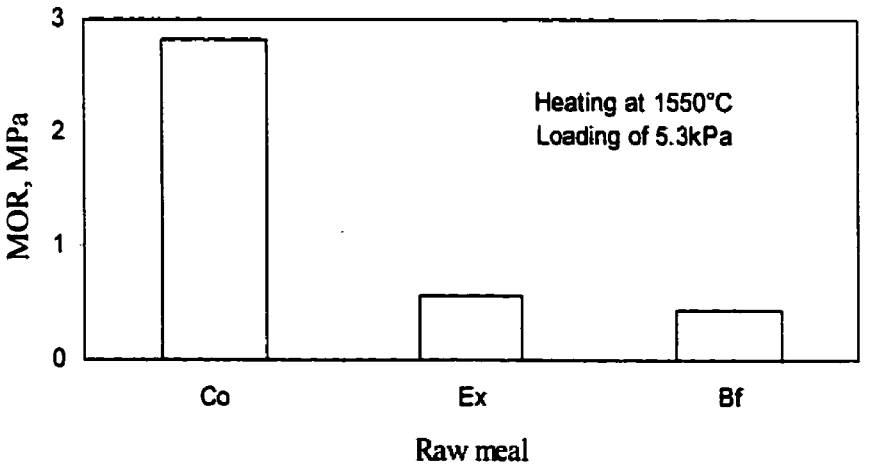

Figure 4.7 Influence of raw meal on adherence strength (HMA3)

4.3.1 Statistical Design of Experiment

A new 2^{4-1} fractional factorial experiment was executed, using two levels for each factor. The three parameters for a given raw meal, in addition to heating rates, were the silica ratio, the alumina ratio, and the particle size. The term 'level' for particle size referred to mean size of raw meal. Silica ratio values were either 2 or 3 weight ratio and alumina ratio values 1 or 1.5 weight ratio, which are normal ranges for Portland cement. St. Constant raw meal was used and modified as needed by adding alumina, silica, and hematite and by grinding. The raw meal was calcinated first in an alumina crucible at 1000°C for 4 hours, the needed amount of tabular alumina (mean size 4.2 μm, Alcoa Industrial Chemicals), ferric oxide (Red-anhydrous, mean size 0.49 μm, Fisher Scientific) and silica powder (mean size 5.02 μm, Anchemia) with purity of 99.9 wt-% were added and well mixed to reach the desired silica ratio and alumina ratio. Each of the mixtures were ground in a vibration mill for 30 hours, by which the mean value of particle size was reduced from ~40 μm to ~5 μm. The particle size of the raw meal was determined using a LS Particle Size Analyzer from Coulter Corporation. The particle size distributions of as-received raw meal and ground raw meal are shown in Figure 4.8.

The design of **I = 1234** in Table 4.1 was used to conduct the experiment. All the sandwiches were prepared by the dry mix method, fired at 1550°C for 30 min under loading of 5.3 kPa, and finally tested for modulus of rupture, as described in the sandwich protocol in Chapter 3. The magnesia based spinel brick -- HMA3 was used in

this experiment to see which factors of raw meal influence its adherence strength mostly. The fractional factorial format and the resulting data were recorded as indicated in Table 4.6.

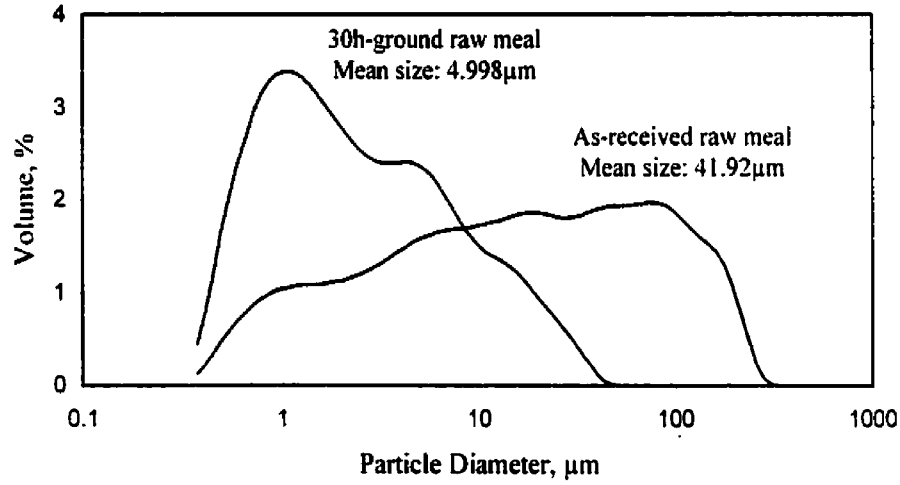

Figure 4.8 Particle size distributions of as-received and ground raw meal

4.3.2 Statistical Analysis of Acquired Data

The acquired data were first dealt with control charts, to know if the measured strength in each run had been controlled or not. The X-bar chart and S chart (standard deviation) are shown in Figure 4.9. In the S chart, none of the points are out of the control limits, and then variability of run is said to be controlled. The X-bar chart shows seven out-of-control runs in a total of eight runs. The different combination of factors from one run to another one leads to very big change of strength. Therefore, silica ratio, alumina ratio, particle size and heating rate exert a tremendous influence on adherence strength.

Table 4.6 The second 2^{4-1} factorial design and MOR responses of magnesia spinel brick

Run	Replicate	Mean particle size μm	Silica ratio(SR)	Alumina ratio(AR)	Heating rate °C/min	MOR MPa
1	1	5	2	1	4	4.09
2	1	5	2	1.5	8	1.05
3	1	5	3	1	8	0.00
4	1	5	3	1.5	4	0.42
5	1	40	2	1	8	0.66
6	1	40	2	1.5	4	1.98
7	1	40	3	1	4	0.00
8	1	40	3	1.5	8	0.39
1	2	5	2	1	4	3.72
2	2	5	2	1.5	8	1.34
3	2	5	3	1	8	0.00
4	2	5	3	1.5	4	0.68
5	2	40	2	1	8	0.79
6	2	40	2	1.5	4	2.39
7	2	40	3	1	4	0.00
8	2	40	3	1.5	8	0.21
1	3	5	2	1	4	4.07
2	3	5	2	1.5	8	0.84
3	3	5	3	1	8	0.00
4	3	5	3	1.5	4	0.81
5	3	40	2	1	8	0.71
6	3	40	2	1.5	4	2.15
7	3	40	3	1	4	0.00
8	3	40	3	1.5	8	0.34

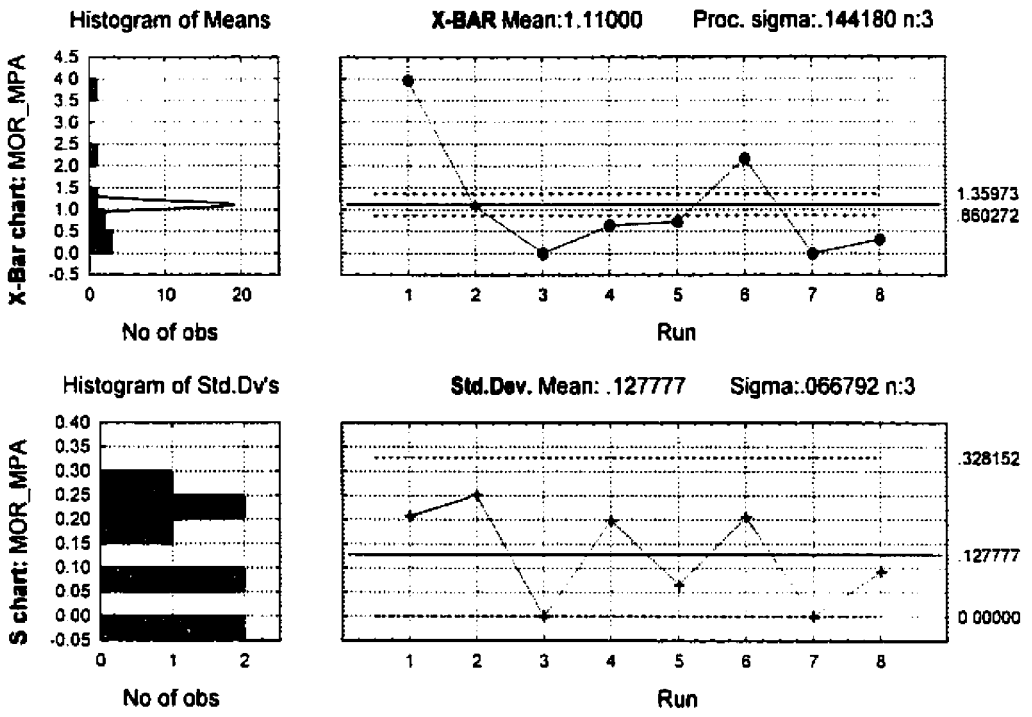

Figure 4.9 The X-bar chart and S chart in second factorial experiment

Next, analysis of variance determines which of the factors significantly affected the dependent variable of interest. As shown in Table 4.7, at $p \leq .005$ the three factors silica ratio, heating rate and particle size, as well as the three interactions, are highly significant to affect adherence strength. Moreover, in Table 4.8 the effect estimates are listed, showing how these factors work. With the exception of the overall *mean/intercept*, these estimates are the deviations of the mean of the negative settings from the mean of the positive setting from the respective factor. If the setting of factor silica ratio is changed from low to high, a reduction in adherence strength by 1.75 can be expected. If the value for factor heating rate is set to its low setting, an improvement in

strength by 1.17 can be expected, and so on. For analyses including interactions, the interpretation of the effect parameters is a bit more complicated. Specifically, the two-way interaction parameters are defined as half the difference between the main effects of one factor at the two levels of a second factor. More attention was paid to the main effects.

Table 4.7 Analysis of variance for the experiment in Table 4.6

Factor	Sum of Square	Degree of Freedom	Mean Square	*F* ratio	*P*-Value
(1)Partic-size	2.28167	1	2.28167	90.7524	.000000
(2)SR	18.27015	1	18.27015	726.6881	.000000
(3)AR	0.08640	1	0.08640	3.4365	.082299
(4)Heat-rate	8.14335	1	8.14335	323.8986	.000000
1 by 2	1.24215	1	1.24215	49.4060	.000003
1 by 3	6.04007	1	6.04007	240.2413	.000000
1 by 4	2.12415	1	2.12415	84.4872	.000000
Error	0.40227	16	0.02514		
Total SS	38.59020	23			

Pareto chart of effects for the second factorial experiment is shown in Figure 4.10. It is easily seen that three main factors are statistically significant showing the largest parameter estimates, in addition to the interactions between particle size and alumina ratio and between particle size and heating rate; thus the setting of these factors are the most important for the resultant strength of adherence. The effect estimates were

negative for all the main factors, which indicated adherence strength decreases with high value of each factor in their respective range. Only alumina ratio was not significant to influence adherence strength at the $p \leq .05$ level of significance.

It is easily understood that the fine powders of raw meal and the slow heating rate are beneficial to reactions that initiate adherence on magnesia spinel brick. The mechanisms to explain the influence of silica ratio and alumina ratio will be tackled in the microstructural analysis afterwards.

Table 4.8 ANOVA effect estimates for the second factorial experiment

Factor	Effect	Std. err.	t(16)	*P*-Value	-95% confidence limit	+95% confidence limit
Mean/ intercept	1.1100	0.0324	34.295	.000000	1.04139	1.17861
(1)P-size	-0.6167	0.0647	-9.526	.000000	-0.75389	-0.47944
(2)Silica r.	-1.7450	0.0647	-26.957	.000000	-1.88223	-1.60777
(3)Alum. r.	-0.1200	0.0647	-1.854	.082299	-0.25723	0.01723
(4)H-rate	-1.1650	0.0647	-17.997	.000000	-1.30223	1.02777
1 by 2	0.4550	0.0647	7.029	.000003	0.31777	0.59223
1 by 3	1.0033	0.0647	15.499	.000000	0.86611	1.14056
1 by 4	0.5950	0.0647	9.192	.000000	0.45777	0.73223

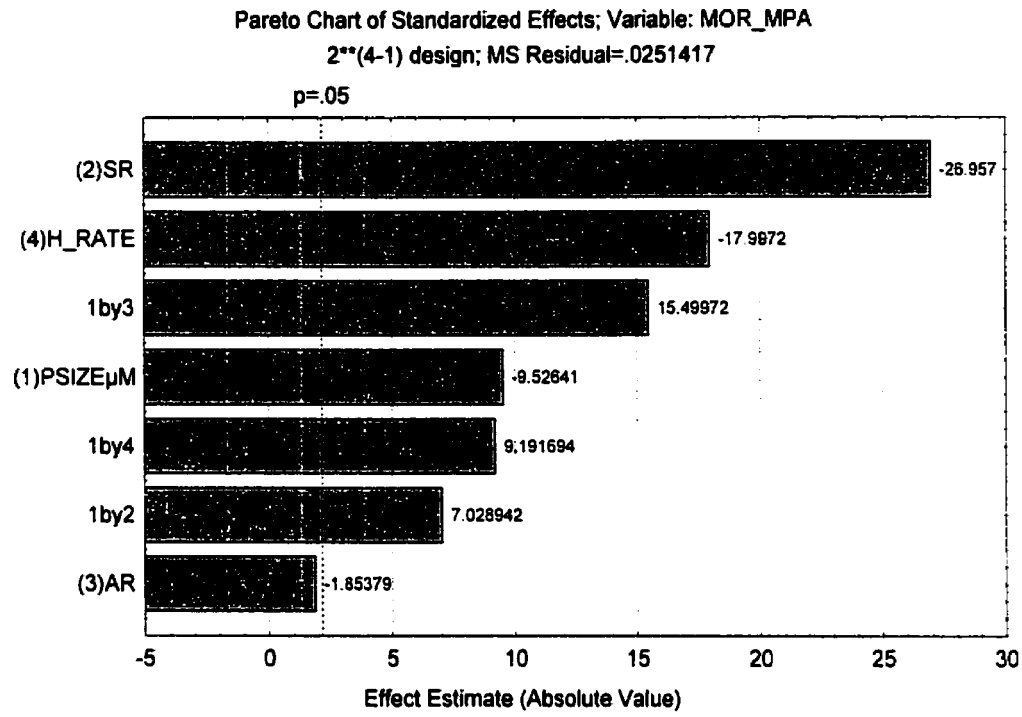

Figure 4.10 Pareto chart of effect estimates for the second factorial experiment

Since the parameter estimates and ANOVA analysis are based on the assumption that the residual are normally distributed, diagnostic plots of residuals should always be made to examine the distribution of the residual values, as shown in Figure 4.11. These are computed as the difference between the predicted values and the observed values. In this plot the actual residual values are plotted along the horizontal X-axis; the vertical Y-axis shows the expected normal values for the respective values, after they were rank-ordered. It is seen that all values fall closely around a straight line and so the residuals follow the normal distribution.

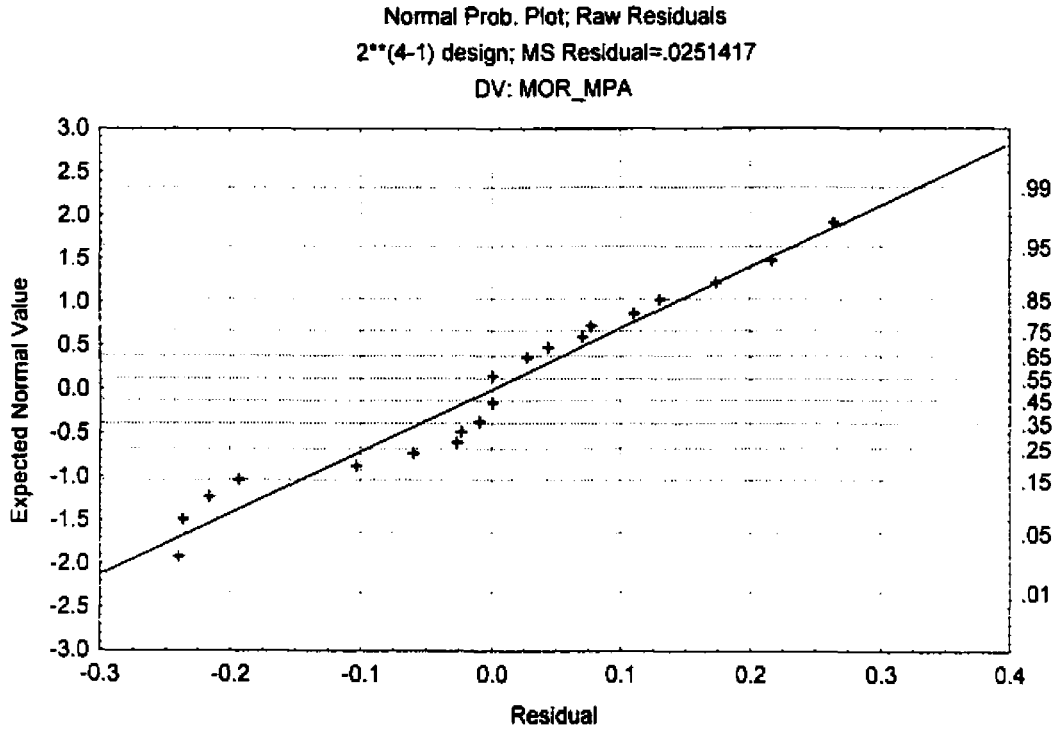

Figure 4.11 Normal probability plot of residuals in the second factorial experiment

4.4 Study of Raw Meal with Doloma Brick

The same design of 2^{4-1} fractional factorial experiment as in Section 4.3 was conducted on doloma brick LD1, with the factors, silica ratio, alumina ratio, and particle size of raw meal, as well as heating rate. Raw meal was prepared in the same way as before. The sandwiches were made following the dry mix method, fired at 1550°C for 0.5 hour under a compressive loading of 5.3 kPa and finally tested in three point bending flexural mode. Modulus of rupture measured on such a doloma brick exposed to clinker are listed in Table 4.9.

Table 4.9 The third 2^{4-1} factorial design and MOR responses of doloma brick

Run	Replicate	Particle size µm	Silica ratio	Alumina ratio	Heating rate °C/min	MOR MPa
1	1	5	2	1	4	2.23
2	1	5	2	1.5	8	2.73
3	1	5	3	1	8	7.67
4	1	5	3	1.5	4	8.93
5	1	40	2	1	8	2.02
6	1	40	2	1.5	4	3.11
7	1	40	3	1	4	5.61
8	1	40	3	1.5	8	6.70
1	2	5	2	1	4	2.44
2	2	5	2	1.5	8	2.62
3	2	5	3	1	8	7.41
4	2	5	3	1.5	4	8.56
5	2	40	2	1	8	2.44
6	2	40	2	1.5	4	2.57
7	2	40	3	1	4	5.65
8	2	40	3	1.5	8	6.20
1	3	5	2	1	4	2.57
2	3	5	2	1.5	8	2.96
3	3	5	3	1	8	7.83
4	3	5	3	1.5	4	8.33
5	3	40	2	1	8	2.38
6	3	40	2	1.5	4	3.06
7	3	40	3	1	4	5.44
8	3	40	3	1.5	8	6.38

The data in Table 4.9 were firstly examined using the control chart shown in Figure 4.12. The S chart shows that the standard deviation for each run is under control, thus it is safe to get information from the X-bar chart. All the points for the eight runs are out of control limit in this chart. Surely, some factors in this 2^{4-1} fractional factorial experiment on doloma brick have a strong impact on adherence strength.

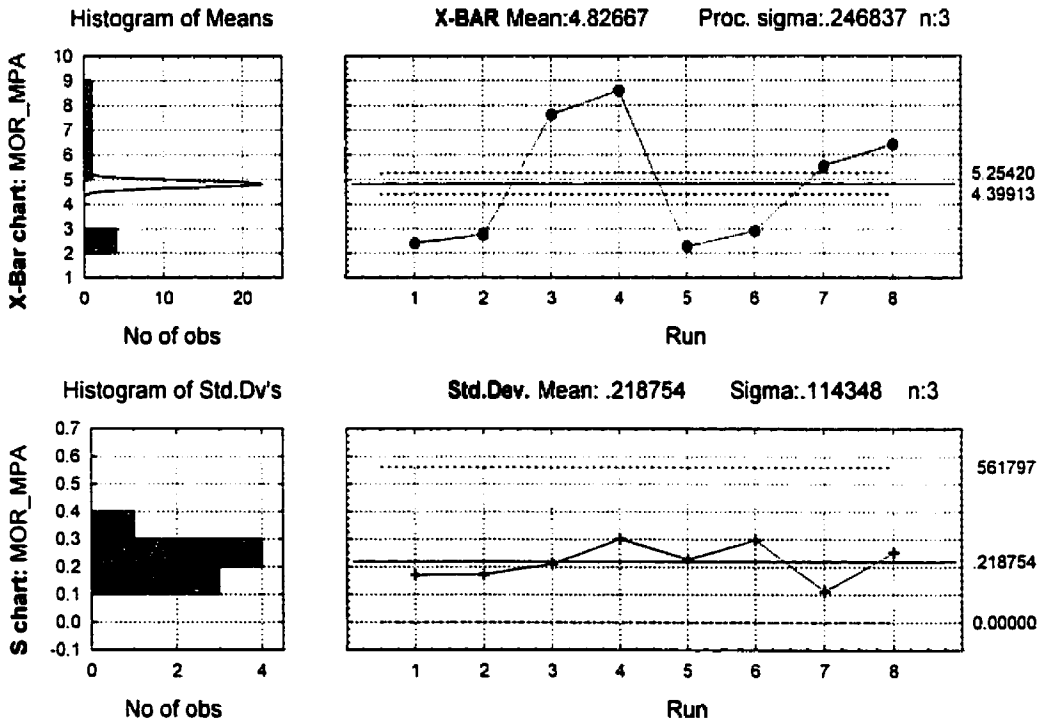

Figure 4.12 X-bar chart and S chart for the third factorial experiment

The ANOVA effect estimates are shown in Table 4.10. The differences in means between two groups can be evaluated using one of the nonparametric alternatives to the *t*-test. The p-level reported with a t-test represents the probability of error involved in

accepting our research hypothesis about the existence of a difference. Each estimated effect in Table 4.10 has a standard error of 0.046, so any effect greater than 2 × 0.046 is statistically significant at the 0.05 level. However, some of effects, such as silica ratio and particle size, have a much greater impact than the others on response of adherence strength. At the $p \leq .01$ level of significance, actually at almost 100% confidence level, factors particle size, silica ratio, and alumina ratio, as well as interaction between particle size and silica ratio, are statistically significant to influence adherence strength on doloma brick.

Table 4.10 ANOVA effect estimates for the third factorial experiment

Factor	Effect	Std. err.	t(16)	*P*-Value	-95% confidence limit	+95% confidence limit
Mean/ intercept	4.82667	0.0464	104.03	.000000	4.7283	4.9250
(1)P-size	-1.0600	0.0928	-11.423	.000000	-1.2567	-0.8633
(2)Silica r.	4.4650	0.0928	48.118	.000000	4.2683	4.6617
(3)Alum. r.	0.70500	0.0928	7.5976	.000001	0.5083	0.9017
(4)H-rate	-0.9667	0.0928	-1.0418	.313013	-0.2934	0.1000
1 by 2	-1.0650	0.0928	-11.477	.000000	-1.2617	-0.8683
1 by 3	0.0417	0.0928	0.4490	.659431	-0.1550	0.2384
1 by 4	0.2100	0.0928	2.2631	.037889	0.0133	0.4067

It is clearer to identify their effects in Pareto chart of Figure 4.13. High silica ratio and alumina ratio are conducive to adherence with positive effect estimates. The coarse raw meal and fast heating is not good to adherence strength due to negative values for particle size and heating rate.

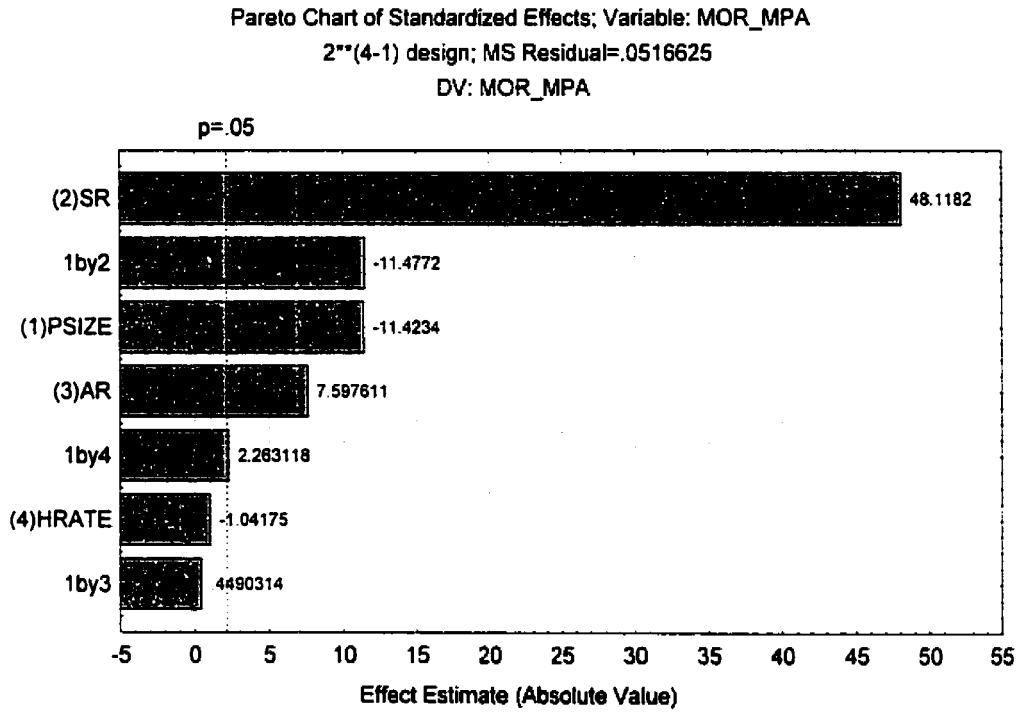

Figure 4.13 Pareto chart for the third factorial experiment on doloma brick

When using as-received raw meal and slowly heating sandwich, i.e., particle size is set to 40 μm and heating rate with 4°C/min, the adherence strength surface can be created by the two variables: silica ratio and alumina ratio. Figure 4.14 is the 3D surface representation of the results. The two horizontal axes are the two variables silica ratio

and alumina ratio (not in real range). The vertical axis shows the expected adherence strength. This just is used to see the relationship of silica ratio and alumina ratio. Different levels of adherence strength predicted by the fitted result models are indicated in the contour plot by different shades of color. Examination of the contour plot shows darker shading in top right corner, suggesting overall high silica ratio and alumina ratio may produce a high strength.

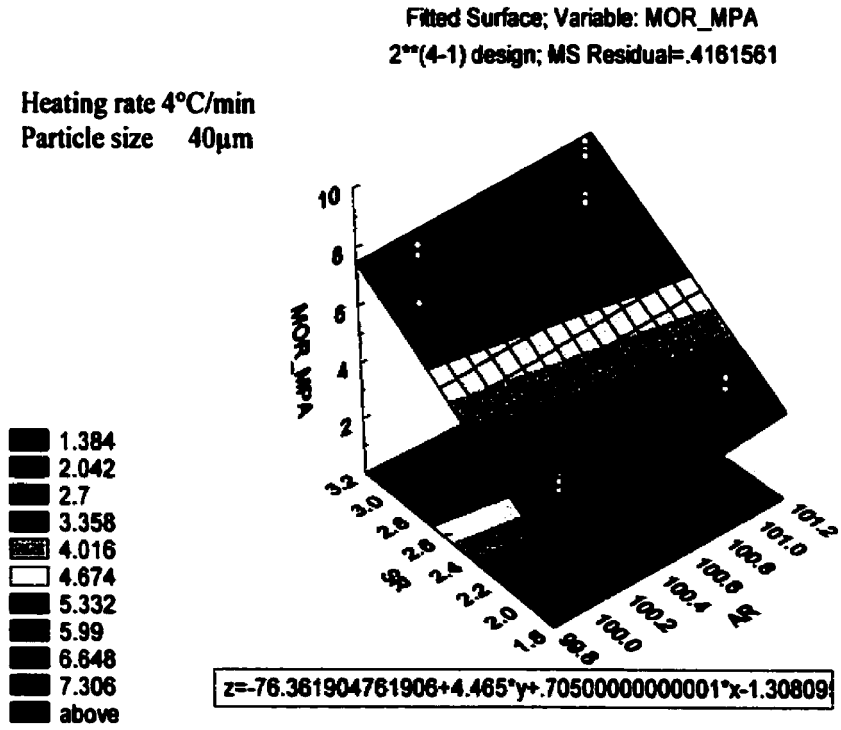

Figure 4.14 Adherence strength surface for doloma brick

Comparison of the same factorial experiment on magnesia spinel brick and doloma brick is as follows. Silica ratio is always highly significant, but have negative effect on

magnesia spinel brick and positive effect on doloma brick. That is, high silica ratio conduces to strong adherence on doloma brick, but yields weak adherence on magnesia spinel brick. Alumina ratio has a significant positive effect on doloma brick, and a small negative effect on magnesia spinel brick. Particle size is significant in both cases. Heating rate is significant for magnesia spinel brick, but not significant for doloma brick.

For examining the fitted model for the main effects, Figure 4.15 represents the predicted values closely falling around the diagonal line. The normal probability plot of the residuals shows no obvious deviation, as seen in Figure 4.16.

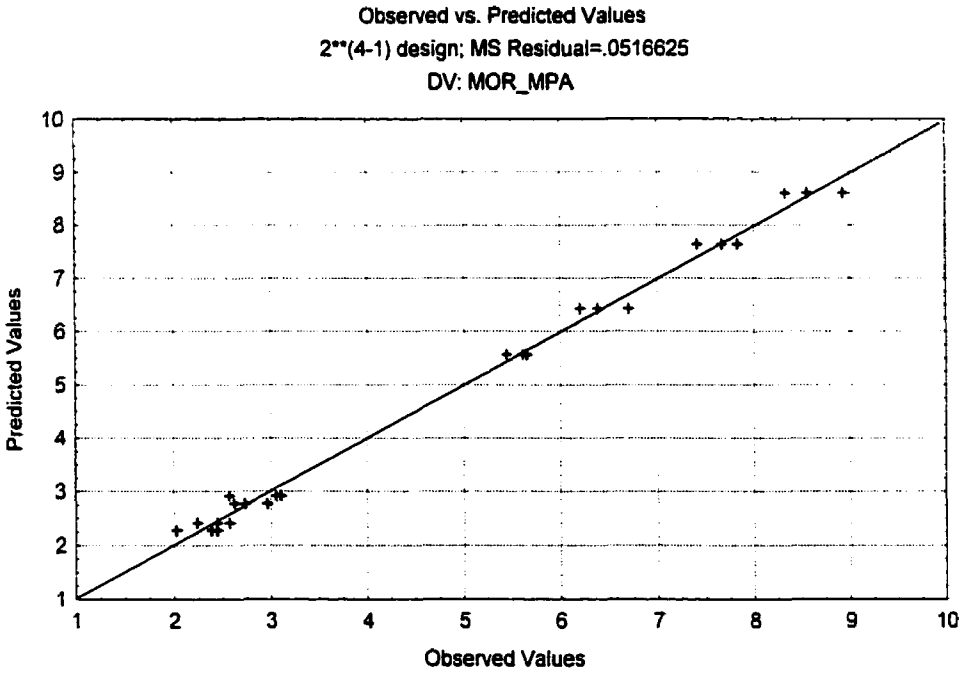

Figure 4.15 Predicted values vs. observed values for the third factorial experiment

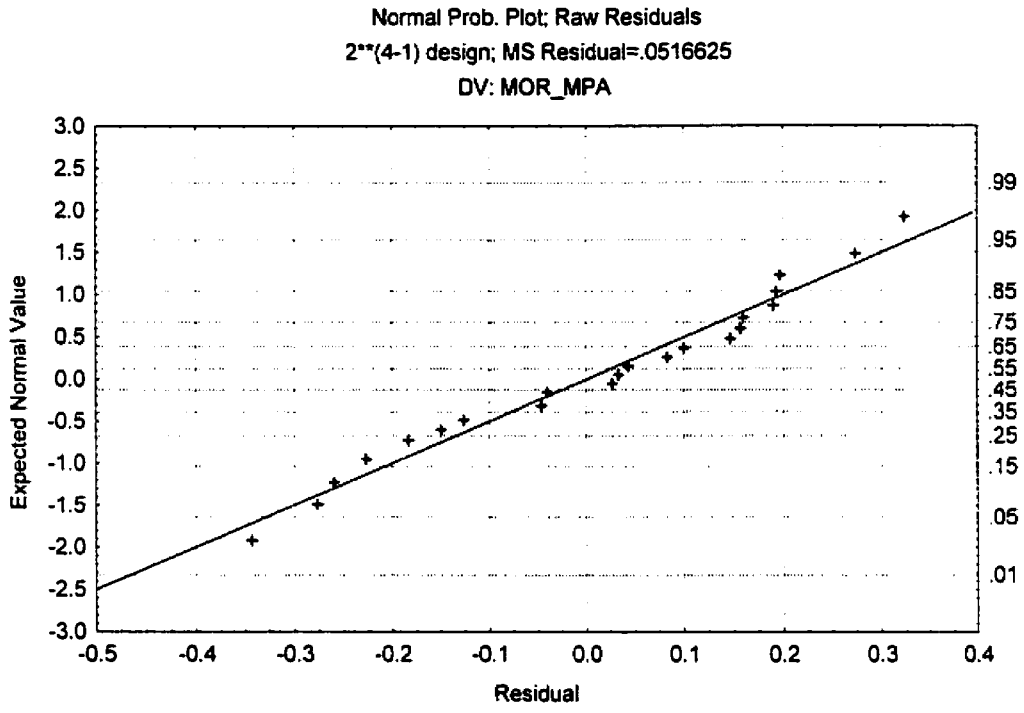

Figure 4.16 Normal probability plot of residuals for the third factorial experiment

4.5 Conclusions of Chapter 4

The following conclusions can be drawn from the three highly successful experiments, which were designed according to 2^{4-1} two-level fractional factorial plans, and analysis of variance (ANOVA).

(1) The most significant effects on adherence strength are the compressive load, the nature of raw meal, the heating temperature, and the holding time, ranked in the reducing order of importance.

(2) Silica ratio of raw meal has highly significant influence on adherence strength, with a negative effect on magnesia spinel brick and a positive effect on doloma brick.

(3) Effect of alumina ratio on adherence strength is not significant on magnesia spinel brick, but is a significant positive effect on doloma brick.

(4) Effect of heating rate on adherence strength is significant only on magnesia spinel brick. Particle size has a significant negative effect on both magnesia spinel brick and doloma brick, which is the finer the particle, the higher the adherence is.

CHAPTER 5. RELIABILITY OF THE SANDWICH TEST

When the main parameters are specified, the sandwich test should produce reliable values of adherence strength. However, it will be checked how sensitive those values are if other variables fluctuate within allowable limits, and how precise the measurement system works.

This chapter will thus document results on statistical ruggedness test and repeatability & reproducibility experiment, as well as reproduction of evaluation results on various basic bricks used in rotary cement kilns, including different doloma and magnesia bricks, some doloma-magnesia and some zirconia containing bricks.

5.1 Ruggedness Test

In studying the sandwich test method, it is necessary to consider the effect of all environmental factors on measured values of adherence strength. If this effect is not considered, the result obtained by the sandwich protocol may not be as accurate as expected. The purpose of the ruggedness test is to know if the variables strongly influence the measurements provided by the sandwich protocol and to determine how closely these variables need to be controlled. Again, a statistical design of experiment was used in ruggedness test, setting two levels for each variable so as not to be greatly different. The design requires the simultaneous change of the levels of all the variables,

and allows the determination of the separated effect of each of the variables on the measured results.

5.1.1 Designing and Conducting the Ruggedness Test -- Following the Paste Method

In the ruggedness test, the three variables tested were as follows:

(1) The thickness of the paste, 2 or 5 mm;

(2) The mixing method to prepare the paste, manually or in a Hobart mixer;

(3) The holding time, 30 or 120 min.

These variables were thought to have an approximately equal chance of influencing adherence strength. A full 2^3 factorial design was selected to quantify these influences. The eight treatment combinations and the design format of runs are shown in Table 5.1 [89]. There are seven degrees of freedom between the eight treatment combinations in the 2^3 design. Three degrees of freedom are associated with the main effect of factors X_1, X_2 and X_3. Four degrees of freedom are associated with interactions, one each with X_1X_2, X_1X_3 and X_2X_3, and one with $X_1X_2X_3$.

In the ruggedness test, the sandwiches were heated at 1550°C under a compressive load of 2.4 kPa, and tested in the usual three-point bending flexural mode. Three replicates were made for each treatment combination. The paste was prepared by mixing calcinated raw meal and about 46% water. Holding time as one of factors in ruggedness

test had a narrow range of 0.5 to 2 hours compared with range of 0.5 to 5 hour in the first fractional factorial test in Chapter 4. The experimental format with data acquired in ruggedness test is shown in Table 5.2.

Table 5.1 The 2^3 factorial design

Run	X_1	X_2	X_3
1	-	-	-
2	-	-	+
3	-	+	-
4	-	+	+
5	+	-	-
6	+	-	+
7	+	+	-
8	+	+	+

5.1.2 Statistical Analysis

The same package of statistical software was used to analyze these data. The first step was made using the control chart shown in Figure 5.1. Before a control chart is constructed to assess performance of ruggedness test, the variability has to be checked to make sure if this measurement system attains a state of statistical control. That is, the data are a population distribution that is stable in time and has a fixed mean. The information about variability is richer when standard deviations are calculated. It is better to use standard deviation of the individual groups to estimate variability. The S chart in Figure 5.1 shows that none of the points are out of the control limits. As a result, ruggedness test has an acceptable variability.

Table 5.2 The experiment format and acquired data in ruggedness test

Run	Replicates	Thickness mm	Holding time min	Mixing mode	MOR MPa
1	1	2	30	Hand	4.20
2	1	2	30	Machine	4.62
3	1	2	120	Hand	4.52
4	1	2	120	Machine	4.10
5	1	5	30	Hand	4.49
6	1	5	30	Machine	3.81
7	1	5	120	Hand	3.89
8	1	5	120	Machine	5.15
1	2	2	30	Hand	5.15
2	2	2	30	Machine	4.47
3	2	2	120	Hand	3.97
4	2	2	120	Machine	5.49
5	2	5	30	Hand	5.38
6	2	5	30	Machine	4.94
7	2	5	120	Hand	4.94
8	2	5	120	Machine	4.12
1	3	2	30	Hand	4.71
2	3	2	30	Machine	4.76
3	3	2	120	Hand	4.78
4	3	2	120	Machine	4.58
5	3	5	30	Hand	4.71
6	3	5	30	Machine	4.98
7	3	5	120	Hand	4.90
8	3	5	120	Machine	4.62

The variability of ruggedness test is shown to be under control, in X-bar chart of Figure 5.1. The intent of X-bar chart is to be able to determine very quickly if the sandwich test is still under control. X-bar chart is sensitive enough to be able to detect shifts, which has been proved by the three fractional factorial experiments in Chapter 4. In this case, the points of the average values of each run fall closely around line of the overall mean, within the upper and lower action and warning limits. Therefore, the three factors in the ruggedness test do not influence adherence strength strongly.

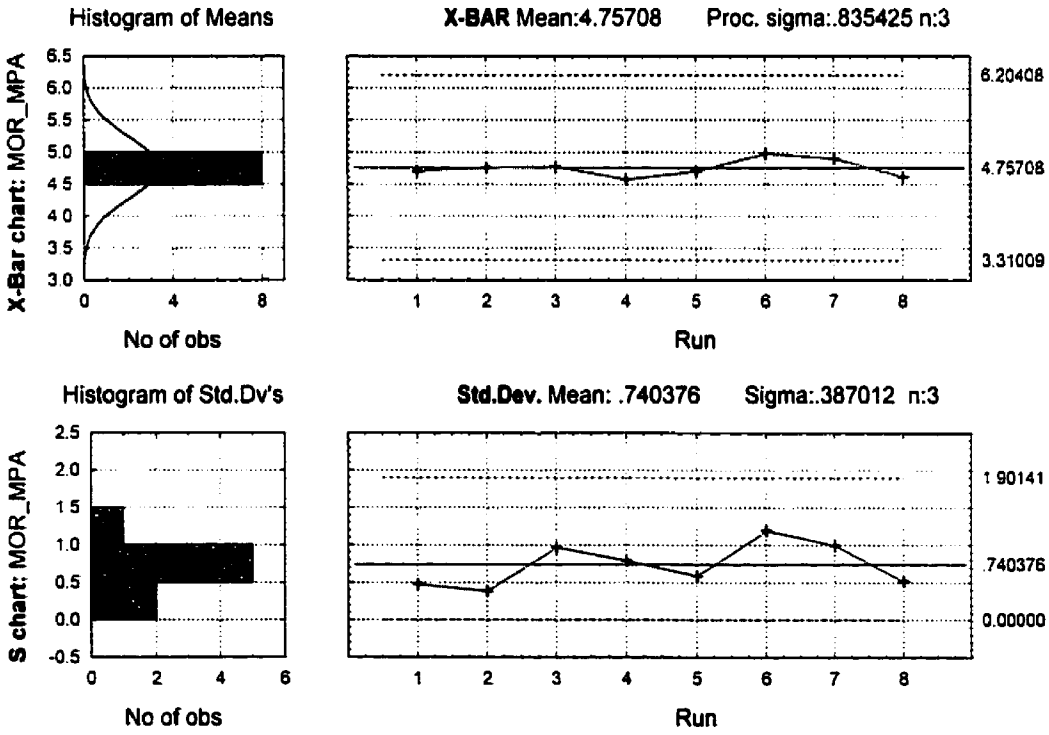

Figure 5.1 The X-bar control chart and S chart for ruggedness test

Results of a software-generated ANOVA for a cubic model involving three factors are shown in Table 5.3. At the 0.05 level of significance, no factor significantly affects adherence strength. This is clearly displayed by Pareto chart of effects, as shown in Figure 5.2.

Table 5.3 Analysis of variance for ruggedness test

Factor	Sum of Square	Degree of Freedom	Mean Square	*F* ratio	*P*-Value
(1)Thickness	0.0551	1	0.0551	0.0885	.7699
(2)Ho-time	0.0287	1	0.0287	0.0461	.8327
(3)Mix-mode	0.0092	1	0.0092	0.0148	.9047
1 by 2	0.0012	1	0.0012	0.0019	.9655
1 by 3	0.0077	1	0.0077	0.0123	.9128
2 by 3	0.2460	1	0.2460	0.3952	.5385
1 by 2 by 3	0.0330	1	0.0330	0.0530	.8208
Error	9.9613	16	0.6226		
Total SS	10.3423	23			

Three related means are presented for determining which effects are significantly different from zero. In the first means, the magnitude of an effect is compared to its estimated standard error. In the second means, a regression model is used in which each effect is associated with a regression coefficient. Then the regression results can be used to conduct the analysis. The third means that uses normal probability plots is discussed finally.

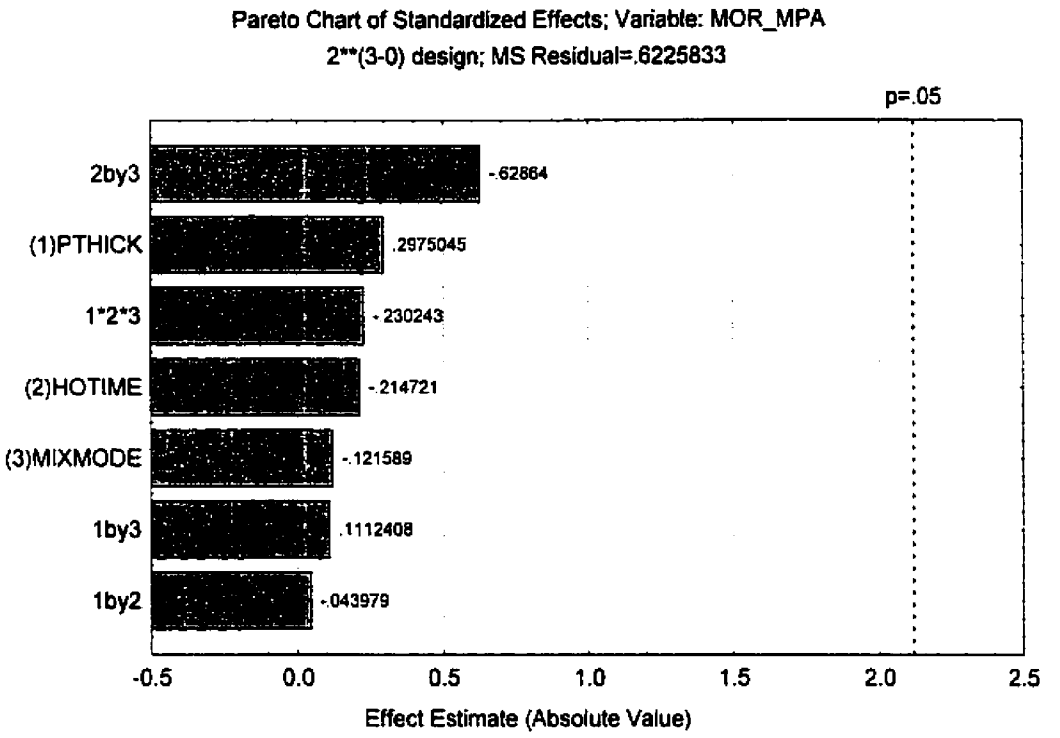

Figure 5.2 Pareto chart of effect for ruggedness test

The magnitude of the effects can be judged by comparing each effect to its estimated standard error. In this 2^3 design with 3 replicates, there are a total of $24 = 3 \times 2^3$ measurements. An effect estimate is the difference between two averages and each average is calculated from half the measurements. In Table 5.4, The numerical estimates and direction of the effects are listed. Each effect is divided by its estimated standard error and the resulting *t* ratio is compared to a *t* distribution with 16 degrees of freedom. The *t* ratio is used to judge whether the effect is significantly different from zero. None of the factors significantly affect adherence strength.

Table 5.4 Effect estimates and regression coefficients for ruggedness test

Factor	Effect	Std. err.	$t(16)$	P-Value	Coefficient	Std. err
Mean/ intercept	4.7571	0.1611	29.5357	--	4.7571	0.1611
(1)Pthick	0.0958	0.3221	0.2975	0.7699	0.0479	0.1611
(2)Htime	-0.0692	0.3221	-0.2147	0.8327	-0.0342	0.1611
(3)Mmode	-0.0392	0.3221	0.1216	0.9047	-0.0196	0.1611
1 by 2	-0.0142	0.3221	-0.0439	0.9655	-0.0071	0.1611
1 by 3	0.0358	0.3221	-0.1112	0.9128	0.0179	0.1611
2 by 3	-0.2025	0.3221	0.6286	0.5385	-0.1012	0.1611
1by2by3	-0.0742	0.3221	0.2302	0.8208	-0.0371	0.1611

In any designed experiment, it is important to examine a model for predicting responses. Furthermore, there is a close relationship between analysis of variance and a regression analysis. An initial regression model is

$$Y = \beta_0 + \beta_1 x_1 + \beta_2 x_2 + \beta_3 x_3 + \beta_{12} x_1 x_2 + \beta_{13} x_1 x_3 + \beta_{23} x_2 x_3 + \beta_{123} x_1 x_2 x_3$$

The thickness of paste, holding time and mixing mode of paste are presented by coded variables x_1, x_2 and x_3, low and high levels of each variables being assigned values –1 and +1, respectively.

The least squares fitted model is

$$Y = 4.7571 + 0.0479x_1 + (-0.0346)x_2 + (-0.0196)x_3 +$$
$$(-0.0071)x_1x_2 + 0.0179x_1x_3 + (-0.1013)x_2x_3 + (-0.0371)x_1x_2x_3$$

where the intercept β_0 is the grand average of all 24 measurements. The estimated coefficient is one-half the effect estimate, shown by the regression analysis in Table 5.4. Because the *p*-value associated with *F* test for the model is big (more than 0.05), none of the effects are important. The *t* test from a regression analysis is identical to the *t* test obtained from the standard error of an effect in a 2^3 design, as shown in Table 5.4. A simpler model that uses only the important effects is the preferred choice to predict the response. Because the *t* tests for all the effects are not significant, these terms are removed from the model. The model then becomes $\boldsymbol{Y = 4.7571}$. That is, the estimate regression coefficient for any effect is the same, regardless of the model considered. Although this is not true in general for a regression analysis, an estimated regression coefficient does not depend on the model in a factorial analysis.

Since the observed values at first run are 4.20, 5.15 and 4.78, the residuals are 4.20 – 4.75 = 0.55, 5.15 – 4.75 = 0.40, and 4.78 – 4.75 = 0.03. Residuals for the other seven runs are obtained similarly. A normal probability plot of the residuals is shown in Figure

5.3. The residuals lie approximately along a straight line. Thus no problem with normality in the data needs to be suspected.

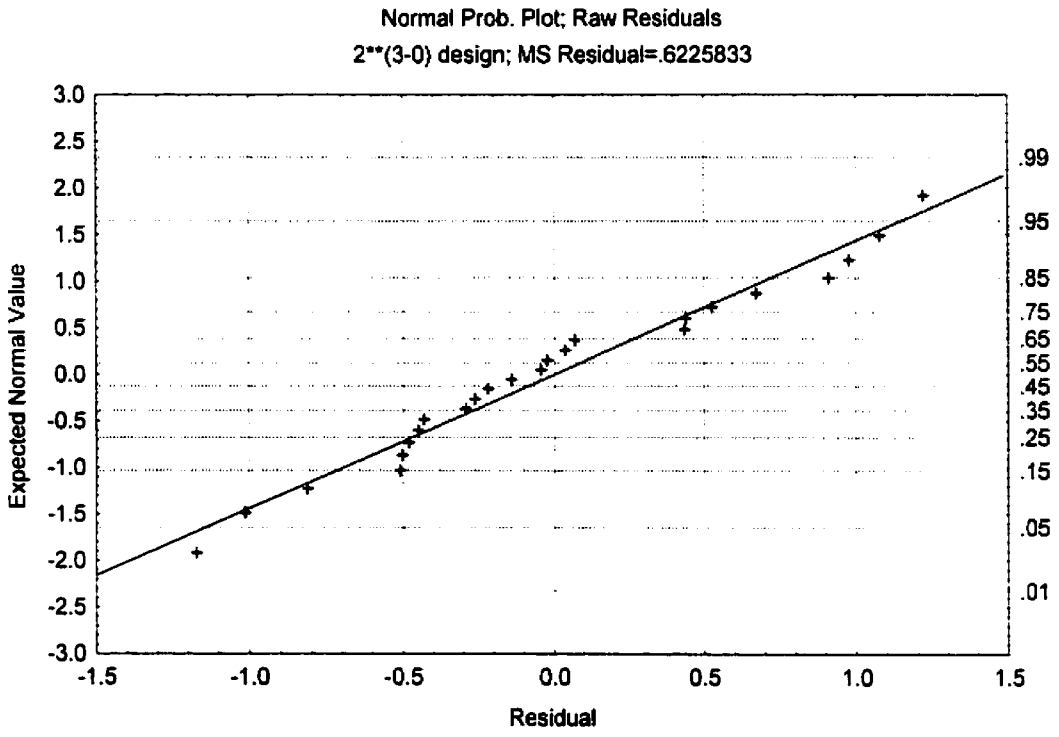

Figure 5.3 Normal probability plot of residuals for ruggedness test

It is now very clear that sandwich test is indeed very rugged, as thickness of the paste, holding time and mixing mode of the paste are concerned within the allowable limits considered. None of the three factors have a direct major influence, nor the binary interactions between the two factors, nor the interaction of all three factors together. It is worth mentioning that holding time in the range of 0.5 to 2 hours does not affect

adherence strength strongly, but significantly impacts from 0.5 to 5 hours in the fractional factorial experiment in Chapter 4.

5.2 Repeatability and Reproducibility Study

5.2.1 Experimental

In this study, repeatability refers to the variability of measurements of the same parts by the same operators across trials; thus, repeatability reflects the variation (measurement errors) in the measurement equipment. Reproducibility refers to the variability of measurements of the same parts across operators. The purpose of repeatability and reproducibility experiments is to determine the proportion of measurement variability that is due to (1) the parts being measured (batch-to-batch variation), (2) the operator (reproducibility), and (3) errors (unreliability) in the measurements over several trials by the same operators of the same parts (repeatability). In the ideal case, all variability in measurements will be due to the part-to-part variation, and only a negligible proportion of variability will be due to operator reproducibility and trial-to-trial repeatability.

In the repeatability and reproducibility study, the sandwiches were prepared by dry mix of calcinated raw meal from St. Constant, fired at 1550°C for 0.5 hour with heating rate of 6°C/min and under a load of 5.3 MPa, and tested by 3-point bending mode with span of 90 mm. Doloma brick BD2 was used as a reference refractory. Three operators were

involved in running this study. Each operator prepared 18 sandwiches and fired 3 sandwiches once for 6 times in an electrically heated furnace. Therefore, 3 operators, 6 parts (firing and measurements) and 3 trials for each operator were used to analyze the data of the repeatability and reproducibility study, as listed in Table 5.5.

5.2.2 Statistical Analysis

The sandwich test is reproducible if different users of the protocol come up with identical or similar measurements. It is repeatable if repeated measurements of the same part produce identical results. Both of these characteristics – repeatability and reproducibility – will affect the precision of the measurement system. The magnitudes of repeatability, reproducibility and variability between parts are estimated, and thus the precision of the measurement system is assessed. In essence, this procedure amounts to an analysis of variance (ANOVA) on an experimental design that includes as factors different parts, operators and repeated measurements (trials). Repeatability can be assessed using variance due to differences across trials, reproducibility by variance due to differences across operators, and variability between parts by variance due to differences across parts. The ANOVA table will also contain an F test – statistical significance test for the operator-by-part interaction, and report the estimated variances, standard deviations, and confidence intervals. Finally, the respective percentages of total variation will be computed, that is, so-called percent-of tolerance statistics.

Table 5.5 The design and resultant data for repeatability and reproducibility study

Operator	Firing	Trial	MOR, MPa
G	1	1, 2, 3	5.82, 5.94, 5.85
G	2	1, 2, 3	6.11, 6.02, 5.98
G	3	1, 2, 3	5.09, 4.95, 4.98
G	4	1, 2, 3	5.35, 5.45, 5.34
G	5	1, 2, 3	6.37, 6.26, 6.13
G	6	1, 2, 3	5.17, 5.02, 5.15
H	1	1, 2, 3	5.58, 5.78, 5.55
H	2	1, 2, 3	6.29, 6.12, 5.93
H	3	1, 2, 3	5.15, 5.09, 4.99
H	4	1, 2, 3	5.31, 5.30, 5.22
H	5	1, 2, 3	6.21, 6.17, 6.16
H	6	1, 2, 3	5.10, 5.39, 5.01
K	1	1, 2, 3	5.60, 5.79, 5.89
K	2	1, 2, 3	5.95, 6.12, 5.81
K	3	1, 2, 3	4.88, 5.06, 4.76
K	4	1, 2, 3	5.00, 5.07, 5.44
K	5	1, 2, 3	5.98, 5.98, 5.89
K	6	1, 2, 3	5.09, 5.06, 4.85

Figure 5.4 is the repeatability and reproducibility summary plot. The individual points plotted in this figure are the deviations of the respective MOR measurements from the average measurement for respective parts. The three measurements made by one operator on the same firing are connected via the vertical line. Excessively long lines identify wide ranges of measurements on the same part, and thus greater imprecision. The points representing the measurements by each operator are enclosed in a box, indicating the general range of measurements taken by the respective individual. The average deviation of the respective operator's measurements is also indicated by the dashed horizontal line in each box. The height of the box is an indication of the variability of measurements across trials. It is obvious that operator G produced less variability across measurements on the same part than the other two operators.

It has to identify outliers among all the parts or firings, that is, to identify those parts that are particularly difficult to measure, and therefore, yield imprecise measurements. The S (sigma) chart for controlling the variability of the sandwich test is shown in Figure 5.5. It is the standard deviation for the three measurements (trials) by each firing for each of the three operators. The average standard deviation is indicated by the solid line at 0.111. The plus 3 times sigma limit for this chart is at 0.285, this upper control limit being indicated by the dashed line. None of the points are out of control limit and thus the variability of the MOR measurements is acceptable. Any outlier above that sigma limit, however, indicates the respective firing produced particularly unreliable measurements for the respective operator.

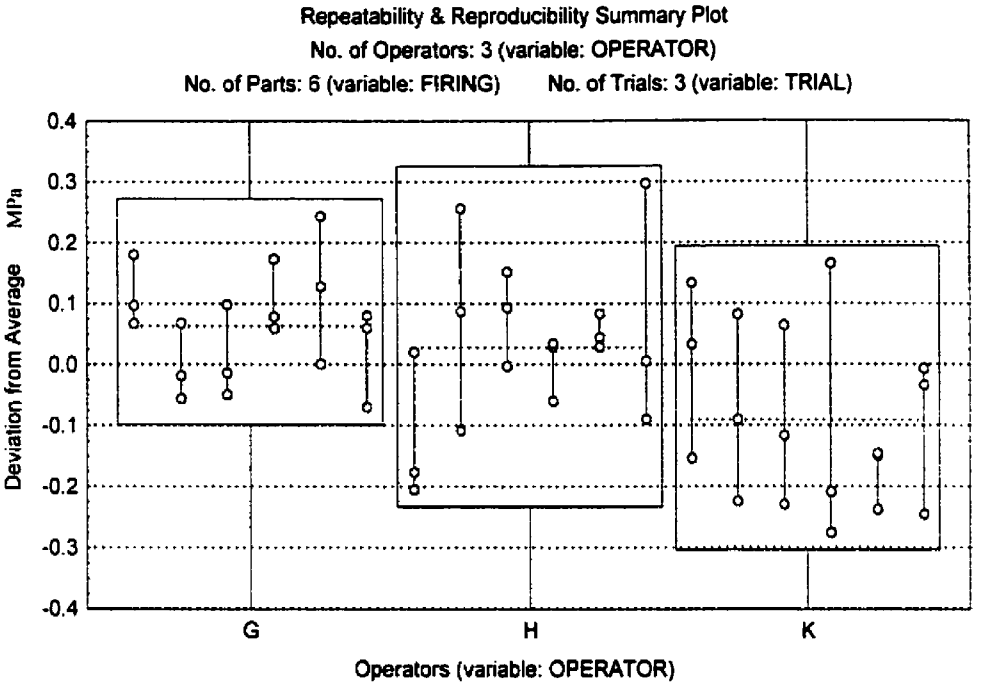

Figure 5.4 Repeatability and reproducibility summary plot

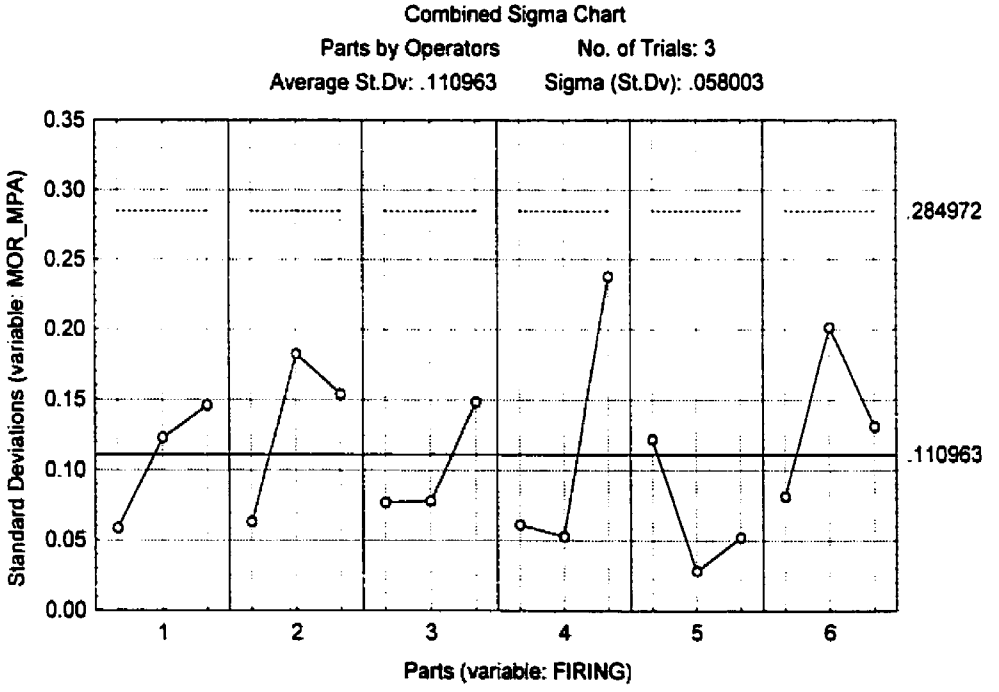

Figure 5.5 The S chart for repeatability and reproducibility study

Box and whisker plot provides another summary of the average measurements across trials and across parts, as shown in Figure 5.6. It also allows examining whether the measurements are normally distributed. For each operator, this plot summarizes the range of average measurements (averaged across trials) as well as the distribution of those average measurements. Based on the distribution from 25% to 75%, the ranges are quite close for the measurements from the three operators. In a normal distribution, the mean is equal to the median and would fall in the center of each box. Obviously, the measurements of operators G and K are closer to normal distribution than that of operator H.

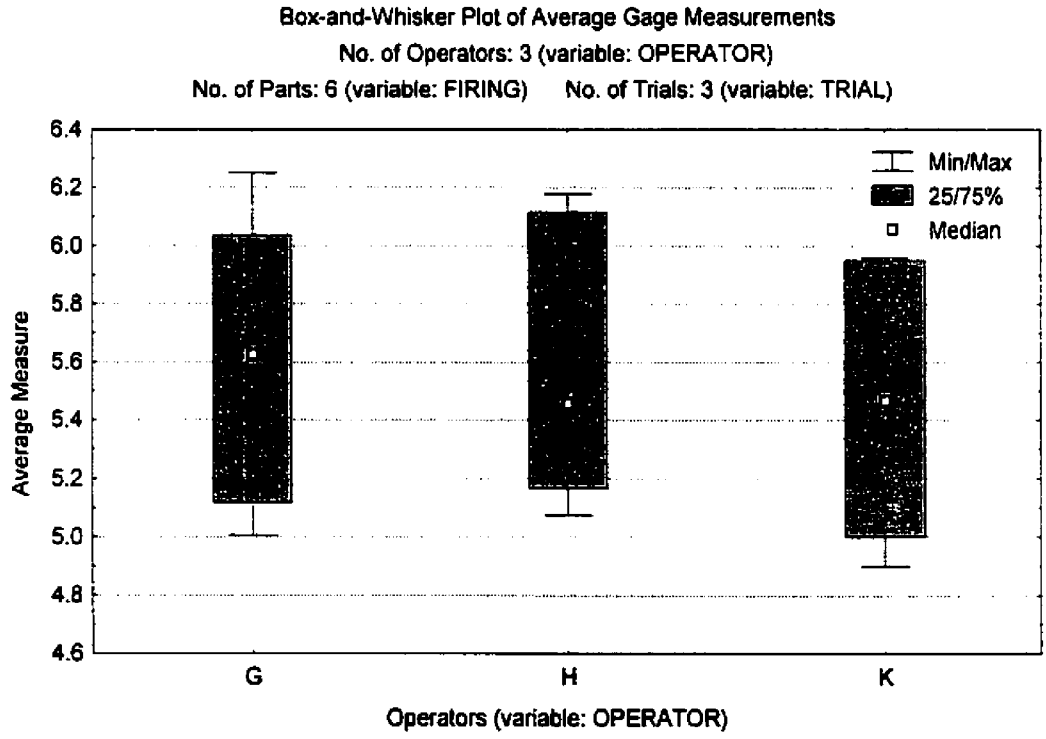

Figure 5.6 Box and whisker plot for repeatability and reproducibility study

The ANOVA on repeatability and reproducibility study is show in Table 5.6, where all variability is partitioned into main effects, two-way interactions, and the three-way interaction. This is a result of fundamental calculation, in which the big mean square may lead to significance influence. It is customarily assumed in repeatability and reproducibility experiments that no interactions exist between parts and trials, operators and trials, parts, operators and trials. Thus, it is assumed that there are no interactions by trials, which appears reasonable because it is difficult to imagine how the measurement of some parts is systematically different in successive trials. When more than one trials — repeated measurements occur, Table 5.6 can transform into Table 5.7, where only the operator-parts interaction is estimated separately and where all remaining variability is treated by trials as error variance. The *F* test of the statistical significance of the operator by part interaction can be performed. It is apparent that the operator by parts variability is not significant.

Table 5.6 The ANOVA (1) for repeatability and reproducibility

Source of Variance	Sums of Square	% of Total	df	Mean Square
Operators	0.23293	1.9700	2	0.1165
Parts (Firing)	10.83796	91.6631	5	2.1676
Trials	0.07752	0.6557	2	0.0388
Operators by parts	0.19208	1.6245	10	0.0192
Operators by trials	0.06588	0.5572	4	0.0165
Parts by trials	0.15364	1.2994	10	0.0154
Operators by parts by trials	0.26369	2.2302	20	0.0132
Total	11.82368	100.0000	53	0.2231

However, the operator by parts interaction may be important. It is conceivable that certain less experienced operators will be more prone to particular biases, and hence will arrive at systematically different measurements for particular parts. If so, then a significant two-way interaction would be expected.

Table 5.7 The ANOVA (2) for repeatability and reproducibility

Statistical Process Analysis Variable: MOR, MPa Mean = 5.547 Std.Dv = 0.472					
Source of Variance	Sums of Square	df	Mean Square	F ratio	P-value
Operators	0.23293	2	0.1165		
Parts (Firing)	10.83796	5	2.1676		
Operators by parts	0.19208	10	0.0192	1.2332	0.3039
Error	0.56072	36	0.015576		
Total	11.82368	53	0.2231		

Since the operator by part interaction is not statistically significant, the variance estimates and their errors are determined in Table 5.8, using the ANOVA method. In this case, the combined repeatability and reproducibility variability is defined as the sum of two components: 75% repeatability (error) and 25% operator variability. The variance components can be expressed in terms of percentage of the total variability. In Table 5.8, the last column of numbers reports the variability due to different sources relative to the total variability in the measurements. Repeatability of measurements accounts for

6.27%, reproducibility across operators accounts for 2.13% of the total variability, the part-to-part variation accounts for 91.6%, and the combined repeatability and reproducibility variability accounts for about 8.4% of the total variability. Thus, most of the variability in measurements is due to differences between parts, as is desirable for a reliable measurement system. Using the common guidelines for evaluating the quality of the measurement system (under 10% = acceptable, 10% to 30% = questionable, above 30% = needs improvement) [90], the performance of the sandwich test is acceptable.

Table 5.8 Variance estimates for repeatability and reproducibility

Source	Estimated Sigma	0.9 Lowr Conf.Lim	0.9 Uppr Conf.Lim	Estimated Variance	% of R&R	% of Total
Repeatability	0.1279	0.1095	0.1547	0.0164	74.64	6.27
Reproducibility	0.0746	0.0334	0.3537	0.0056	25.36	2.13
Part-to- parts	0.4889	0.3128	1.0345	0.2390		91.60
Combined R&R	0.1327	0.1327	0.3763	0.0219	100.0	8.40
Total	0.5108			0.2609		100.0

The tolerance analysis was made to compute the percent tolerance values, i.e., to express the variability due to reproducibility and repeatability errors relative to the engineering tolerance. As shown in Table 5.9, the second column contains the respective estimates of sigma in Table 5.8 times the number of sigma intervals = 5.15. The percent total contribution is the percentage values relative to the total variance. The percent process variation is the respective percentage values (for the ranges in the second column)

relative to the total variation range. Repeatability of measurements accounts for 25.0%, reproducibility across operators accounts for 14.6% of the total variability, the part-to-part variation accounts for 95.7%, and the combined repeatability and reproducibility variability accounts for 28.9% of the total process variability. Therefore, these percentages indicate that the performance of the sandwich test is marginal at best, and it may have to be improved.

Relative to the acceptable tolerance for the respective process, the repeatability and reproducibility errors account for 8.2 and 4.8, respectively. The variability introduced by repeatability and reproducibility errors combined account for 9.5% of the tolerance. Thus, this measurement system seems to be acceptable, given the tolerance value of 8.

Table 5.9 Percent Tolerance analysis for repeatability and reproducibility

Source	Measrmnt unit	% proc. variation	% total contribution	% of tolerance
Repeatability	0.6588	25.0427	6.2714	8.2353
Reproducibility	0.3841	14.5981	2.1310	4.8006
Part variation	2.5178	95.7066	91.5967	31.4731
Combined R&R	0.7626	28.9869	8.4024	9.5323
Total proc. variation	2.6308	100.0000	100.0000	32.8849
Tolerance	8.0000			100.0000

Similarly, another not-well-statistically-designed experiment was conducted by two operators to verify repeatability and reproducibility of adherence strength on doloma bricks of reference with a compressive load of 2.4 kPa on sandwiches fired at 1550°C for 30 minutes holding time. Five batches of sandwiches were tested with maximum six ones fired at once in the furnace used, obtaining twenty-six values of adherence strength. As shown in Figure 5.7, the mean adherence strength is 4.1 MPa with a standard deviation of 0.4 MPa, which is the same level as that in Figure 3.14. This confirms the results of the statistically designed repeatability and reproducibility experiment.

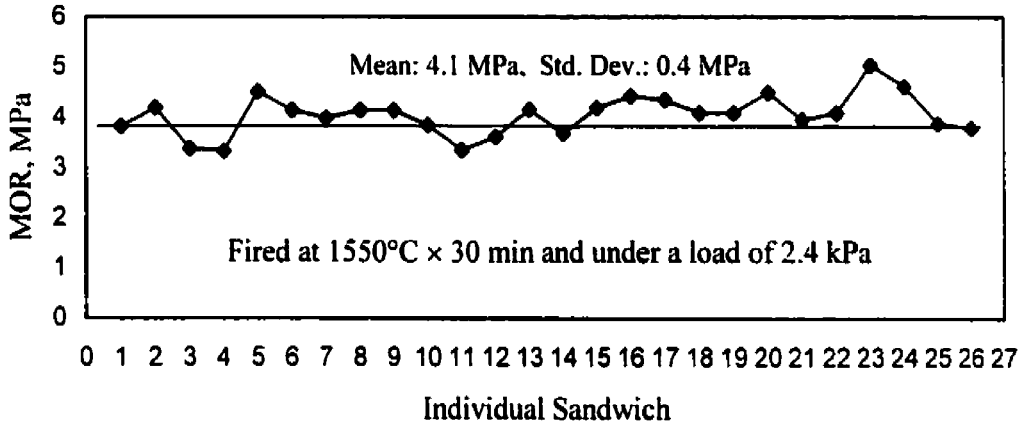

Figure 5.7 Repeatability and reproducibility test results on doloma brick LD1

To summarize, the sandwich test is repeatable (small variability across trials) and is reproducible (small variability across operators) relative to the variability between parts. The mean value of adherence strength for doloma brick is 5.55 MPa with standard deviation 0.47 MPa, obtained after firing at 1550°C for 30 min under a load of 5.3 kPa.

5.3 Evaluation of Various Basic Bricks for Rotary Cement Kiln

Some eight brands of basic bricks have been tested to differentiate their adherence strength using the sandwich test. Two sets of results, shown in Figure 5.8, are from sandwiches made using a wet paste of the calcinated raw meal from St. Constant plant, and fired at a clinkerization temperature of 1450°C for 30 min and under a load of 2.4 kPa, obtained at six months interval. The reproducibility is considered acceptable for the brands that have been tested twice. Values of adherence strength are ranked in the order from the highest to the lowest: doloma, doloma-zirconia, doloma-magnesia and magnesia-spinel, which is consistent with their performance in rotary cement kilns.

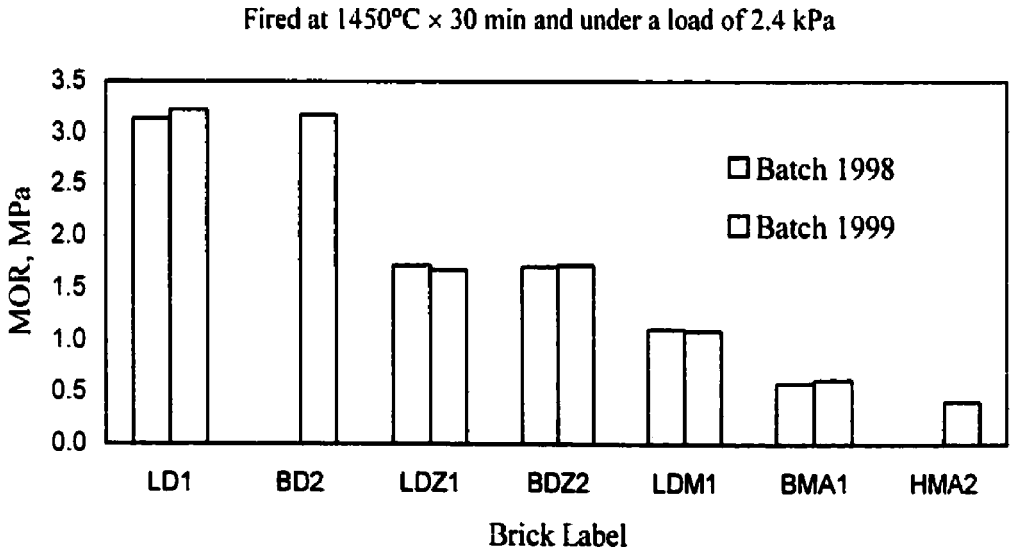

Figure 5.8 Adherence strength of various basic bricks using wet paste

Adherence strength of various basic bricks, using sandwiches made by dry mix instead of a wet paste and fired at temperature of 1550°C for 30 min and under a load of 5.3 kPa, is illustrated in Figure 5.9. Once more, although the temperature of firing sandwiches is different in both cases, the ranking order, in terms of adherence strength. is the same as follows:

Doloma > doloma-zirconia > doloma-magnesia > magnesia-spinel

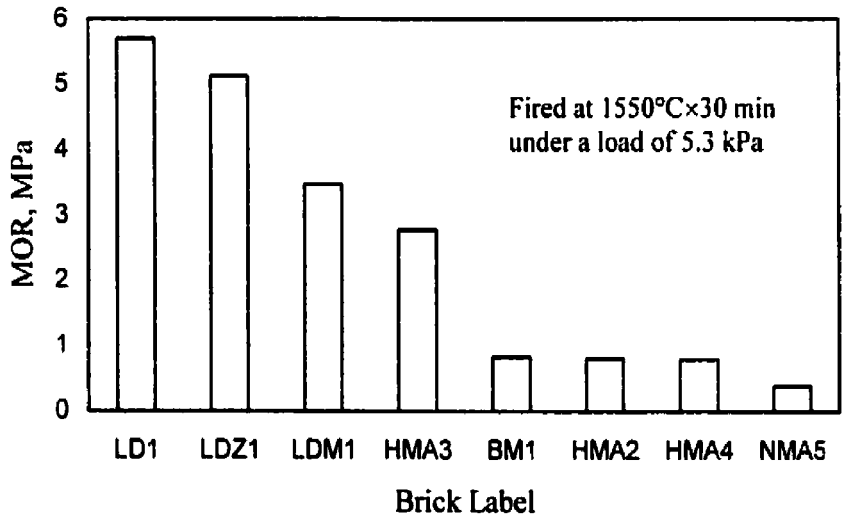

Figure 5.9 Adherence strength of various basic bricks using dry mix

The fact that the measurements are significantly different from one brand to another brand reveals the meaningful value of this simple laboratory test protocol. The results of testing various basic bricks have reflected their coatability performed in rotary cement kilns.

5.4 Conclusions of Chapter 5

The following conclusions can be reached from ruggedness test, repeatability and reproducibility study, and evaluation of various basic bricks.

(1) From a statistical analysis of the results of ruggedness test, it is concluded that the sandwich test is rugged: none of the variables, from within the domain chosen, have a direct major effect on the response. Therefore the sandwich test is insensitive to minor changes such as holding time, paste thickness and mixing mode of the paste.

(2) The sandwich test is repeatable with small variability across trials, and is reproducible, having small variability across operators, relative to the variability between batches of firing. The standard deviation of 0.47 MPa has been obtained, for adherence mean value -- 5.5 MPa on doloma brick fired at temperature of 1550°C for 30 min and under a load of 5.3 kPa.

(3) The sandwich test is able to differentiate the coatability of various basic bricks in laboratory. The results reflect coating performance of basic bricks in rotary cement kilns. It is a reliable test.

CHAPTER 6. EFFECT OF BRICK TEXTURES ON COATABILITY

So far, the sandwich test enables to obtain reliable values of adherence strength for a specific refractory and to differentiate the coatability of various basic bricks. In this chapter, some explanations are to be provided to interpret why doloma-based bricks perform better in terms of coatability than magnesia spinel bricks, and why one given brand of basic brick may have totally different coatability from another one. It will be shown that it is possible to correlate coatability to the microstructure of the bricks.

6.1 Sample Preparation

Some samples of the sandwich test have been carefully polished. Using reflected light on polished samples properly etched enables details of structure to be better discerned. Preparing samples involves the following steps:

(1) Impregnating and embedding the sandwich with clinker coating in synthetic epoxy;

(2) Preparing a small piece of sample by sawing;

(3) Mounting and impregnating the sample in a ring mold with epoxy again;

(4) Grinding and polishing the sample, Alcohol was used instead of water;

(5) Etching and staining the polished surface of the sample.

Some details of preparing sample, similar to polishing clinker sample, were introduced in Section 3.15 in Chapter 3. For etching of the cement clinker, the polished section was held for 20 seconds in a solution made of 1 gram of ammonium nitrate (NH_4NO_3), in 150 ml isopropyl alcohol, 20 ml water, 20 ml ethyl alcohol and 10 ml acetone. Then the polished section was sprayed with alcohol. After drying, the sample was immersed in a second solution containing 0.2 gram of salicylic acid, 25 ml isopropyl alcohol and 25 ml water.

For magnesia spinel bricks, in order to distinguish periclase (MgO) from spinel, the polished section was exposed to a 30% solution of sulfuric acid for 2 minutes, which results in etching the crystals of MgO with spinel remaining intact.

Cathodoluminescent technique was helpful in microstructure observations to distinguish spinel from alumina grains.

6.2 Coating on Doloma Based Bricks

6.2.1 Textures of Typical Bricks

Pure Doloma Brick is produced by pressing a combination of sized doloma grains with an organic binder. Direct bonding between the doloma grains is achieved after firing the bricks through a kiln. Essentially, doloma brick is made up of direct bonded doloma

grains. High purity doloma grains are basically composed of rounded magnesia crystallites embedded in a continuous matrix of lime, as shown in Figure 6.1. It is the CaO phase that provides the direct-bond and is responsible for the chemical properties of the brick. Direct-bonding between doloma grain is shown in Figure 6.2.

Figure 6.1 Microstructure of doloma grain LD1 ×300

Doloma brick is a basic kiln liner which exhibits excellent coatability and retention characteristics. Coating is formed by virtue of the brick's free lime reacting with silicates from clinker to form the stable C_3S phase. It is this chemical compatibility with cement chemistry which promotes rapid coating formation and strong refractory bond at the brick/coating interface. On account of the highly basic characteristic, alkalis do not react

with doloma components MgO and CaO. Doloma is then not susceptible to corrosion by alkalis. Doloma is also highly resistant against REDOX conditions because the direct bond between MgO and CaO, as well as CaO, is predominant and the only reducible phase – C_2F represents only a minute portion of the matrix. However, sulfur and chloride can react with CaO in the brick which may result in loss of bonding strength. Due to its limited spall resistance, doloma brick is intended for use only in the burning zone, under stable operation conditions.

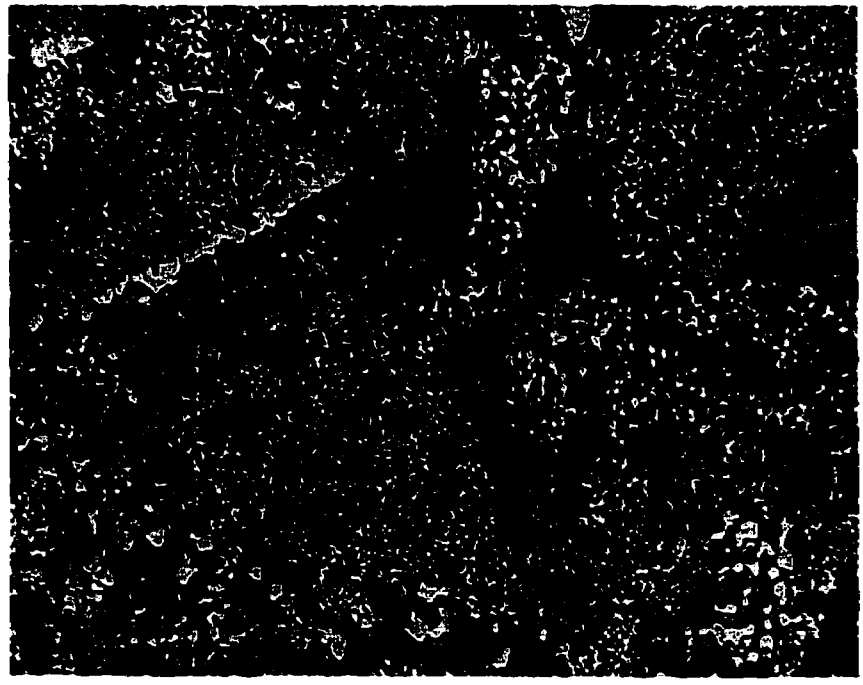

Figure 6.2 Direct-bonding between doloma grains LD1 ×20

Doloma Containing Zirconia retains all the favorable characteristics of fired doloma brick but has improved spalling resistance via the inclusion of some 2% zirconia. Figure

6.3 shows that the addition of high purity zirconia grain decreases the extent of direct solid bonding by the formation of microcracks within the structure, and creates microcracks in the brick's matrix which interrupt spalling crack propagation through the brick. In other ceramic systems incorporating ZrO_2, microcrack formation is attributed to the zirconia phase transformation. But in doloma brick, microcracking was primarily due to the formation of a new compound, calcium zirconate. This reaction phase is developed via diffusion of the lime into the zirconia grain. The reaction is noted to be of an expansive nature and it is this expansion that is the major cause of microcrack formation in a doloma brick, and not the expansion due to phase transformation. A second mechanism of microcrack formation is also shown in Figure 6.3, as thermal expansion differences between calcium zirconate, zirconia, calcia and magnesia, exist and all these contribute to a general opening up of the brick matrix. At any rate, the formation of microcracks results in significant improvements in the thermal shock resistance of doloma bricks.

Doloma-Magnesia Containing Zirconia – A portion of the doloma is replaced by magnesia while retaining the benefit of a zirconia addition. Figure 6.4 shows microstructure of doloma-magnesia brick with zirconia addition. Doloma grains are bonded by magnesia matrix. The particularly active portion of fine doloma particles is substituted with considerably less active particles of magnesia in order to eliminate the influence of sulfatization and recarbonatation upon doloma. Normally, an enrichment of the fines with burned magnesia is selected at a magnitude of 30%.

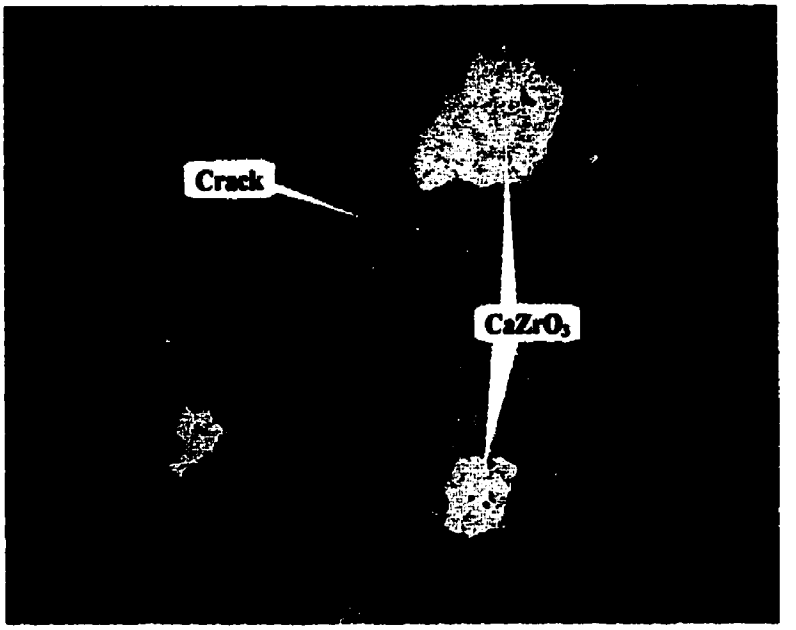

Figure 6.3 Microstructure of doloma zirconia brick LDZ1 ×20

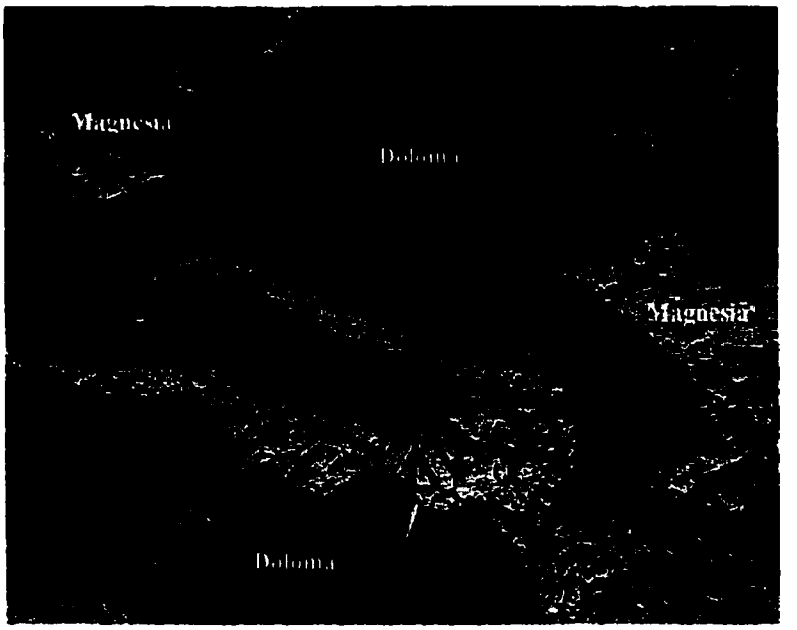

Figure 6.4 Microstructure of doloma-magnesia brick BDM2 ×20

6.2.2 Coating Formation

Figure 6.5 shows adherence strength for three typical doloma-based bricks, including pure doloma LD1, doloma zirconia LDZ1 and doloma-magnesia BDM2. The sandwich was prepared with dry mix of calcinated St. Constant raw meal, fired at 1550°C for 0.5 hour and under a compressive load of 5.3 kPa, then tested for modulus of rupture at room temperature. Again, adherence strength of doloma brick is the highest, followed by doloma zirconia and then doloma-magnesia bricks. Their sandwich samples after testing were examined by microstructural analysis, to illustrate how the adherence is built up and what reactions take place at the clinker/brick interfaces.

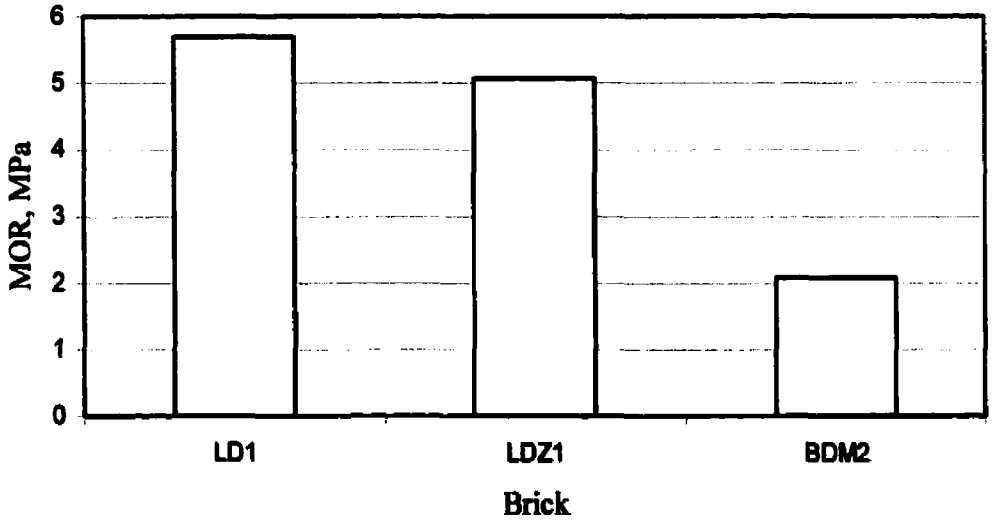

Figure 6.5 Adherence strength of three typical doloma-based bricks

There is less adhesion when the reactivity of refractory components to clinker is low. Due to presence of inert MgO and $CaZrO_3$, restricting CaO contact with clinker leads to

decrease of adherence strength, from doloma to doloma zirconia, doloma magnesia bricks. Figure 6.6 shows the reaction interface at the clinker/doloma brick boundary. Four zones can be clearly distinguished as § Clinker § MgO-agglomerated zone § Fine crystals of alite and belite – MgO zone § CaO-MgO regular doloma structure §. Clinker remains alite as the dominant crystalline phase, the details being indicated in Section 3.1.5, page 48. MgO-agglomerated zone, with thickness of about 100 μm, contains predominantly 10-20 μm round periclase crystals and interstitial phases – calcium ferrites. Around 1000 μm thick layer between MgO-agglomerated zone and the unaltered zone of the doloma brick is composed of fine crystals of alite and belite with C_3A and C_4AF liquid phases, as well as small periclase grains that are very rich in this layer.

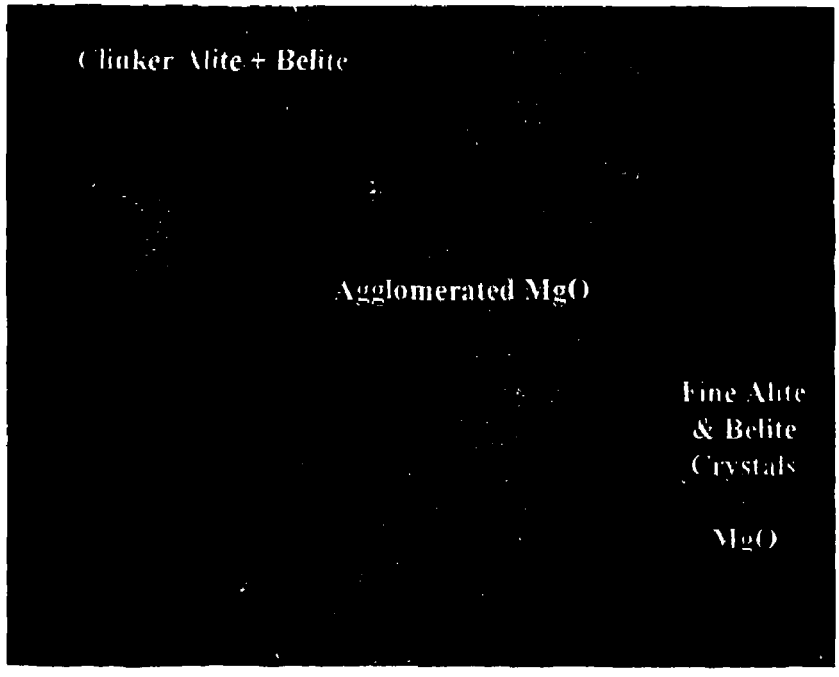

Figure 6.6 Microstructure of the doloma/clinker interface ×150

Obviously, doloma brick's CaO near the clinker/brick interface reacts with clinker, leaving MgO from doloma grains to agglomerate at the interface, as indicated by the zone of the round shape of periclase grains of Figure 6.6. The liquid phases in clinker penetrate into doloma brick to promote their reactions, and greatly contribute to the mass transport necessary for the formation of calcium silicates. It is shown by the relatively high content of liquid phases in MgO agglomerated zone at the interface. The excess of CaO at the interface leads to formation of C_3S zone, which is highly beneficial to coating formation.

Doloma-zirconia brick contains a small amount of $CaZrO_3$ crystals. Investigation of $CaZrO_3$ showed that it is not chemically reactive when fired with compounds in cement clinker [91]. $CaZrO_3$ is structurally stable on firing and not subjected to polymorphic structural conversions. However, $CaZrO_3$ crystals existing at the interface of clinker/doloma-zirconia brick may block contact of lime in doloma grain with clinker in limited area, as shown in Figure 6.7. This may reduce, more or less, the bonding between clinker and doloma grains, which results in a little lower adherence strength of doloma zirconia than that of pure doloma brick.

Doloma-magnesia brick consists of doloma aggregates bonded by magnesia matrix, as well as calcium zirconate. Any mutual reaction between clinker, MgO, and $CaZrO_3$ was not observed. The effective adherence still forms between doloma grains and clinker, but with reduced contact area. Figure 6.8 shows the boundary of clinker/doloma-magnesia brick.

Figure 6.7 Microstructure at the interface of clinker/doloma-zirconia brick ×150

6.2.3 Influence of Silica Ratio

The factorial plan of experiments in Section 4.4 of Chapter 4 has revealed that silica ratio is the most significant factor to influence adherence strength among the parameters of the raw meal. It is confirmed in Figure 6.9, which shows that adherence strength increases with rising silica ratio in the range of 2 to 3 as the other conditions are alumina ratio of 1.5, heating rate of 4°C/min, on doloma brick BD2. It is noticed that the two brands of pure doloma bricks, LD1 and BD2 from different manufacturers, show no differences on adherence strength with the same clinker.

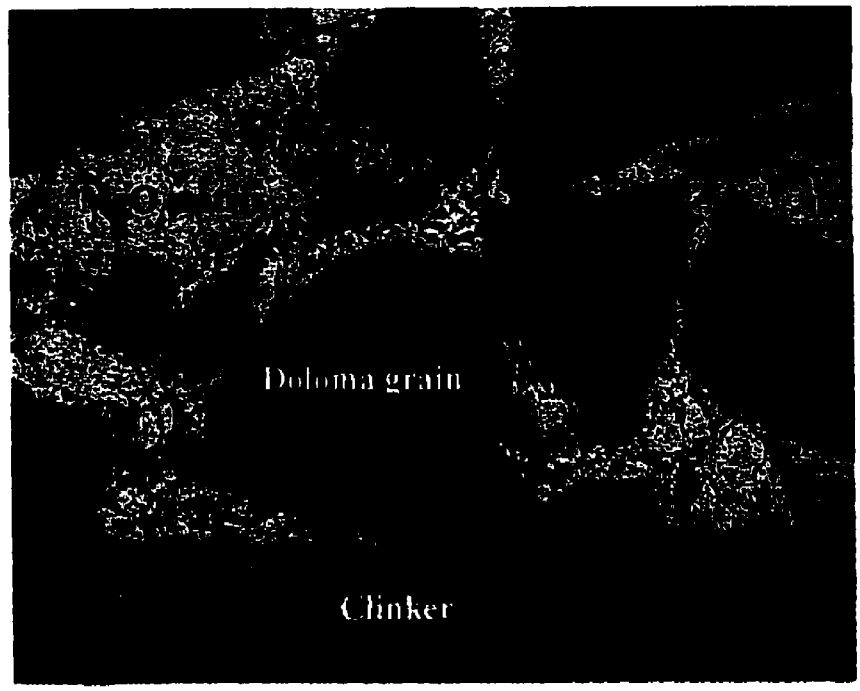

Figure 6.8 Microstructure at the interface of magnesia-doloma brick ×20

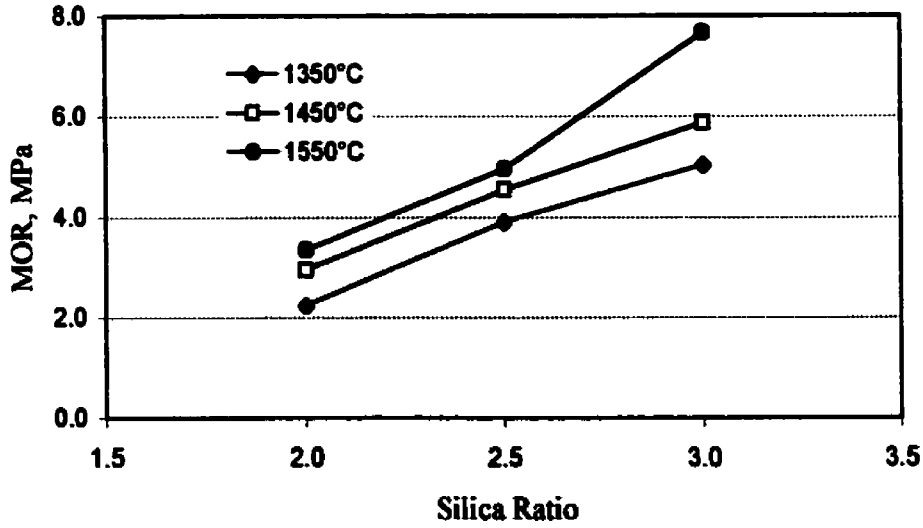

Figure 6.9 Influence of silica ratio on adherence strength

According to the following equations,

$$SR = \frac{SiO_2}{Al_2O_3 + Fe_2O_3} = \frac{C_3S + 1.325C_2S}{1.434C_3A + 2.046C_4AF}$$

$$AR = \frac{Al_2O_3}{Fe_2O_3} = 0.64 + \frac{1.15C_3A}{C_4AF}$$

Silica ratio varies with ratio of silicate minerals to flux minerals. If silica ratio of clinker is too high, amount of liquid during burning reduces significantly and it is very hard to clinkerize. With low silica ratio, plenty of liquid forms in clinker at high temperature. Alumina ratio represents viscosity of liquid during burning of clinker. With high alumina ratio, more C_3A and less C_4AF result in more viscous liquid formed in clinker. Reversibly, low alumina ratio leads to forming liquid with low viscosity.

In the first run of the factorial plan of experiments in Section 4.4, Table 4.9 in page 95, the clinker has a lower silica ratio and a lower alumina ratio. It means that more CaO from raw meal can react to form C_3A and C_4AF since there is more fluid liquid in the clinker, compared to a clinker with higher silica ratio and alumina ratio as in the fourth run. The microstructure of the sandwich sample of the first run is shown in Figure 6.10. The liquid in clinker penetrates over 500 μm deep into doloma brick and reacts with lime, transferring magnesia to the interface. MgO grains precipitate to form a continuous

50-100 μm thick layer, which reduces bonding between clinker and doloma brick, as shown in Figure 6.11.

Figure 6.10 Microstructure of doloma brick exposed to clinker with SR=2.0 & AR=1.0 ×30

In the sandwich with raw meal of high silica ratio and alumina ratio, there is less liquid in the clinker, and it is a viscous liquid. Figure 6.12 reveals the microstructure of the sandwich sample of the fourth run. It shows much thinner altered zone at the interface of clinker/doloma brick than in the sample with low silica ratio clinker (see Figure 6.11). Periclase grains are bonded by calcium silicates and liquid phases. Silica in clinker just reacts with lime near the interface, as indicated by some small residual MgO. There is no

significant penetration of liquid clinker. It seems that retaining original doloma structure near the interface is very helpful to obtain higher adherence strength.

Therefore, lower silica ratio leads to more liquid formation in clinker, which accelerates reaction between clinker and doloma brick. However, due to growth and agglomeration of dissociated MgO from doloma grains at the interface, a continuous layer of MgO is detrimental to adherence strength of doloma brick. Higher silica ratio clinker, with less and more viscous liquid at high temperature, strongly adheres on doloma brick just through reactions with lime at the interface, to form C_3S.

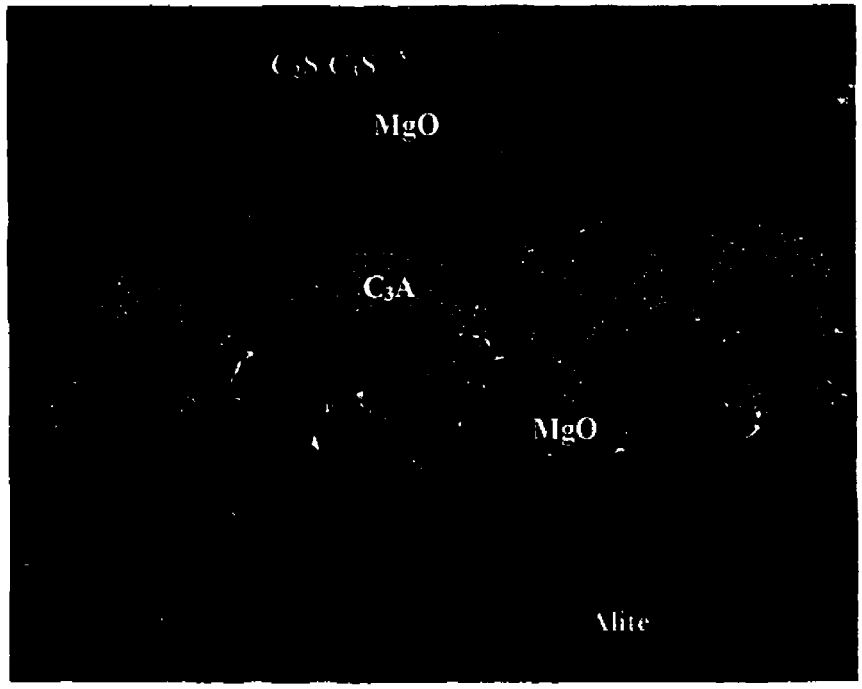

Figure 6.11 MgO agglomerated layer at the interface of doloma brick/clinker with SR=2.0 & AR=1.0 ×400

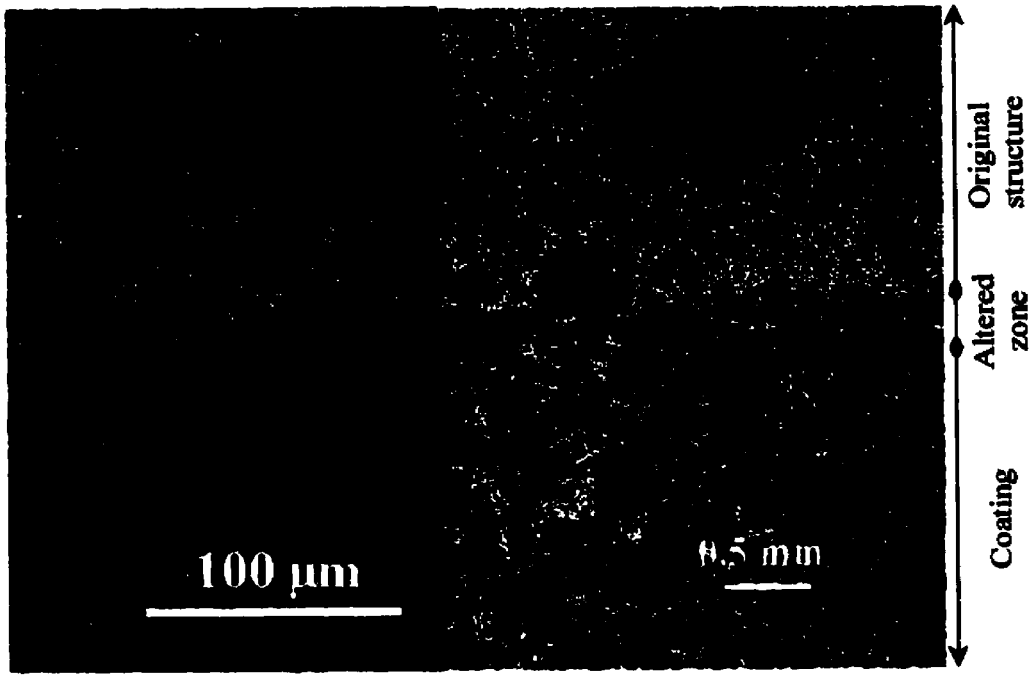

Figure 6.12 Microstructure of the interface of doloma brick/clinker with SR=3.0 & AR=1.5

6.3 Coating on Magnesia-Spinel Bricks

6.3.1 Textures of Samples

The two kinds of magnesia spinel bricks, tested HMA3 and NMA5, have quite similar chemical and physical properties, as listed in Table 3.7, but very dissimilar adherence strength with the same clinker, as shown in Figure 5.9, page 125. Brick HMA3 is typically developed to have higher resistance to the attack of sulfur and chlorine, and contains reinforced spinel bonding in the brick's matrix. Placement of fine, crystalline spinel in the matrix shields the more vulnerable matrix from attack of acidic species, and

generally improves the strength and overall physical properties of the brick. This brick contains both coarse, pre-reacted spinel and fine, crystalline spinel in the bond phase, as shown in Figures 6.13 and 6.14.

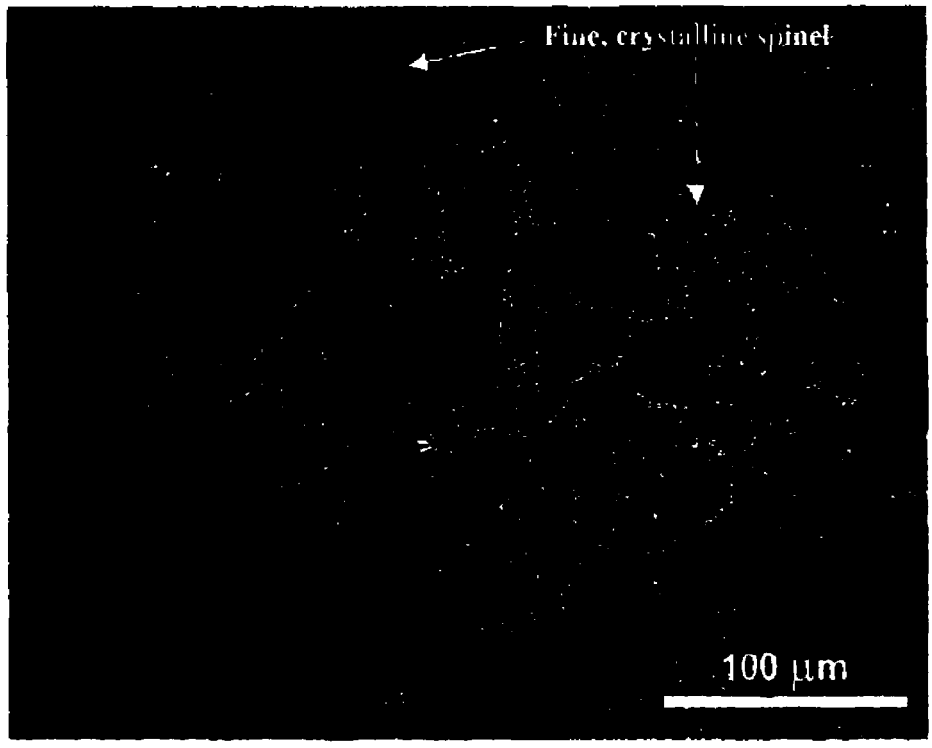

Figure 6.13 Fine, crystalline spinel in the matrix of brick HMA3

The coarse, pre-reacted spinel containing brick possesses excellent structural flexibility that absorbs and dissipates mechanical and thermal shock stress before catastrophic damage occurs to the brick's structure. A high purity matrix and careful addition of pre-reacted spinel assure the brick properties necessary for consistent service life. The fine and crystalline spinel is generated by the addition of pure alumina powder, which leads

to advanced thermal shock resistance with improved coating attraction properties relative to only pre-reacted spinel containing magnesia spinel brick.

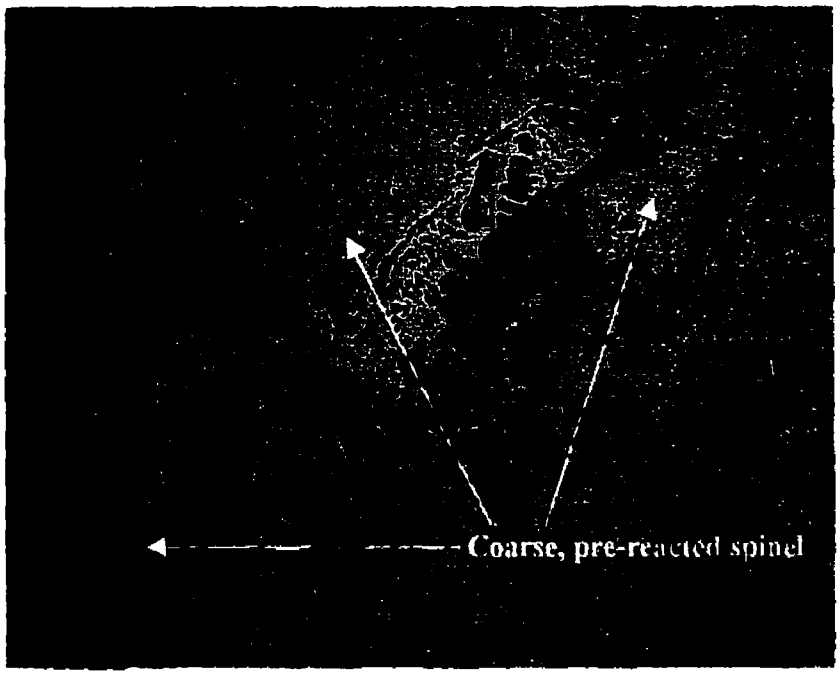

Figure 6.14 Coarse, pre-reacted spinel in brick HMA3 ×100

Figure 6.15 shows microstructure of brick NMA5, which consists mainly of sintered magnesia grains and fused alumina grains. Spinel rings were formed around coarse, fused alumina grains, as clearly shown in Figure 6.16. On the top-left corner of Figure 6.15, alumina grain and spinel ring were distinguished by using cathodoluminescence technique. No pre-reacted spinel is found in this brick. Void ring formation between spinel and fused alumina grain is important to interrupt spall crack propagation and to reduce thermal conductivity through the brick.

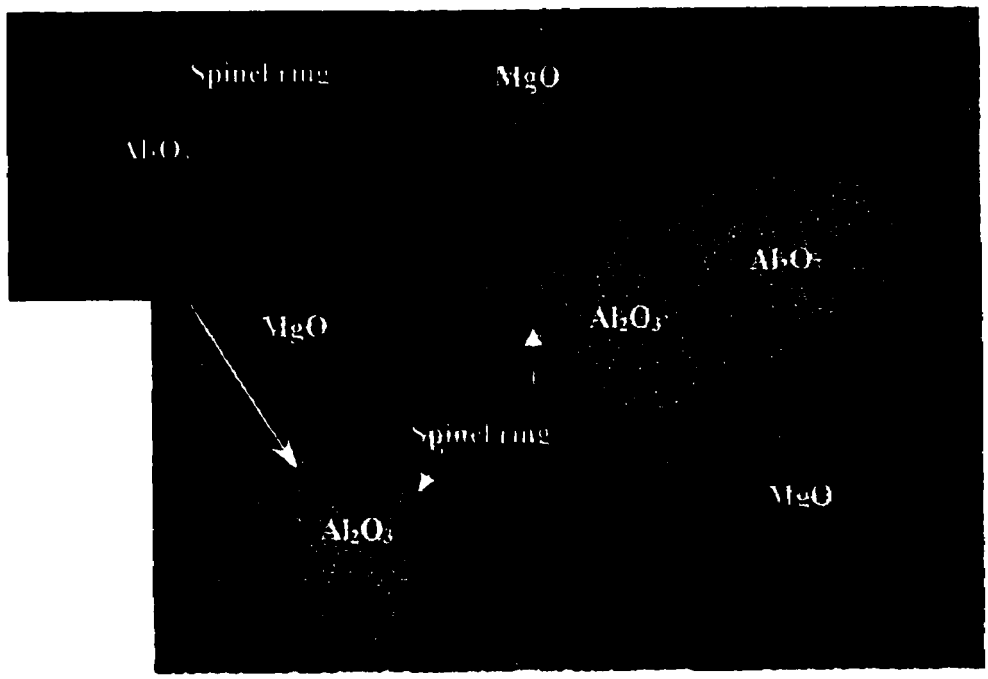

Figure 6.15 Microstructure of magnesia spinel brick NMA5 ×100

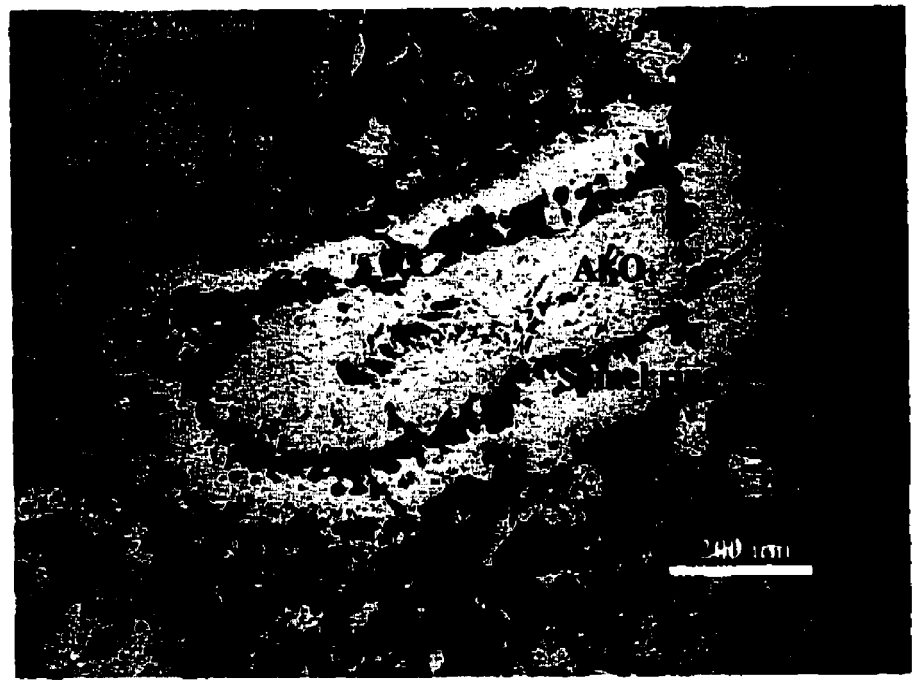

Figure 6.16 Spinel ring in magnesia spinel brick NMA5

6.3.2 Coating Mechanisms

Figure 6.17 shows the microstructure of a sandwich sample of magnesia-spinel brick HMA3. There are two obvious features in such a sandwich. Firstly, the phase composition of clinker adjacent to the brick is belite and in the center, alite. The coating is hence due to a belite layer (blue colored) on the magnesia spinel brick. Secondly, the liquid phase of the clinker deeply penetrates into the brick's matrix, up to a thickness of 3 mm, which is much deeper than that found in the doloma brick. Clinker penetration and dissolution of magnesia aggregates are observed along their grain boundaries in this brick.

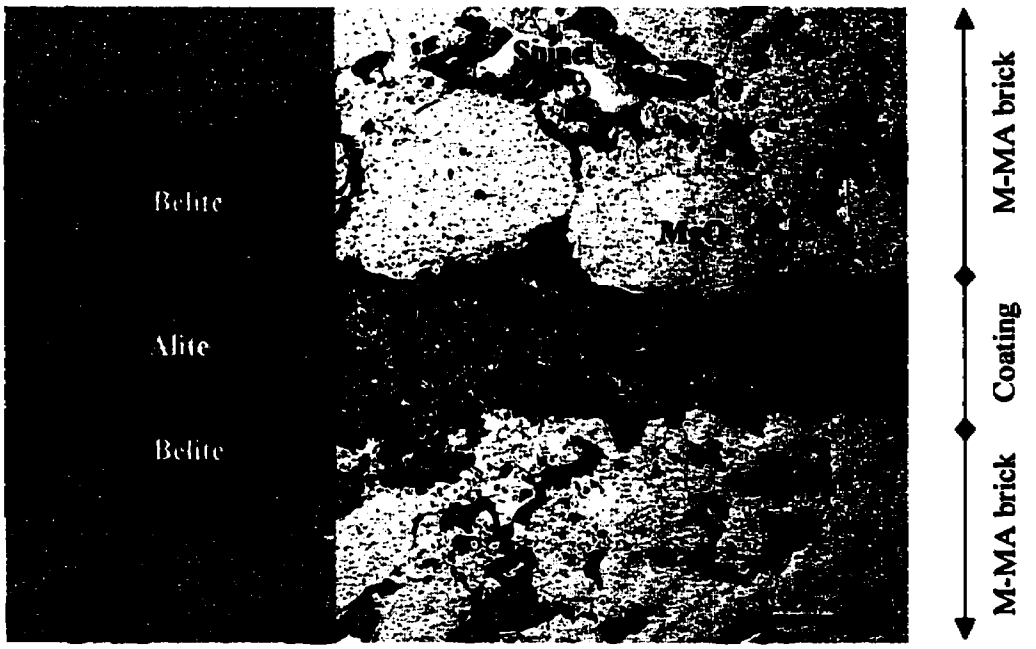

Figure 6.17 Microstructure of sandwich sample of magnesia spinel brick HMA3

The major constituent of magnesia spinel brick, MgO, can coexist with all of the major cement-clinker minerals, i.e., alite (C_3S), belite (C_2S), three-calcium aluminate (C_3A) and brownmillerite (C_4AF). Periclase will not react with either of them, but will be dissolved in the melt of CaO-SiO_2-Al_2O_3-Fe_2O_3 that form low melting eutectics under 1350°C with MgO. Those four components containing mixtures are the penetrating media into the grain boundaries of MgO aggregates and can form the only possible connection between MgO aggregates and cement clinker. In fact, this process can be considered as a sintering process in the presence of liquid phase with all of the typical phenomena characteristic of sintering.

Magnesium-aluminate, which is the second major constituent of the brick, can not coexist with either lime, or three-calcium silicate. The reaction of spinel with free lime and C_3S are found to be the most intensive and could be illustrated by the following equations [91].

$$MA + C_3S = C_2S + C_3A\,(C_{12}A_7)\,(C_5A_3) + M$$

$$MA + C = C_3A\,(C_{12}A_7)\,(C_5A_3) + M$$

As a result of those reactions, MgO is released from spinel and more liquid phases are formed in the system. Spinel is then consuming some lime, or three-calcium silicate, to form C_2S at the interface as it was found in Figure 6.17. This could explain why the adjacent layers of clinker to the brick are substantially richer in belite. Plenty of fine

spinel in the matrix of the brick consumes some lime from the raw meal to form belite, not leaving enough lime for full conversion to alite near the interface of clinker/magnesia-spinel brick. Spinel is compatible with di-calcium silicate, and no reaction was found between them.

Figure 6.18 shows SEM image of the sandwich sample of brick HMA3. All fine, crystalline spinel in altered zone has been reacted, forming a great quantity of liquid. It is obvious that the liquid in clinker penetrates first to dissociate $MgAl_2O_4$ spinel with formation of more liquid and then Al_2O_3 rich liquid reacts with C_3S phase in clinker to form C_2S phase. Reactions between spinel and clinker do not form any solid connection at high temperature because of low melting eutectics in the system. Some amounts of fine spinel in the brick is necessary for enhancing the liquid phase formation at the brick/clinker interface and thus accelerating the sintering processes that is essential for developing strength and building sustained coating on surface of the brick.

For magnesia spinel brick, it is obvious that the ability of coating will be much more sensitive to the very careful design of the brick's texture and composition, than it is in the case of the doloma bricks. Brick NMA5 is the other type of magnesia spinel brick being considered. The dissociation of part of spinel ring is observed just at the clinker/brick interface, as shown in Figure 6.19. Due to limited reactions occurring between clinker and the brick with weak bonding, adherence strength of brick NMA5 is much lower than that of brick HMA3.

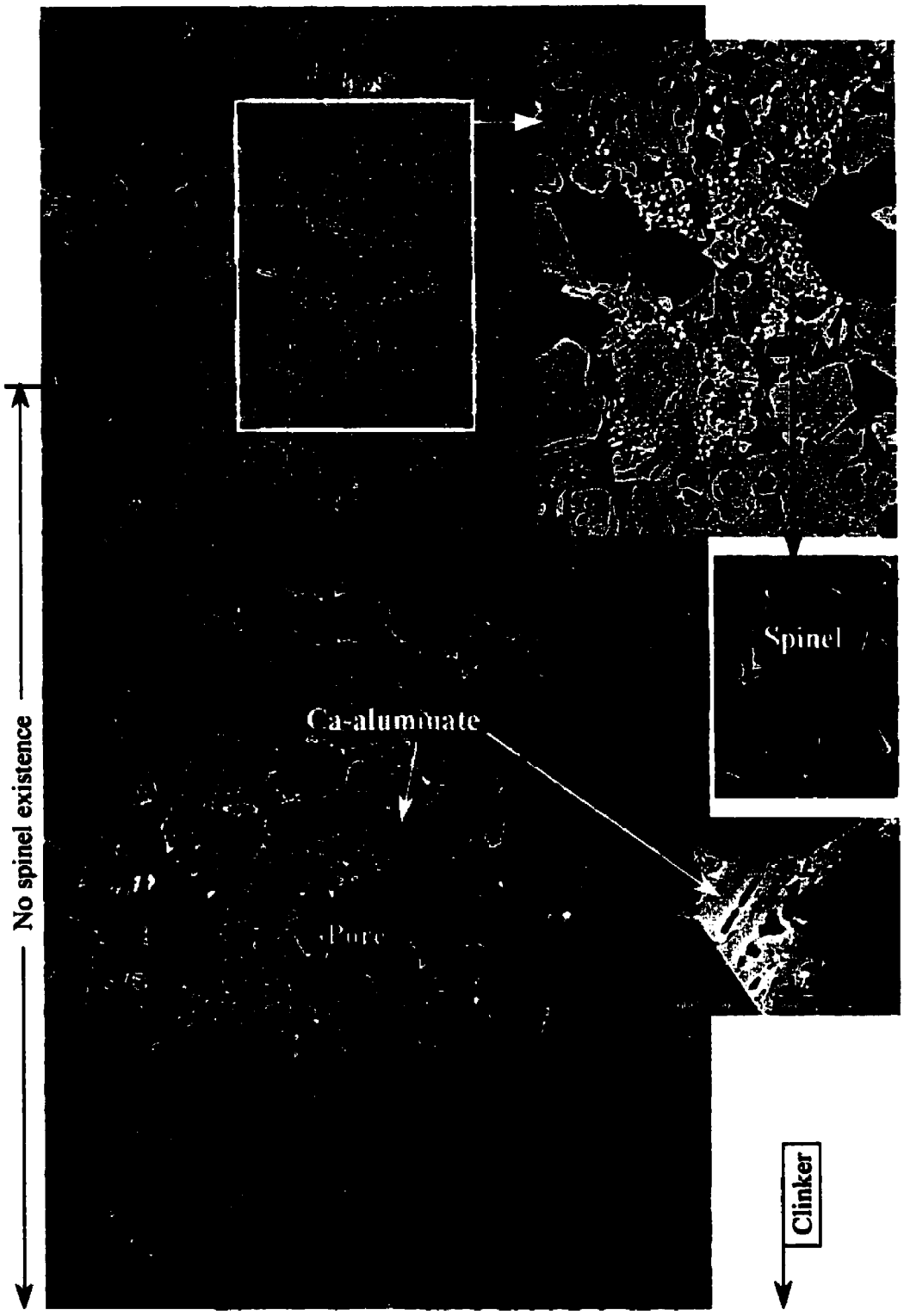

Figure 6.18 SEM image of magnesia spinel brick HMA3 exposed to clinker ×250

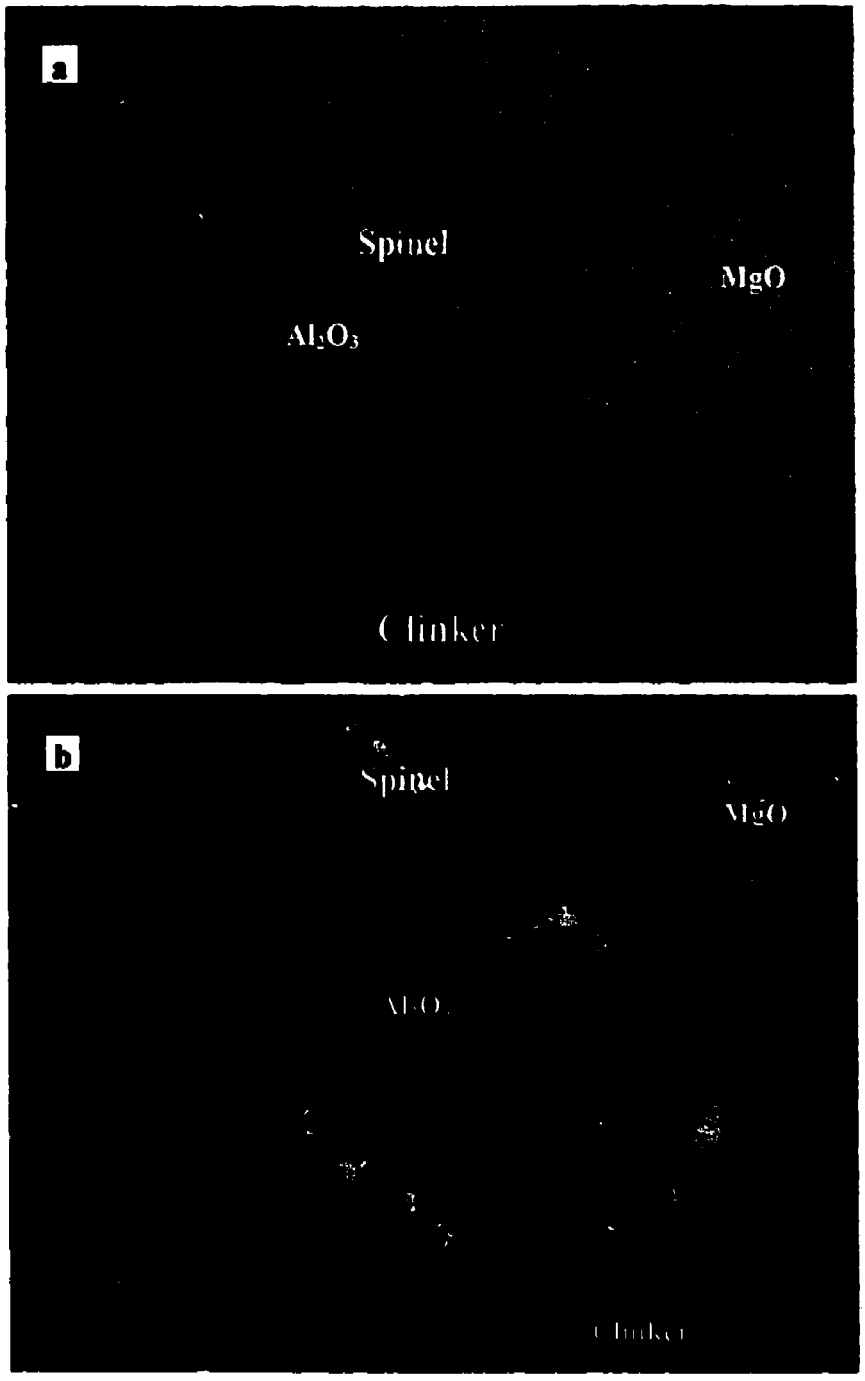

Figure 6.19 Image of the interface between clinker-brick NMA5

a. Reflected light ×100 b. Using cathodoluminescence ×150

6.3.3 Influence of Silica Ratio

Silica ratio also has a significant effect on adherence strength of magnesia spinel brick, as shown in Section 4.3, page 89, but this time the higher the silica ratio, the lower the adherence strength is. The effect is shown in Figure 6.20 for sandwich with a load of 5.3 kPa and a heating rate of 4 °C/min. This is contrary to doloma brick.

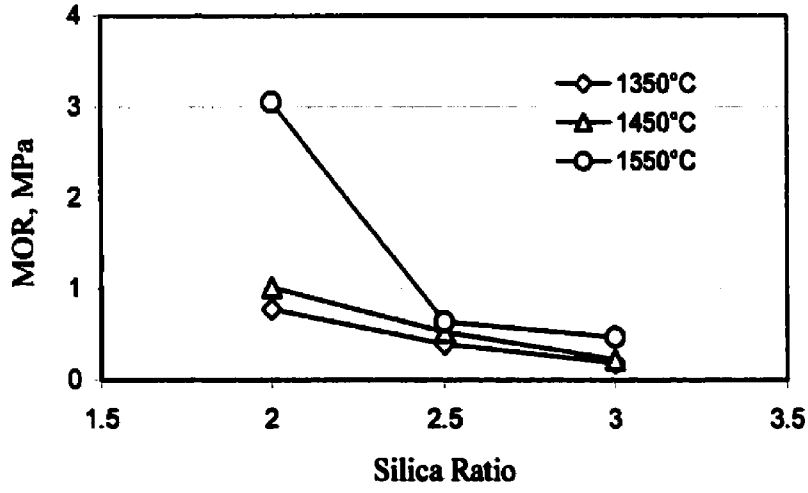

Figure 6.20 Influence of silica ratio on adherence strength of magnesia spinel brick

Influence of temperature on adherence strength of magnesia spinel is very substantial only in the case of low silica ratio of 2 and high temperature of 1550°C. Since lower silica ratio means higher amount of liquid phases in clinker, a great amount of liquid phase in clinker deeply penetrates into the brick and dissociates fine spinel to form more

liquid in the brick and more C_2S at the interface, which all contribute to higher adherence strength. Figure 6.21 shows microstructure of magnesia spinel brick exposed to raw meal with low silica ratio of 2, at temperature of 1550°C. Near the clinker/brick interface there are appreciable penetration of clinker liquid and formation of belite in the clinker. The blue colored calcium silicates are also found between MgO grains. Reaction of fine spinel with CaO containing phases plays a key role in adhering clinker on magnesia spinel brick. The C_2S (blue-colored) formed at the interface is beneficial to adherence strength.

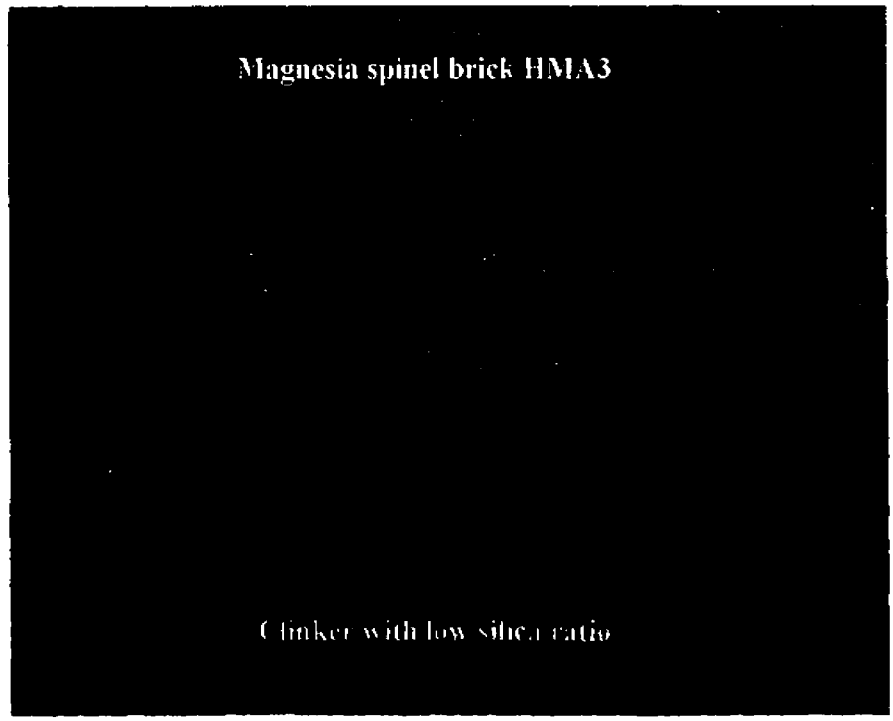

Figure 6.21 Microstructure of the interface of magnesia spinel brick HMA3 exposed to clinker with SR=2 & AR=1 ×150

In the case of high silica ratio of 3, reaction between spinel and CaO containing phases is restricted at the immediate clinker/brick interface due to less liquid formation in clinker and limited liquid penetration into the brick. There are less belite formation at the interface and little penetration in the brick HMA3, as shown in Figure 6.22. Therefore, adherence strength is very low for magnesia spinel brick exposed to clinker with high silica ratio.

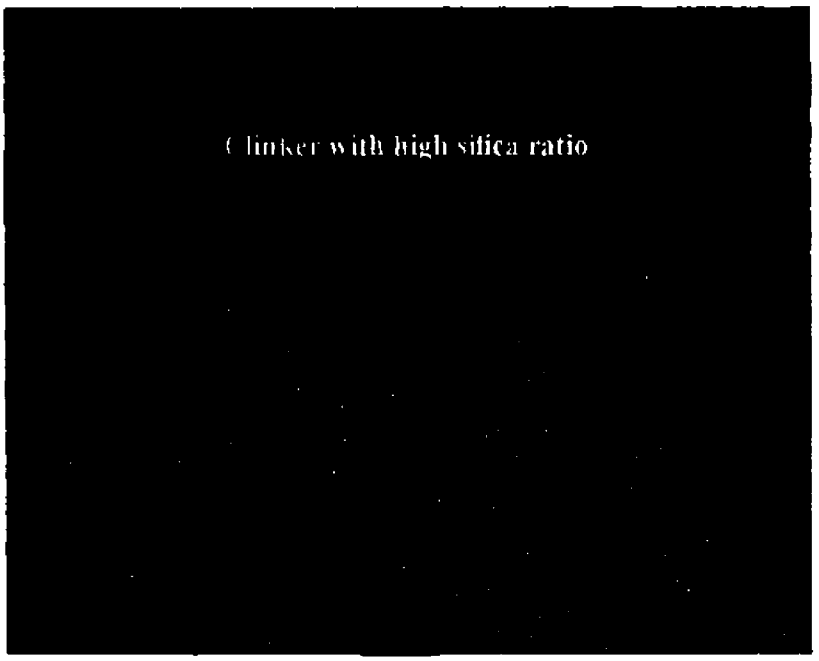

Figure 6.22 Microstructure of the interface of magnesia spinel brick HMA3 exposed to clinker with SR=3 & AR=1.5 ×150

6.4 Conclusions of Chapter 6

Microstructural analysis can be concluded as follows:

(1) Adherence mechanism of cement clinker on doloma brick is due to participation of lime from doloma brick in clinkerization of raw meal, to form alite phase. High adherence strength can be obtained in the case of raw meal with high silica ratio. The more liquid existing in clinker with low silica ratio accelerates reactions between doloma grain and silica from raw meal to form a continuous layer of agglomerated MgO, which reduces adherence strength. There is no reaction found between MgO and clinker phases.

(2) Magnesia-doloma brick has the microstructure of doloma grains bonded by magnesia. Magnesia presence decreases the possible contact between lime and clinker phases, thus explaining the lower adherence strength of doloma-magnesia brick over doloma brick.

(3) Fine crystalline spinel, evenly-distributed in one brand of magnesia-spinel brick, easily reacts with lime containing phases from clinker to form low melting phases and belite zone at the clinker/brick interface; this insures the adherence on magnesia spinel brick. The high content of liquid in clinker with low silica ratio accelerates reaction between spinel and clinker while limited reaction occurs at the brick/clinker interface with high silica ratio.

(4) In a brick consisting of magnesia and fused alumina grains, there are some spinel rings formed around fused alumina grains. When the brick is exposed to clinker,

little liquid penetration occurs and limited reactions are found at contact areas between spinel rings and clinker, which results in very low adherence strength. Therefore, careful design of magnesia spinel bricks' texture is important to enhance their adherence with clinker.

CHAPTER 7. COMPREHENSIVE DISCUSSION, CONCLUSIONS AND RECOMMENDATIONS

A new protocol has been developed to measure adherence of cement clinker on basic refractory bricks to test their coatability. The test is based on a sandwich configuration, with raw meal squeezed between two similar refractory samples. Some 600 sandwiches have been tested (1) in order to clarify the importance of compressive load, heating temperature, composition and particle size of raw meal, (2) to assess the reliability of the sandwich protocol in terms of ruggedness, repeatability and reproducibility, (3) to compare the adherence evaluation of various basic bricks to "known" coating performance in rotary kilns, (4) to uncover the adherence mechanisms with different raw meals and to correlate bricks' texture with adherence by microstructural analysis.

All the aforementioned objectives have been reached, although developing coating and making precise measurements were big challenges under laboratory conditions. At this point, it is believed that the technique developed will prove to be a useful evaluation technique for refractories in the cement industry.

It was proven that the coating simulation, in a short rotary kiln, is not appropriate to obtain quantitative data because of unreliable ratio of the coated area. Traction mode for mechanical testing was also verified to be unacceptable since the standard deviation could not considered for small values of measurements, tensile strength being less than 1

MPa. The protocol for the new sandwich test is adequate to develop solid adherence. Exerting a compressive load during heating the sandwiches plays a key role to generate strong and reproducible adherence on basic refractory bricks. A dead load of 5.3 MPa is recommended to obtain high adherence strengths. As far as influence of heating temperature is concerned, adherence strength increment with rising temperature is obviously demonstrated only in the case of a load of 5.3 MPa rather than 2.4 MPa.

Having shown that measuring adherence strength in traction mode is inadequate, adoption of three point bending mode was another major achievement of the sandwich testing protocol.

Using calcinated raw meal to make sandwich is a feature of the protocol, either in a form of wet-paste or with dry mix. Investigations of raw meal indicate that there is up to 60% free lime when raw meal is calcinated at 1000°C. Free lime can react with water in the paste to form a temporarily hydraulic bond of the sandwich at room temperature. But the paste sometimes lost this function due to the non-wettability of wax impregnated doloma brick. On the other hand, the consistency of the paste should be carefully controlled to avoid influencing clinker's adherence. Thus, dry mix of calcinated raw meal is preferred with equal adherence and great convenience in the later stage of the work for this thesis. Other trials have been carried out to make sandwich using as-received raw meal. Different treatments of the same raw meal can generate almost equal levels of adherence strength, Appendix 2 showing the results for the adherence of four kinds of basic bricks

using untreated raw meal. Therefore, it will be possible to modify and simplify the protocol, using untreated raw meal, instead of pre-calcinated raw meal.

The particle sizes of the 3 as-received raw meals tested in this thesis are mostly distributed between 0.5 and 125 μm. Although it is not evident to correlate particle size distribution of those raw meals with their adherence strength, the enhanced differences of particle size of the raw meal indeed influence adherence strength. Microstructures of clinker fired at different temperatures illustrate that most liquid phases have been formed over 1350°C and there are still some clusters of free lime at 1450°C in raw meal with high content of dolomite or ankerite. It is then a good choice to execute the sandwich test at 1550°C, at least for high dolomite or ankerite containing raw meal.

It was clearly shown that the repeatability and reproducibility of the sandwich test are also adequate. Hence, the following conclusions can be drawn:

(1) The compressive load, the nature of raw meal, the heating temperature and the holding time have significant effects on adherence strength. They are here ranked in their order of importance. Effect of heating rate on adherence strength is noticeable on magnesia spinel brick. Whenever a group of basic bricks is to be evaluated, those parameters must be specified.

(2) For different raw meals, silica ratio has a highly significant influence on adherence strength, with a negative effect on magnesia spinel brick and a positive effect on

doloma brick. Effect of alumina ratio on adherence strength is not significant on magnesia spinel brick, but is a significant positive effect on doloma brick. Particle size has a significant effect on both magnesia spinel brick and doloma brick.

(3) The sandwich test is rugged in terms of holding time, paste thickness and mixing mode of the paste. The insensitivity to minor changes on those factors allows different operators to obtain similar results.

(4) Using the guidelines of American Society for Quality Control, it was shown that the sandwich test is repeatable with small variability across trials, and is reproducible. having small variability across operators, relative to the variability between batches of firing.

(5) An acceptable standard deviation of 0.47 MPa has been obtained, for adherence mean value 5.5 MPa on doloma brick fired at 1550°C for 30 min and under a load of 5.3 kPa. The sandwich test generates distinguishable adherence values on various basic bricks and is able to differentiate their aptitude to coatability in laboratory. The results reflect the same accepted coating performance of basic bricks, in rotary kilns. It is then a reliable test. It is highly recommended to proceed now with a new well-organized inter-laboratories round robin testing, following the state of the art rules for such a test.

From the microscopic analysis, coupled to a cathodoluminescence technique and a scanning electronic microanalyzer, the following conclusions have been reached:

(1) On doloma brick, the adherence is due to the presence of sufficient lime at the brick/clinker interface, forming an alite-bonding zone. Higher adherence strength can be obtained in the case of raw meal with high silica ratio because of further alite formation with more silica. The more liquid existing in clinker with low silica ratio accelerates reactions between doloma grain and clinker phases to form a continuous layer of agglomerated MgO, which reduces adherence strength. There is no reaction found between MgO and clinker phases.

(2) On magnesia-doloma brick, MgO presence decreases the possible contact between lime and the clinker phases, thus explaining the lower adherence strength of doloma-magnesia brick over doloma brick.

(3) On magnesia spinel brick, it is evident that fine crystalline spinel easily reacts with lime containing phases from clinker to form low melting phases and belite zone at the clinker/brick interface; this insures adherence on magnesia spinel brick. More liquid in clinker with low silica ratio accelerates reaction between spinel and clinker while limited reaction occurs at the immediate interface of the brick/clinker with high silica ratio.

(4) On a brick consisting of magnesia and fused alumina grains, there are some spinel rings formed around fused alumina grains. After the brick being exposed to clinker, little liquid penetration occurs and limited reactions are found at contact areas between spinel rings and clinker, this leads to very low adherence strength. Therefore, careful design of magnesia spinel bricks' texture is important to enhance their adherence with clinker.

Conditions, which prevail to perform the sandwich test, are much more limited than those prevailing in rotary cement kilns. Some recommendations for further improvements and studies are as follows:

(1) Further work is needed to confirm the possibility of using as-received raw meal to simplify the protocol.

(2) The life of basic bricks in rotary kilns has been shortened in recent years due to the increased use of wastes as raw material and fuel. Alkalis are always identified in the used bricks. It is believed that alkalis also have big influence on coatability of clinker on basic brick. Some trials have been made to evaluate alkali attack (see Appendix 3), but the attempts failed. The sandwich can be considered to be in a big enough chamber of induction furnace to test alkalis attack on adherence.

(3) It is to be reinforced that a full round-robin testing between laboratories needs to be launched, using dry mix of calcinated or as-received raw meal, since both

challenging and inconclusive results, at the time, had been obtained, in two other laboratories. See Appendix 4.

REFERENCES

1. XELLER, H. (1984). Development of burning technology in the cement industry and demands on the refractory lining. InterCeram, Special Issue on Refractories, Vol. 33, 7-10.

2. BARTHA, P. and KILISCHAT, H. J. (1999). Present state of refractory lining for cement kilns. Ceramic News, Special Refractories, Vol. 6(3), 31-38.

3. MACEY, C. L. (1997). Refractory solution for high wear in cement kiln transition zones. Proceedings of UNITECR'97, Nov. 4-7, 1997, New Orleans, USA, Vol. 3, 1625-1631.

4. LIU, G. R. (2000). Development of refractories for cement kilns in China. The Refractories Engineer, Nov. 2000, 2-7.

5. PARTRIDGE, T. J. (1997). Cement kiln refractories for the chrome-free solution. The Refractories Engineer, July 1997, 2-6.

6. KOMATSU, H., ARAI, M. and UKAWA, S. (2000). Current and future status of chrome-free bricks for rotary cement kilns. Taikabutsu Overseas, Vol. 19(4), 5-8.

7. KLISCHAT, H. J. (1999). Variation of physical and chemical parameters as a tool for the development of basic refractory bricks. Proceedings of UNITECR'99, September 6-9, 1999, Berlin, Germany, 204-207.

8. SANCHEZ, J. A. R. and TOLEDO, O. D. (1989). New developments of magnesite-chrome brick and magnesite-spinel for cement rotary kilns higher thermal shock

resistance and higher coating adherence. Proceedings of UNITECR'89, Nov. 1-4, 1989, Anaheim, USA, Vol. 2, 968-979.

9. BARTHEL, H. and KALTNER, E. (1987). The basic refractory lining of cement rotary kilns to conform to changed requirements. Proceedings of the 2nd International Conference on Refractories, Nov. 10-13, 1987, Tokyo, Japan, Vol. 2, 623-639.

10. RADOVANOVIC, S. V. (1995). The reactions between zirconia from MgO-ZrO_2 refractories and the compounds of Portland cement clinker. Proceedings of UNITECR'95, Nov. 19-22, 1995, Kyoto, Japan, Vol. 1, 224-232.

11. PRANGE, R., BONGERS, U., HARTENSTEIN, J. and STRADTMANN, J. (1995). Present state and future trends in the use of basic refractories in cement and lime kilns. Proceedings of UNITECR'95, Nov. 19-22, 1995, Kyoto, Japan, Vol. 1, 248-255.

12. POLESNIG, W. and ZEDNICEK, W. (1984). The behaviour of basic refractory lining materials in oil- and coal-fired rotary kilns in the cement industry. InterCeram, Special Issue on Refractories, Vol. 33, 49-53.

13. TANEMURA, F. and HONDA, T. (1981). Problems and developments in cement-kiln refractories. Taikabutsu Overseas, Vol. 1(1), 89-96.

14. RIGAUD, M., CHERIF, K. and KOVAC, V. (1997). Development of methods to measure the ability to coat and the adherence of coating on refractories. Bibliographical Review for Portland Cement Association, CIREP -- Ecole Polytechnique, March 15, 1997. p.1-34.

15. TAYLOR, H. F. W. (1997). Cement Chemistry, 2nd Edition, published by Thomas Telford Service Ltd., London, Great British, p.1-28.

16. LEA, F. M. and PARKER, T. W. (1934) Investigation of a portion of the quaternary system $CaO-Al_2O_3-SiO_2-Fe_2O_3$: the quaternary system $CaO-C_2S-C_5A_3-C_4AF$. Philosophical Transactions of Royal Society, No. 234, p.731-737.

17. CZERNIN, W. (1980). Cement Chemistry and Physics for Civil Engineers, 2nd English Edition, published by Foreign Publications, New York, USA, p.13-30.

18. http://continentalcement.com -- Continental Cement Company, LLC.

19. HEWLETT, P. C. (1998). Lea's Chemistry of Cement and Concrete, 4th Edition, published by Arnold Publishers, London, Great British, p.95-239.

20. WEI, S., WENXI, H. and PANYONG, M. (1990). Process Technology of Portland Cement, in Chinese, published by Polytechnic University Publishers, Wuhan, China, p.6-83.

21. BOGUE, R. H. (1955). The Chemistry of Portland Cement, 2nd Edition, published by Reinhold, New York, USA, p.793.

22. CHRISTENSEN, N. H. (1981) Modeling of the clinker reaction. World Cement Technology, June 1981.

23. CHRISTENSEN, N. H. and JOHANSEN, V. (1979). Role of liquid phase and mineralizers. Cement Production and Use, New Hampshire. Engineering Foundation Conference, p.55-69.

24. PETERSEN, I. F. (1983). Isothermal sintering of Portland cement raw mixes. World Cement Technology, June and July/August 1983.

25. GLASSER, F. P. and MARR, J. (1980). Sulfates in cement clinkerizing, immiscibility between sulfate and oxide mutes at 1350°C. Cement and Concrete Research, 10, 753-758.

26. TIMASHEV, V. V. (1980). The kinetics of clinker formation: the structure and composition of clinker and its phases, Proceedings of the 7th International Congress of the Chemistry of Cement, Paris, France, Vol. 1, 1-31.

27. ISHIGAYA, Y., NARA, K. and MATSUZURU, M. (1988). Improvement of basic brick for burning zone of cement kiln. Taikabutsu Overseas, Vol. 8(1), 40-42.

28. HONDA, T. and OHTA, S. (1997). Evaluation techniques for refractories used in rotary cement kilns. Taikabutsu Overseas, Vol. 17(4), 50-58.

29. IMLACH, J. A and MULLER, H. P. (1980). Practice relevant test for the determination of coating behavior in the burning zone of rotary cement kilns. Zement-Kalk-Gips, Vol. 33(11), 575-580.

30. IGAWA, T., YAMAMOTO, H., KIMOTSU, H., HAYASHI, Y., MATSUZURU, M. and UKAWA, S. (1995). Chrome-free bricks with good adhesion of coating in cement rotary kiln. Taikabutsu Overseas, Vol. 15(3), 36-40.

31. HIRAGUSHI, K., SHIKANO, H. and OHISHI, M. (1989). Cement clinker sticking properties of basic bricks in cement kilns. Taikabutsu Overseas, Vol. 9(4), 15-19.

32. KOZUKA, H., KAJITA, Y., TUCHIYA, Y. HONDA, T. and OHTA, S. (1993). New kind of chrome-free (MgO-CaO-ZrO_2) bricks for burning zone of rotary cement kiln. Proceedings of UNITECR'93, Oct. 31 - Nov. 3, 1993, Sao Paulo, Brazil, 1026-1037.

33. KOZUKA, H., KAJITA, Y., TUCHIYA, Y. HONDA, T. and OHTA, S. (1995). Further improvement of MgO-CaO-ZrO_2 bricks for burning zone of rotary cement kiln. Proceedings of UNITECR'95, Nov. 19-22, 1995, Kyoto, Japan, Vol. 1. 256-263.

34. BONGERS, U. and STRADTMANN, J. (1995). Basic refractories for the burning and transition zones of cement kilns. Zement-Kalk-Gips International, Vol. 48(4), 231-240.

35. KOCK, H. (1980). Coating test with practical applications for determining coating behavior in the burning zone of cement rotary kilns: I. Zement-Kalk-Gips, Ed. A, Vol. 33(2), 77-83.

36. HARA, K., KUSUNOSE, H. and TOKUNAGA, K. (1985). Refractories for cement industry. Taikabutsu Overseas, Vol. 5(1), 39-50.

37. NACHTWEY, W. and WEIBEL, G. (1988). Theory and Practice of thermal insulation of basic lined zones in rotary kilns, Zement-Kalk-Gips International, Refratechnik Report No. 33. Vol. 41(3), 125-128.

38. MILLER, T. (1981). Characterization of clinker coatings in rotary cement kilns. I.E.E.E. Cement Industry Technical Conference, Lancaster, Pennsylvania, USA, May 10-14, 1981.

39. WAJDOWICZ, A. A. (1993). Correlation of basic refractory brick development with the evolution of cement industrial kilns. Proceedings of UNITECR'93, Oct. 31 - Nov. 3, 1993, Sao Paulo, Brazil, 173-197.

40. YAMAGUCHI, A. (1989). Dolomite refractory and atmosphere in burning zone of cement kiln. Taikabutsu Overseas, Vol. 9(4), 3-11.

41. YASUDA, Y. and TAKEMOTO, M. (1989). Influence of alkali oxide and sulfur on the wear of dolomite bricks in cement kilns. Taikabutsu Overseas, Vol. 9(4), 30-32.

42. HONDA, T. (1989). Thermodynamic consideration of dolomite bricks used in a rotary cement kiln. Taikabutsu Overseas, Vol. 9(4), 47-51.

43. YOSHIDA, T., WAKAMOTO, E., OHARA, M. and OJIMA, T. (1996). Development of MgO-CaO type bricks for sintering zone of cement rotary kiln. Taikabutsu Overseas, Vol. 16(1), 45-49.

44. SATO, A., TSUCHIYA, I., TAKAHASHI, H., ISHII, T., TAKERBAYASHI, K. and KAWAKAMI, T. (1988). Effect of thermal shock on the structure changes of the basic refractories for cement rotary kiln. Taikabutsu Overseas, Vol. 8(1), 37-39.

45. ISHII, H., ENDO, S., YASUDA, Y., and TAKEMOTO, M. (1988) Experience with dolomite bricks in large cement rotary kiln. Taikabutsu Overseas, Vol. 8(1), 33-36.

46. ODANAKA, S., HARA, K., KUSUNOSE, H. and TOKUNAGE, K. (1986). Refractories for cement production, history and current status. Taikabutsu Overseas, Vol. 6(2), 62-71.

47. NAEFE, H., NAZIRE, M., and WALK, H. (1993). Optimum chrome-free burning zone lining for rotary cement kilns. Zement-Kalk-Gips International, Vol. 46(4), 204-210.

48. KUENNECKE, M., WIELAND, K. and FAIZULLAH, M. (1986). The correlation between burning zone linings and operation of cement rotary kilns – Part 1. World Cement, Vol. 17(5), 189-198.

49. UZAKI, N., TSUCHIYA, I., TAKAHASHI, H., KAWAKAMI, T., KAWASHIMA, K. and TAKEBAYASHI, K. (1988). Study on spalling resistance of magnesia-dolomite brick. Taikabutsu, Vol. 40(2), 106-108.

50. COCHELIN, M. M. (1978). Etude des facteurs de stabilité du croutage. Internal Report of Lafarge Coppée Recherche.

51. TOKUNAGA, K., KOZOKA, H., HONDA, T. and TANAMURA, F. (1991). Further improvement in high temperature strength, coating adherence, and corrosion resistance of magnesia spinel bricks for rotary cement kiln. Proceedings of UNITECR'91, 2nd Ed., September 23-26, 1991, Aachen, Germany, p.431-435.

52. WIESBADEN, M. M. (1981). Service life of refractory linings in the transition zone of large rotary kilns, results obtained by the VDZ working committee-refractory. Zement-Kalk-Gips, Vol. 34(8), 403-406.

53. SCHULTZ LOUP, M. and SEGADAES, A. M. (1991). Refractory castables in the cement rotary kiln: chemical corrosion versus thermal shock. Proceedings of UNITECR'91, 2nd Ed., September 23-26, 1991, Aachen, Germany, p.440-443.

54. SCHUBIN, W. I., GNEDINA, I. A. and SOKOLINSKAJA, T. A. (1986). Rapid method for checking the coating and lining in the burning zone of the rotary kiln. Zement-Kalk-Gips, Vol. 35(9), 410-411.

55. SCHEUBEL, B. (1989). Raw material properties and temperature profile factors influencing clinker quality and refractory lining. Zement-Kalk-Gips, Vol. 42(10), 532-538.

56. SAXER, B. (1980). Estimating the fatigue strength of rotary kilns tyres. Zement-Kalk-Gips, Vol. 33(6), 314-318.

57. GROSSE-DALDRUP, H. and SCHEUBEL, B. (1996). Alternative fuels and their impact on refractory lining. Reprint from World Cement, March 1996, Refratechnik Report No. 45.

58. BAYLE, A. F. (1985) Aptitude au croutage des crus de frangey. Internal Report of Lafarge Coppée Recherche.

59. WALTER, H. and WEIBEL, G. (1992). Lining recommendation for high thermally stressed lime recovery kilns. Reprint from World Cement, December 1992. Refractechnik Report No. 40.

60. NAKAJIMA, E., TSUCHIYA, Y., TOKUNAGA, K., OHTA, S., HONDA, T. and KOSUKA, H. (1995). Relationship between the ovality of a cement kiln and wear rate of refractories. Taikabutsu, Vol. 47(7), 353-360.

61. HEIN, J. C. (1982). Contribution to the determination of stresses, strains and ovalities in rotary kilns, taking accounts the stiffening effect of the lining. Zement-Kalk-Gips, Vol. 35(9), 464-477.

62. ERNI, H. and SCHNEIDER, F. (1979). Deformation of rotary kilns and their effect in lining life. Zement-Kalk-Gips, Vol. 32(5), 236-243.

63. STEINBIB, E. (1979). Effect of tyre clearance and tyre ovality on kiln shell deformation. Zement-Kalk-Gips, Vol. 32(12), 604-608.

64. ADERSON, K. T. (1981). Loads and overloads on kiln supports. Zement-Kalk-Gips, Vol. 34(4), 197-201.

65. IMLACH, J. A. (1996). Private communication. October 1996.

66. WACKERLE, H. (1986). SIDRAM—an apparatus for the early detection of coating failure in the rotary cement kiln. Zement-Kalk-Gips, Vol. 39(3), 143-145.

67. BARTHEL, H. and MULLER, I. (1984). The influence of alkali oxide, sulphur and chlorine on the wear of magnesia chrome bricks in rotary cement kilns. InterCeram. Special Issue on Refractories, Vol. 33, 18-21.

68. CHATTERJEE, A. K., BISWAS, S. K., GHOSH, D. and NARAYANAN, S. (1986). Laboratory method for testing of the compatibility of burning-zone bricks with respect to kiln feeds. Zement-Kalk-Gips, Vol. 39(7), 399-402.

69. OHTA, Y. and MATSUZURU, M. (1988). Study on the evaluation method for MgO-Cr_2O_3 bricks to be used in the sintering zone of cement rotary kiln. Taikabutsu, Vol. 40(12), 728-730.

70. JAIN, M. K. and RICHTER, T. (1993) Magnesia-alumina spinel refractories based on residue from a plasma dross recovery process. Proceedings of UNITECR'93, Oct. 31 - Nov. 3, 1993, Sao Paulo, Brazil, p.1039-1049.

71. DREIZLER, I. E. (1981). Microscopic examinations of high magnesia type clinker as a contribution to clarify the causes of expansion due to magnesia. Proceedings of the Third International Conference on Cement Microscopy, edited by Gouda, G. R. March 16-19, 1981, Houston, USA, p.33-55.

72. GOUDA, G. R. (1981). Study of the reactivity of a cement raw mix by SEM. Proceedings of the Third International Conference on Cement Microscopy, edited by Gouda, G. R. March 16-19, 1981, Houston, USA, p.127-139.

73. Lhoist Réfractaires. (1994). Product data sheets.

74. Baker Refractories. (1998). Product data sheets.

75. DOMAN, R. C., BARR, J. B., MCNALLY, R. N. and ALPER, A. M. (1963). J. Am. Ceram. Soc., Vol. 46(7), 314.

76. Harbison-Walker Refractories Company. (1996). Product data sheets.

77. North American Refractories Co. (1997). Product data sheets.

78. ALPER, A. M., MCNALLY, R. N., RIBBE, P. G. and DOMAN, R. C. (1962). J. Am. Ceram. Soc., Vol. 45(6), 264.

79. ASTM C 874-85. (1995). Practice for rotary slag testing of refractory materials. Annual Book of ASTM Standards, Vol. 15.01, 1999.

80. ASTM C 860-91. (1995). Practice for determining and measuring consistency of refractory concretes. Annual Book of ASTM Standards, Vol. 15.01, 1999.

81. TSUCHIYA, I., TAKAHASHI, H., KAWAKAMI, T. and KADOTA, Y. (1984). Proof testing of basic refractories for the cement rotary kiln. InterCeram, Special Issue on Refractories, Vol. 33, 79-82.

82. ASTM C 133-97. (1997). Test methods for cold crushing strength and modulus of rupture of refractories. Annual Book of ASTM Standards, Vol. 15.01, 1999.

83. DEL VECCHIO, R. J. (1997). Understanding Design of Experiment: A Primer for Technologists, published by Hanser Publishers, Munich, Germany, p.3-7.

84. SCHMIDT, S. R. and LAUNSBY, R. G. (1994). Understanding Industrial Designed Experiments, 4th Edition, published by Air Academy Press, Colorado Springs, USA.

85. SNEE, R. D. and HARE, L. B. (1985). Experiments in Industry Design, Analysis and Interpretation of Results, published by American Society for Quality Control, Milwaukee, USA.

86. DEAN, A. and VOSS, D. (1999). Design and Analysis of Experiments, published by Springer – Verlog New York, Inc., USA.

87. MONTGOMERY, D. C. (1997). Statistical Design and Analysis of Experiments, published by John Wiley & Sons, Inc., New York, USA.

88. STATISTICA, 6.0, '98 Edition, StatSoft, Inc.

89. FRIGON, N. L. and MATHEWS, D. (1997). Practice Guide to Experimental Design, published by John Wiley & Sons, Inc., New York, USA.

90. Fundamental Statistical Process Control Reference Manual, (1991). Published by ASQC/AIAG – American Society for Quality Control and Automotive Industry Action Group, p.127.

91. RADOVANOVIC, S. V. (1997). Reaction behavior of spinel, zirconia and monocalcium zirconate under working conditions of cement kilns. Proceedings of UNITECR'97, Nov. 4-7, 1997, New Orleans, USA. p.1613-1623.

92. JAWED, I. and SKALNY, J. (1977). Alkalies in cement: a review I. Forms of alkalies and their effect on clinker formation. Cement and Concrete Research, Vol. 7(9), 719-730.

93. WANG, J. Z., ZHANG, J. Y. and CHEN X. F. (1993). Study on interaction between cement clinker and basic refractories. Refractories (in Chinese), Vol. 27(6), 352-355.

94. GONSALVES, E. G., DUARTE, K. A. and BRANT, O.R.C.P. (1993). Magnesia-spinel brick for cement rotary kilns. Am. Ceram. Soc. Bull., Vol.72(2), 49-54.

95. GONSALVES, E. G., WAJDOWICZ, A. A. and DUARTE, K. A. (1996). Recent improvement of a low permeability refractory brick for lower transition zone of rotary cement kiln. Proceedings of the International Symposium on Refractories, Haikou, China, p.312-318.

96. KOMATSU, H. and UKAWA, S. (1998). Experimental method for evaluation of damages caused in bricks by condensed alkali salts in cement rotary kilns. Taikabutsu Overseas, Vol. 18(2), 12-18.

97. KAJITA, Y., OZEKI, F., KOZUKA, H., HONDA, T. and OTA, S. (1999). New magnesia-spinel brick for cement rotary kiln utilizing waste as raw material and fuel in large quantity. Proceedings of UNITECR'99, Sept. 6-9, 1999, Berlin, Germany, p.208-211.

98. OHYAMA, T., IMAI, K., KANAI, N., TAKADA, T., KENMOCHI, I. and KUSUNOSE, H. (2000). Influence of alkali salts on magnesia-spinel bricks for rotary cement kilns. Journal of the Technical Association of Refractories, Japan, Vol. 20(3), 184-188.

APPENDIX 1. ETCHING PROCEDURES FOR CEMENT CLINKERS[72]

Structure To Be Viewed	Etchant Composition	Treatment
Aluminates and free lime	Distilled water	Immerse the polished surface for 3-5 seconds
Silicates	1% solution of NH_4Cl in water or 1% HNO_3 in ethyl alcohol	Immerse the polished surface for 5-10 seconds
Interstitial glass	10% KOH in water	Immerse the polished surface for 10-15 seconds. The best results can be achieved at etchant's temperature of 30°C.
Stain to resolve alite and belite	1 g NH_4NO_3 150 ml isopropyl alcohol 20 ml ethyl alcohol 10 ml acetone <u>Salicylic acid:</u> 0.2 g salicylic acid 25 ml isopropyl alcohol 25 ml water	Useful as an alite stain with 25-30 seconds immersion. Alite and belite will be resolved if followed by immersing in salicylic acid for 30 seconds.

APPENDIX 2. INFLUENCE OF UNTREATED RAW MEAL

The results, shown in Figure AP2-1, were obtained by using untreated raw meal from St. Constant cement plant. The sandwich was heated up at the heating rate of 4°C/min and fired at 1550°C for 0.5 h and under a load of 5.3 kPa. Modulus of rupture was measured as adherence strength, in three-point bending flexural mode.

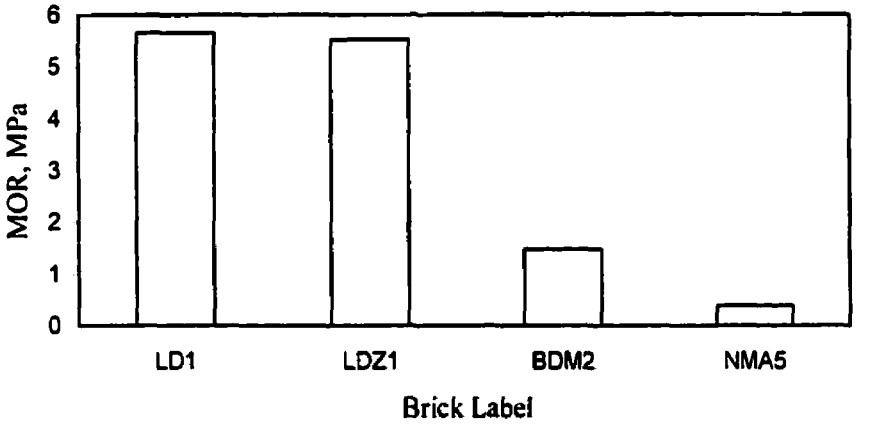

Figure AP2-1 Adherence strength of basic bricks exposed to untreated raw meal

APPENDIX 3. ROLE OF ALKALIS

1. Alkalis in Rotary Cement Kiln

Alkalis in rotary kilns originate from the raw meal used for the manufacture of Portland cement, i.e., clay, limestone, chalk and shale. Alkalis can also come from coal ash if coal is used as the primary fuel. Most of alkalis present in raw meal are volatilized in the kiln between 800° and 1000°C. Usually, potassium compounds are more volatile than those of sodium [92]. The circulation of alkalis is facilitated by cycles involving the transportation of specific elements or combinations of elements. Sulfur, introduced in fuel, is mostly coupled with the movement of alkalis. The flow of raw meal through the kiln is opposite in direction to gas flow; this is deliberate, to facilitate thermal economy by using hot gas from the burning zone to heat incoming raw meal. However, recycling of alkali-containing kiln and baghouse dusts tends to increase the amount of alkali in circulation within the kiln.

These volatile components penetrate the pores of the refractory lining. After recombination the alkali sulfate condenses at their respective solidus temperatures. The molar alkali/sulfur ratio determines whether the infiltration reacts with the brick matrix or does not chemically reacts [40, 67]. Excessive CO_2 and SO_3 present in kiln's atmosphere would react with free lime of the brick, forming calcium carbonate and/or calcium sulfate. The reaction products need a larger volume than the original lime

portion. Free alkali, however, can be absorbed by CaO in solid solution without physical alteration. In the transition zone, alkali salts have significant effects on the wear of the brick lining. As the result of alkali migration to commonly used magnesia spinel brick, the texture of the brick is often destroyed by the accompanying increase in expansion coefficient. For this reason lower permeability and higher hot strength of the brick are highly recommended.

Post-mortem analysis indicated that K_2SO_4 amounts varied from 8% to 17% in a residual magnesia spinel brick removed from the altered zone [93]. Excessive alkalis resulted in surprisedly high thermal expansion at temperatures between 400° and 700°C. Two types of magnesia spinel bricks were collected in the lower transition zone of a kiln operating under severe alkali and sulfate circulation [94]. The brick bonded by dicalcium silicate had much better resistance against alkali sulfate than the other containing calcium aluminate, which was completely destroyed by alkali sulfate. The amount of K_2O in the hot face of the brick varied between 3.0% and 6.5% and that of SO_3, between 4.5% and 5.9%. An intensive alkali penetration in the used brick was up to 120 mm in depth from hot face [95].

In the conditions of the reducing atmosphere by sulfur incomplete combustion, influence of alkali on coating formation was studied by addition of alkalis and coke in clinker as fluxing reagents for brick coating [31]. The results indicated that the coating tendency was reduced by coke and alkali salts and some alkali attacks occurred on the bricks.

Strong reactions were observed with magnesia spinel brick. It was probable that alkali salts infiltrated into the brick in the gaseous phase and condensed in the cold layer, accelerating the structure change and disintegration of brick.

It is difficult for doloma brick to form a low-melting point phase with cement clinker. However, the deposit of alkali sulfate or chloride is the main factor to lead to wear of doloma brick because of reduced spalling resistance. When the $(K_2O + Na_2O)/(SO_3 + Cl)$ molar ratio, converted from their content in the hot faces (approx. 20 mm deep) of 27 used doloma bricks, was around 1, coating adhered to doloma brick with alite formation on the interface, performing long duration. The bricks had a short life with acid surplus and an extremely low molar ratio of alkalis to sulfur [41].

It is highly intensified that alkalis are rich in cement kiln and have severe attack on refractories by using the increased amount of industrial wastes in recent years. Several studies have been made to test alkalis attack on magnesia spinel bricks [96-98]. Furthermore, it is necessary to evaluate influence of alkalis on coating adherence in order to increase and maintain coatability of cement clinker on basic refractory bricks in rotary cement kiln.

2. Approaches of Alkali Test

2.1 Gas Furnace Set-Up

In order to simulate the influence of a kiln's atmosphere and impose measurable thermal gradients, in within the tested bricks, a gas-fired cylindrical chamber was built, as illustrated in Figure AP3-1. 10 g of Na_2SO_4 powder was packed into Φ20 × 20 mm hole in the top of 67 × 67 × 198 mm bottom sample HMA4 and the other same size sample HMA4 was then superimposed, bonding by the paste of calcinated raw meal. The furnace was heated by gas, to reach 1550°C in about one hour and then to keep around this temperature for half an hour. Once cooled, coating between two samples, bottom surface layer of upper sample and the cup bottom were analyzed by X-ray diffraction. The results indicated that phase composition of HMA4 was little changed, either directly exposed to alkali salt or to alkali vapor at high temperature. Alkali minerals were not found in coating, either. Strong gas flow flushed all the alkalis in the limited-size chamber. Therefore, it is difficult to test alkali attack on coating in this way.

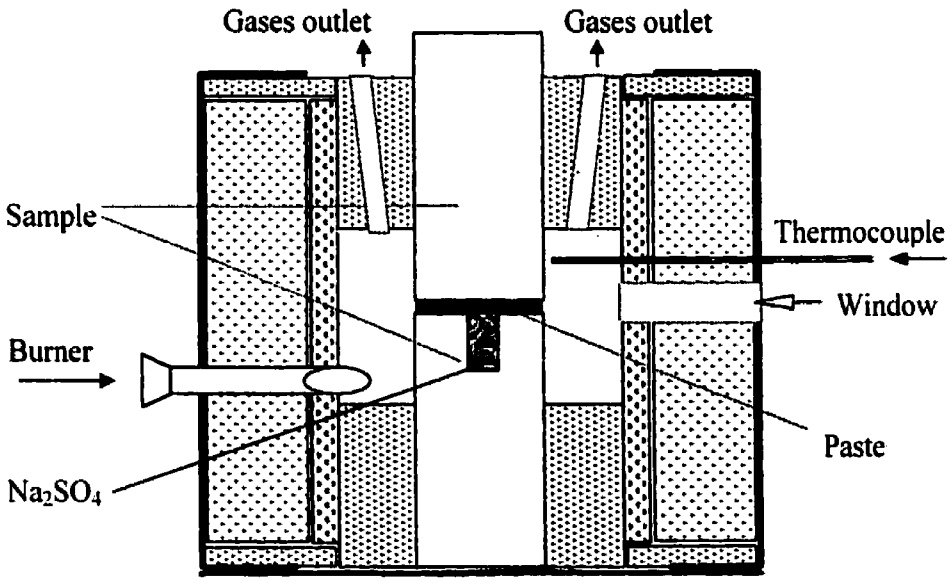

Figure AP3-1 Schematic view of the gas furnace

2.2 Electrically Heated Furnace Set-Up

An electrically heated furnace was designed to study the influence of alkalis under reducing conditions, in an enclosed environment, as shown in Figure AP3-2. The sample

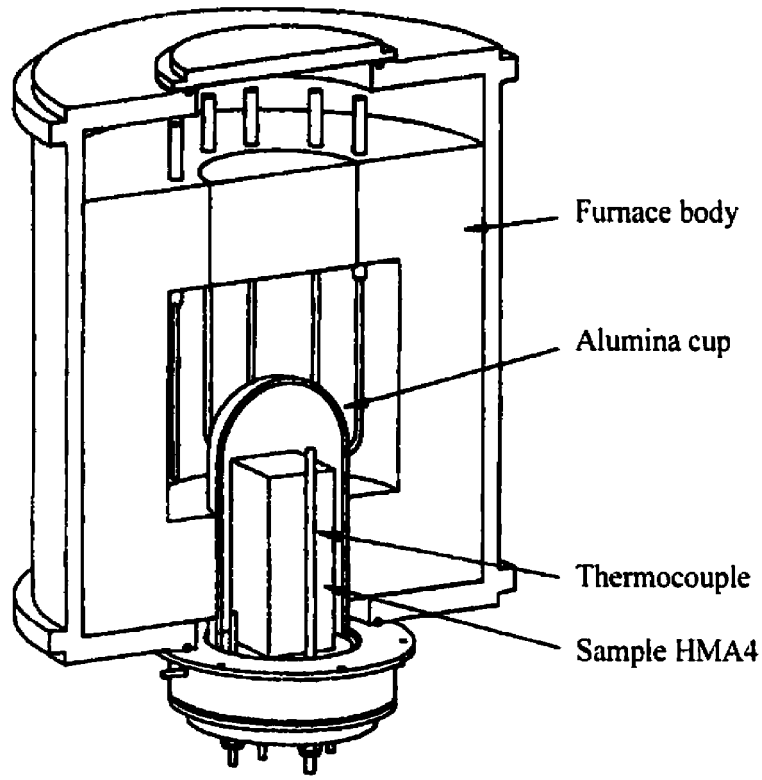

Figure AP3-2 Electrically heated furnace, with a close enclosure

assemblage was similar to that for testing in the gas furnace. However, the thermal gradient was well controlled by cooling water on the cold face. To prevent thermal shocks on the alumina cup, the heating rate and cooling rate were very slow at 1.5°C/min. Once at temperature of 1550°C, the holding time was 30 min. Sandwich was

made by HMA4 brick samples and the mixture of 90% calcinated raw meal and 10% $KCl + Na_2SO_4$ (1:1).

After testing in this closed set-up, clinker and its contact zones of upper and bottom portions of sandwich were analyzed by X-ray diffraction. The color of those areas changed to green. As listed in Table AP3-1, the results indicated that no alkalis were retained in the samples. It is strange that some free lime was detected in the clinker. Sulfur reacted with lime to form anhydrite $CaSO_4$. In the contact zones of both samples, the major phases, MgO and spinel of the original brick, existed and there was no clinker phase and penetration found in the brick.

Table AP3-1 Relative composition of the samples after alkali test

Coating	Percentage, %	Sample	Percentage, %
Larnite C_2S	39	*Upper*	
Periclase MgO	9.7	Periclase	95.0
Lime CaO	12.8	Spinel	3.8
Spinel MA	3.5		
Mayenite $C_{12}A_{14}O_{33}$	4.6	*Bottom*	
C_3S	18.2	Periclase	94.7
Anhydrite $CaSO_4$	7.5	Spinel	4.5
Titanate $CaTiSiO_5$	3.1		

Further tests were made to pack 30 g Na_2SO_4 in a vertical hole Φ25 × 25 mm in the middle of the bottom sample and then cover with paste and an other brick sample. Again, alkali was not detected in the sandwich. When 100 g Na_2SO_4 was packed in a vertical hole Φ25 × 145 mm of the bottom sample, after testing more than half of Na_2SO_4 had evaporated and some were left in the bottom of the hole due to the thermal gradient.

This test needs very long time (about 17 hours) to heat up. Alkalis had evaporated during heating. The electrically heated furnace set up was given up finally.

2.3 Induction Furnace Set-Up

A feasible furnace is to keep alkalis to condense in some part of the sample, not to leak alkali vapor everywhere. Finally, a set up of induction furnace was established, which allowed to heat up very quickly so as to avoid alkali evaporation. As shown in Figure AP3-3, 37 × 37 × 76 mm sample was embedded in 100 g of raw meal with or without 5% alkalis mixture (K_2SO_4 : $KHCO_3$: Na_2CO_2 = 1 : 1 : 1). They were fired to 1250° or 1550°C in 6-8 min and held at this temperature for 20 min. Doloma magnesia brick BDM2 and magnesia spinel brick NMA5 were tested in the induction furnace. In order to obtain evident attack, some of both samples were also exposed to the mixture of raw meal and alkalis by four times.

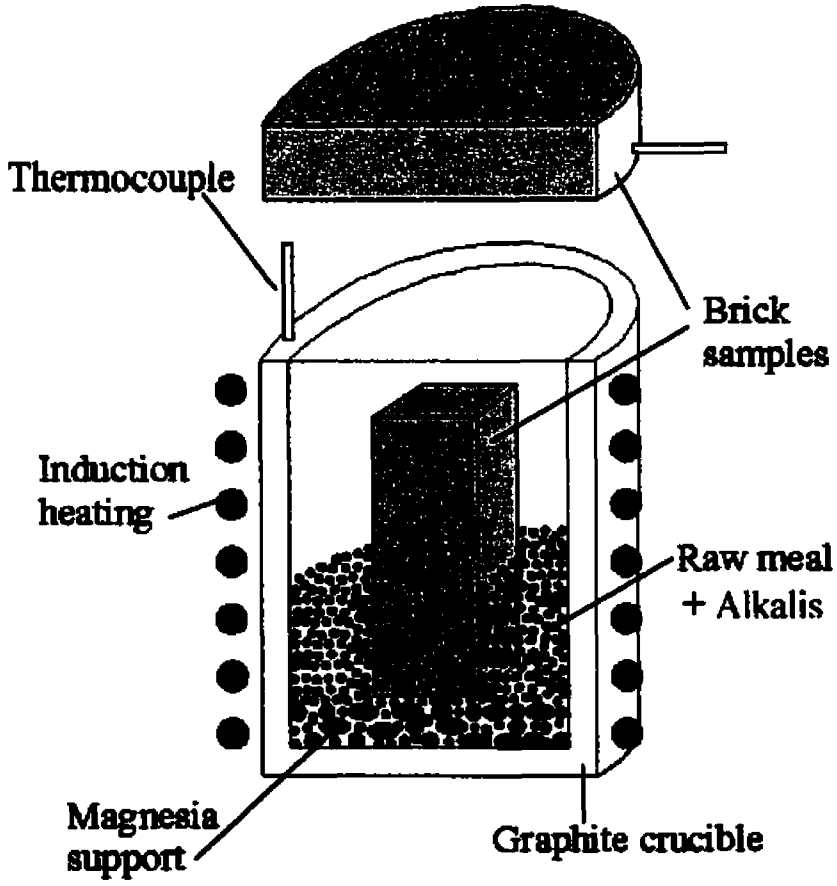

Figure AP3-3 Induction furnace for alkalis attack on refractories

Vertically cut sections of the tested samples are shown in Figure AP3-4 for BDM2 and in Figure AP3-5 for NMA5. It is seen that color change only occurs on the fringe of sample exposed to raw meal without alkalis. However, the sample exposed to mixture of raw meal and alkalis shows color change everywhere. The alkalis migrated in the sample at high temperature. The repeated tests made the samples show more significant

evidence of alkali attack. Cracks were formed in the alkalis attacked samples. It seems that doloma brick had more damage than magnesia spinel brick.

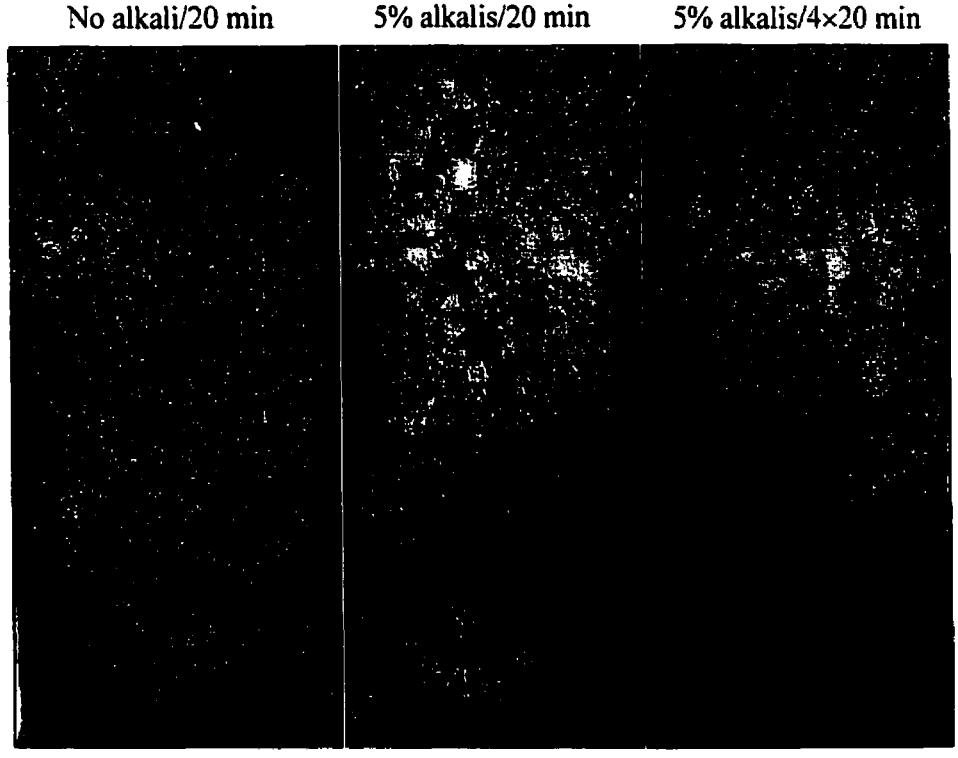

Figure AP3-4 Doloma magnesia brick BDM2 exposed to raw meal with and without alkalis addition

3. Summary

Three set-ups have been tried to investigate alkalis attack on basic bricks and their coatability. Gas furnace and electrically heated furnace need long time to heat up and allow alkalis evaporating during heating. It is possible to test alkali attack by using

induction furnace. A large amount of alkali (100-300 g) is necessary for evident attack results in each test.

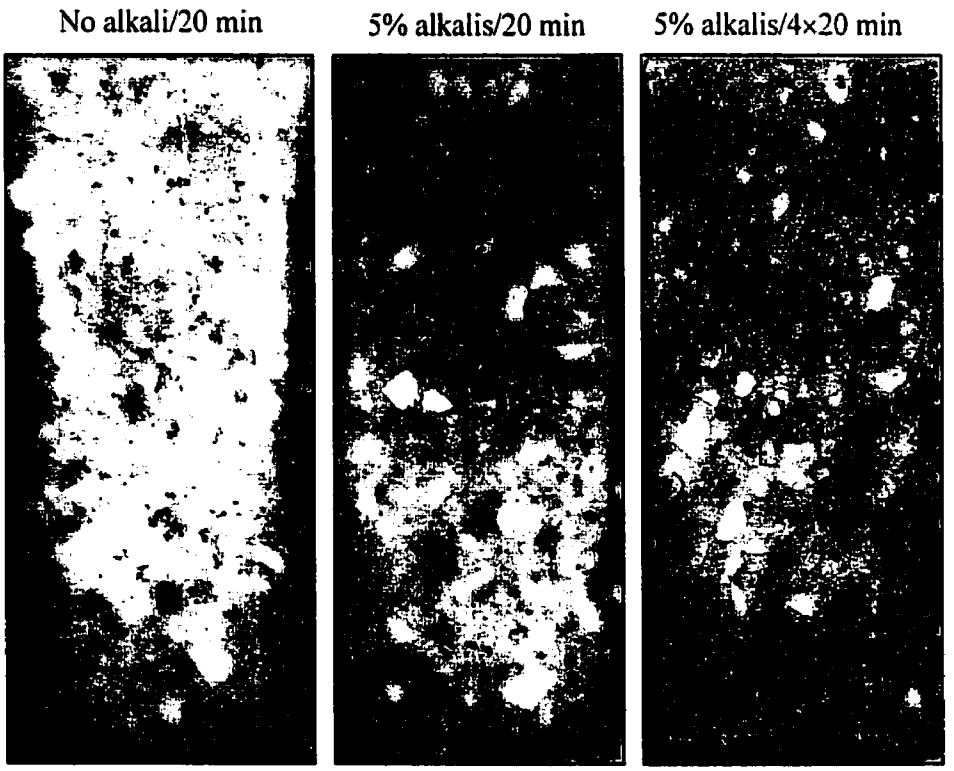

Figure AP3-5 Magnesia-spinel brick NMA5 exposed to raw meal with or without alkalis addition

APPENDIX 4. FIRST ATTEMPT TO A ROUND ROBIN TESTING PROCEDURE

Evaluation of our adherence test was conducted in two independent laboratories, at mid-term in our research program. The results were considered to be not truly conclusive. It has been shown, since, that the test is sensitive to several key parameters. This attempt to setup a round robin has to be rejected. A new round robin should now be organized.

1. The Paste Method in Baker Refractories

Doloma, doloma-zirconia, and doloma-magnesia-zirconia bricks were tested using paste of calcinated raw meal from St. Constant cement plant. A dead weight of 600g was applied on top of each sandwich, which was a load of 2.4 kPa, instead of 5.3 kPa recommended. The sandwiches were heated in a gas fired muffle furnace, with heating rate of 11.4 °C/min from room temperature to 1370°C, and of 1 °C/min to 1550°C. Modulus of rupture was measured using a Tinius Olsen machine; 76.2 mm span; strain rate of 1.27 mm/min. Adherence strength for the basic bricks was obtained, as shown in Figure AP4-1.

The results confirmed the same trend, that is, clinker's adherence of doloma, doloma-zirconia, and doloma-magnesia-zirconia bricks varies in the same order as found in this thesis. Since compressive load, heating rate, span value and strain rate have not been

respected, as stipulated in the suggested sandwich protocol, no other conclusion can be drawn. It did reveal however that adherence is indeed sensitive to all those factors, which hence have to be specified for testing.

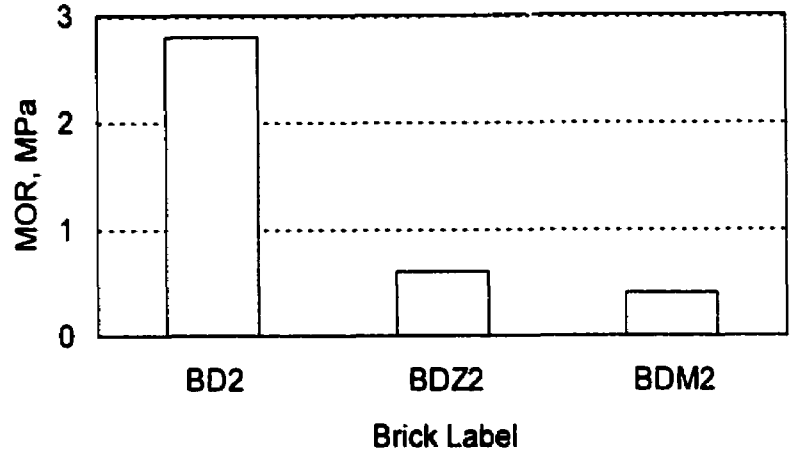

Figure AP4-1 Testing results from Baker's, February 18, 1999

2. The Dry Mix Method in Harbison-Walker Refractories

Doloma and doloma-zirconia bricks were tested using dry mix of clacinated raw meal from St. Constant cement plant. No detail of the test conditions was fed back. The results are shown in Figure AP4-2.

Those values are in accordance with those found in our laboratory; hence it reinforces the need, to proceed now with a new well-organized and well-followed inter-laboratories round robin testing.

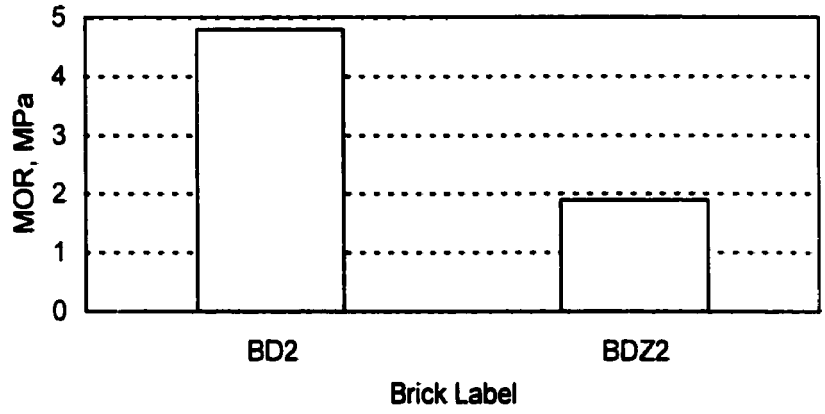

Figure AP4-2 Testing results from Harbison-Walker's, November 5, 1999